

Martin-Luther-Universität Halle-Wittenberg
Fachbereich Biochemie/Biotechnologie

**Approaches to isolating a cDNA encoding thebaine synthase
of morphine biosynthesis from opium poppy *Papaver
somniferum* L.**

Dissertation

zur Erlangung des akademischen Grades
doctor rerum naturalium (Dr. rer. nat.)

vorgelegt der
Mathematisch-Naturwissenschaftlich-Technischen Fakultät
(mathematisch-naturwissenschaftlicher Bereich)
der Martin-Luther-Universität Halle-Wittenberg

von Herrn Khaled Sabarna
geb. am 10.10.1969 in Palestine

Gutachter 1. Prof. Dr. Toni M. Kutchan
2. Prof. Dr. Martin J. Müller

Halle (Saale), den 12.06.2006

Verteidigungsdatum: 16.11.2006

urn:nbn:de:gbv:3-000010922

[<http://nbn-resolving.de/urn/resolver.pl?urn=nbn%3Ade%3Agbv%3A3-000010922>]

*With all love I dedicate this work to
my mother, may God bless her*

Khaled

Content

I. Introduction	1
I.1 Plant secondary metabolism	1
I.2 Modern methods of gene discovery	2
I.3 Single- cell genomic	3
I.4 Enzymes of plant secondary metabolism	4
I.4.1 Substrates and products	4
I.4.2 Evolution and function	5
I.5 Multiple levels of regulation of plant secondary pathways	6
I.5.1 Metabolon formation and metabolic channeling in secondary metabolism	6
I.5.2 Morphine biosynthesis regulation in <i>Papaver somniferum</i>	8
I.5.2.1 Benzyloquinoline alkaloids (BAIs) and morphine biosynthesis	8
I.5.2.2 Cell-specific localization of morphine biosynthesis key enzymes	10
I.6 Yeast two-hybrid system and protein-protein interaction	13
II. Materials and Methods	15
II.1 Materials	15
II.1.1 Organisms	15
II.1.1.1 Plant system	15
II.1.1.2 Bacteria	15
II.1.1.3 Yeast	16
II.1.2 DNA	16
II.1.2.1 Vectors and control plasmids	16
II.1.2.2 Primers	17
II.1.3 Chemicals	18
II.1.4 Molecular-biological kits and enzymes	18
II.1.5 Equipments	18
II.2 Methods	20
II.2.1 Subcloning	20
II.2.1.1 Polymerase Chain Reaction (PCR)	20

II.2.1.2 Gel electrophoresis	20
II.2.1.2.1 Agarose gel electrophoresis of DNA	20
II.2.1.2.2 Formaldehyde agarose (FA) gel electrophoresis of RNA	20
II.2.1.2 Isolation of DNA fragments from agarose gels	21
II.2.1.3 Ligation	21
II.2.1.4 DNA transformation using frozen competent cells	21
II.2.1.5 Isolation of plasmid DNA	22
II.2.1.6 Identification of insert size (Digestion)	22
II.2.1.7 Sequencing analysis	22
II.2.2 cDNA Library construction	23
II.2.2.1 Isolation of total RNA	23
II.2.2.2 Isolation of poly (A) ⁺ RNA	24
II.2.2.3 First-strand synthesis of cDNA.	24
II.2.2.4 Second-strand synthesis of cDNA.	24
II.2.3 Cyto Trap yeast two-hybrid system	25
II.2.3.1 Preparation of yeast host strain	25
II.2.3.2 Preparation of yeast competent cells	25
II.2.3.3 Library screening	25
II.2.3.3.1 Co-transformation.	25
II.2.3.3.2 Identification of “putative positive” interactors	26
II.2.3.3.3 Isolating of library plasmid from yeast cells	26
II.2.4 Alkaloid analysis (HPLC & HPLC-MS)	26
II.2.5 Protein over-expression and purification	27
II.2.5.1 Bacteria as an expression system	27
II.2.5.2 Protein purification	27
II.2.5.3 Protein concentration assay	28
II.2.5.4 SDS-PAGE electrophoresis	28
II.2.5.5 Gel staining/destaining	29
II.2.6 Macroarrays analysis	29
II.2.6.1 cDNA preparation	29
II.2.6.2 Membrane spotting	30

II.2.6.3 Random- prime cDNA labelling and northern hybridisation	30
II.2.6.4 Array analysis	30
II.2.7 Enzymes activity assays	30
II.2.7.1 Enzymatic products analysis	31
III. Results	33
III.1 Bait plasmid construction	33
III.1.1 Cloning of salutaridinol 7- <i>O</i> -acetyltransferase (SalAT) from <i>P. somniferum</i>	33
III.1.2 Verifying expression and interaction specificity of bait protein and target proteins	35
III.2.1 pMyr target vector construction	35
III.2.1 cDNA synthesis from <i>P.somoniferum</i>	35
III.2.2 Cloning of cDNA Library from <i>P. somniferum</i> into pMyr target vector	36
III.2.3 Verifying the insert percentage and size	37
III.3 Yeast transformation	39
III.3.1 Preparation of cdc25H Yeast competent cells	39
III.3.2 Transformation of control plasmids	40
III.3.3 Library screening & identification of “putative positive” interactions	42
III.4 Interactions of SalAT through morphine biosynthesis pathway	44
III.4.1 Cloning of salutaridine reductase (SalR) and norclaurine 6- <i>O</i> - methyltransferase (6OMT) from <i>P. somniferum</i> into pMyr target vector	44
III.4.2 Yeast transformation and detection of protein-protein interaction	46
III.5 Analysis of SalAT protein interactors from <i>P. somniferum</i>	46
III.5.1 Sequencing of library plasmids	46
III.5.2 Comparative macroarrays analysis of SalAT interactors	49
III.6 Alkaloid analysis in <i>P.somniferum</i> L.	58
III.6.1 Accumulation of alkaloids in <i>P.somniferum</i> seedlings	60
50	
III.7 Bacteriology and gene expression	62

III.7.1 Over-expression and purification of recombinant salutaridinol 7- <i>O</i> -acetyltransferase (SalAT) from <i>P. somniferum</i> L.	62
III.7.2 Over-expression and purification of recombinant major latex protein 146 (MLP 146) from <i>P. somniferum</i> L.	63
III.8 Enzymatic activity assays	64
III.8.1 Recombinant salutaridinol 7- <i>O</i> -acetyltransferase (SalAT) activity	64
III.8.2 Salutaridinol 7- <i>O</i> -acetyltransferase (SalAT) and major latex protein 146 coupled activity assay	67
IV Discussion	72
IV.1 Cyto Trap yeast two-hybrid system and identification of putative positives	72
IV.2 Macroarrays analysis and alkaloid profiling	75
IV.3 The enzymatic activity assays for SalAT and MLP 146	77
IV.4 Spontaneous reactions in the biosynthesis of secondary compounds	77
IV.5 Thebaine as the major product for SalAT	78
V Summary	81
VI References	84
VII Appendix	95

Abbreviations

(°)C	(degree) celsius
μA	microampere
μg	microgram
μl	microliter
μM	micromolar
6OMT	Norclaurine 6-O methyl Transferase
A	ampere
aa	amino acid
AD	Activation domain
AMVRT	Avion myeloblastosis virus reverse transcriptase
APS	ammonium persulfate
bp	base pair
BSA	bovine serum albumin
cDNA	complementary deoxyribonucleic acid
CNMT	(S)-Coclaurine N-Methyl transferase
CoII	Collagenase
cpm	count(s) per minute
dATP	2'-deoxyadenosine-5'-triphosphate
DBD	DNA binding domain
dCTP	2'-deoxycytidine-5'-triphosphate
dGTP	2'-deoxyguanosine-5'-triphosphate
DMSO	Dimethyl sulfoxide
DNA	deoxyribonucleic acid
DNase	deoxyribonuclease
dNTP	2'-deoxynucleotide-5'-triphosphate
DTT	dithiothreitol
dTTP	2'-deoxythymidine-5'-triphosphate
EDTA	ethylenediaminetetraacetate
EST	Expressed Sequence Tag
FPLC	fast protein liquid chromatography
g	gram
Gal	galactose
Glu	glucose
GSP	gene specific primer
HPLC	high performance liquid chromatography
hSos	Human Sos
IPTG	iso-propyl-β-thiogalactoside
kb	kilo-base pair
kDa	kilodalton
L	Leucine
l	liter
LB (medium)	Luria-Bertani
LC-MS	liquid chromatography mass spectrophotometry
M	molar
MCS	multi cloning site
min	minute(s)
ml	milliliter

MLP	Major Latex Protein
mM	millimolar
MMLV-RT	Molnoey murine leukemia virus
MOPS	morpholinopropane sulphonic acid
Myr	Myristylation signal
NADPH	nicotinamide adenine dinucleotide phosphate reductive
NaOAc	sodium acetate
OD	optical density
OMT	<i>O</i> -Methyltransferase
ORF	Open reading frame
PCR	polymerase chain reaction
<i>Pfu</i>	polyvinylpyrrolidon
pmol	picomole
RNA	ribonucleic acid
RNase	ribonuclease
rpm	round(s) per minute
SalAT	Salutaridinol-7- <i>O</i> -Acetyltransferase
SB	Sos-binding
SD	Synthetic dropout
SDS-PAGE	sodium dodecyl sulphate polyacrylamide gel electrophoresis
sec	second(s)
sp	storage protein
<i>Taq</i>	<i>Thermus aquaticus</i>
TEMED	N, N, N', N'-tetramethylenediamine
TLC	thin layer chromatography
Tris	Tris-(hydroxymethyl)-aminomethan
U	unit(s)
-U	-Uracil
UPM	universal primer mixture
UV	Ultra-violet
V	(enzyme) velocity
v	volume
w	weight
X-Gal	5-Bromo-4-chloro-3-indol- β -D-galactopyranosid

I. Introduction

I.1 Plant secondary metabolism

Plants are capable of synthesizing an overwhelming variety of small organic molecules, called secondary metabolites, usually with very complex and unique carbon skeleton structures and many of them of high interest to the pharmaceutical and chemical industry. For instance, plant derived pharmaceuticals represent a large market value; about 25% of today's pharmaceuticals contain at least one active ingredient of plant origin (Rischer et al., 2006). By definition, secondary metabolites are not essential for the growth and development of a plant, but rather are required for the interaction of plants with their environment (Kutchan and Dixon, 2005). Many secondary compounds have signalling functions; among them are plant hormones which will be discussed later in more details. They influence the activities of other cells, control their metabolic activities and co-ordinate the development of the whole plant. Other substances flower colours serve to communicate with pollinators (Atsatt, 1996) or protect the plants from feeding by animals or infections by, producing specific phytoalexins after fungi infections that inhibit the spreading of the fungi mycelia within the plant (Atsatt, 1996). Plant secondary metabolites have been a fertile area of chemical investigation for many years, driving the development of both analytical chemistry and of new synthetic reactions and methodologies. The subject is multi-disciplinary with chemists, biochemists and plant scientists all contributing to our current understanding. One overall goal is to genetically characterise the molecular mechanisms driving secondary metabolite biosynthesis in plant cells. Identifying key elements involved in these processes will allow generating novel tools for metabolic engineering of plant cells. Even so, only a little fraction of the enormous biosynthetic potential of plant cells is being exploited. Metabolic engineering of plant cells so far has added little to the problem, since insight into the molecular mechanisms driving plant secondary metabolism is still very limited. Genetic maps of biosynthetic pathways are still far from complete and the regulation of these pathways is hardly understood. However, technological advances in analytical chemistry, in particular in the development of high-field nuclear magnetic resonance spectroscopy and Fourier

transform-ion cyclotron mass spectrometry, have facilitated the elucidation of structures of secondary metabolites that are presents even at low levels within a plant.

I.2 Modern methods of gene discovery

Genetic approaches have been successful in unraveling the metabolic network for phenylpropanoid and flavonoid metabolism, as well as in finding transcriptional regulators of structural genes in the genetically tractable plant species maize, petunia, snapdragon and, more recently, *Arabidopsis* (Davies *et al.*, 2003). The revolution in views on phenylpropanoid metabolism demonstrates the power of genetics and shows that long-term and worldwide research efforts that employed biochemical approaches have failed to correctly describe the basic network of intermediates and enzyme activities in this pathway. Enormous advances have also been made in understanding the basic network of glucosinolate biosynthesis, and its relationship to auxin homeostasis, in *Arabidopsis* (Memelink, 2005). A powerful tool in phenotype-driven genetics is gain-of-function mutagenesis with a strong constitutive promoter that is carried on an insertion element such as *Agrobacterium tumefaciens* T-DNA. T-DNA activation tagging causes dominant gain-of-function mutations that are caused by the over-expression of the genes that flank the T-DNA insertion (Memelink, 2005). It allows the recovery of mutant phenotypes that are conferred by functionally redundant genes. In addition, the T-DNA tag allows gene recovery from the primary transformant without a need for genetic crosses. T-DNA activation tagging has been successfully used in the model species *Arabidopsis* to identify the transcriptional regulator PAP1 (Production of anthocyanin pigment1) (Borevitz *et al.*, 2000). Over-expression of this MYB-type protein up regulates multiple genes that are involved in anthocyanin biosynthesis and gives the transformant a purple color. In non-model plant species, the use of genetic approaches (with the exception of some reverse-genetic RNAi approaches) appears to have come to an almost complete standstill. For example in opium poppy, codeinone reductase (COR), a terminal enzyme in morphine biosynthesis, has been knocked out by RNAi using a chimerical inverted repeat that targets all seven members of the gene family, leading to a significant reduction in the morphine and codeine levels of the transgenic poppy latex (Allen *et al.*,

2004). Surprisingly, none of the morphine-type precursors that are normally present in the latex were detectable. Instead, the transgenic latex accumulated rare alkaloids. These included the upstream precursor reticuline, which is located seven enzymatic steps before the COR-mediated reaction in the biosynthesis pathway, and several methylated derivatives of reticuline. The reasons for the apparent shutdown of the complete morphine-specific branch, resulting in a drastic switch in the alkaloid pattern, are not clear. It has been demonstrated that some genetic approaches, such as T-DNA activation tagging, can be successful with non-model species but this has not led to the expected explosion of similar approaches in a variety of plant species. The picture is far from complete, however, and how the expression and the activities of these transcription factors are regulated remains largely mysterious (Von Endt *et al.*, 2002).

I.3 Single- cell genomics

Particular emphasis is placed on genomic-based single-cell approaches for an improved understanding of the biosynthesis of specialized metabolites. Alkaloids, such as morphine and codeine, and rubber polymers are found in exudates derived from laticifer cells (Mahlberg, 1993), lignin-like polymers are synthesized in vascular tissue cells (Ye, 2002), UV-absorbing phenylpropanoids are present in epidermal cell layers (Harborn and Williams, 1992), and a variety of metabolite classes that function in the defense against insects and pathogens are localized to secretory trichomes (Wager *et al.*, 2004). Protocols for the isolation of specialized cells usually allow the cell type of interest to be pooled, which increases the amounts of analyses available and thus enables direct interfacing with various post-genomic technologies (Markus, 2005). However, care must be taken to ensure that the collection of a specialized cell type does not bias subsequent analyses. Direct access to the cellular contents of individual cells is facilitated by Pico liter-scale sampling using micro capillaries. Isolation of specialized cell types Glandular secreting trichomes are more easily accessed by mechanical means than are cells or components of cells that are embedded within plant tissues (Heath *et al.*, 2003). Biosynthetically competent secretory cells of peppermint (*Mentha x piperita*) and basil (*Ocimum basilicum*), which are responsible for the biosynthesis and secretion of the signature

essential oils of these plants, have been isolated by surface abrasion with glass beads in a complex medium. cDNA libraries were then generated from these cells and randomly selected clones (i.e. expressed sequence tags [ESTs]) (Lange *et al.*, 2000). Laser-capture microdissection (LCM) is a highly effective tool for the isolation of target cells from heterogeneous tissues that has recently been adapted for collecting material from plant sections (Kehr, 2003). The detection of the most abundant proteins and metabolites at the single-cell level has been achieved using a variety of platforms (Tomos *et al.*, 2001), but the potential for multiplexing is limited. Thus, an important challenge in overcoming these current difficulties is the development of more sensitive assays, possibly by advancing the use of nanotechnology in the analysis of biomolecules. Bioanalytical nanotechnology microarrays are used widely to profile thousands of transcripts in parallel and, when interfaced with prior RNA amplification techniques, are powerful tools for single-cell analysis. Microarray analyses might not, however, detect the expression of low abundance transcripts (Czechowski *et al.*, 2004). An alternative transcript-profiling technology, termed massively parallel signature sequencing (MPSS), involves the cloning of DNA molecules onto microbeads and reveals the expression levels of virtually all of the genes that are expressed in a sample by counting the number of individual mRNA molecules produced from each gene. One intriguing possibility is the use of cell-type-specific promoters, which might enable the modulation of essential oil composition in glandular trichomes (Mahmoud *et al.*, 2004) or alkaloid production in laticifers (Frick *et al.*, 2004) by genetic engineering, without causing adverse effects attributable to the ectopic expression of trans-genes.

I.4 Enzymes of plant secondary metabolism

I.4.1 Substrates and products

The ‘classical’ approach to discover enzymes is to start with a given product and to ask what enzymatic reaction is responsible for its formation, and what the substrate is. Substrates can be hypothesized on the basis of biochemical principles and current knowledge of metabolic pathways and types of enzymes. In other words, identification of the enzymatic properties of a newly discovered protein still depends on prior biochemical

knowledge relating to the family of enzymes to which the candidate protein belongs. Thus, many new methyltransferases, terpene synthases, acyl transferases, and glucosyltransferases have been discovered because we already know representative enzymes of these types and can therefore make an informed guess regarding the potential substrates with which to test candidate proteins. New methods of inactivating gene expression, such as the insertion of T-DNAs and transposable elements and RNA interference (RNAi) techniques, could be extremely powerful in combination with metabolic profiling techniques. However, gene identification by such techniques must also be followed by biochemical characterization of the protein (Simkin *et al.*, 2004) because the lack of final product in the mutant does not guarantee that the substrate has been correctly identified. Gene suppression techniques might also lead to misleading results if several similar genes that encode enzymes with different substrates are suppressed by the same construct. In summary, the combination of the new techniques of metabolic and gene expression profiling with classical techniques of enzymatic analysis will allow the identification of the function of the majority of the genes in plant genomes. The challenge is to develop standardized and automatable methods for enzyme analysis.

I.4.2 Evolution and function

The chemical diversity of plants is the result of ongoing evolutionary processes. Recent advances in the molecular biology of plants, particularly in the area of large-scale genomics (Borvitz and Ecker, 2004), are revealing how enzymes of natural product biosynthesis arise through mutation and gene duplication, leading to the continued elaboration of new chemical structures that will be selected for if they impart an adaptive advantage on the plant (Pichersky and Gang, 2000). Structural biology provides an important tool set for the detailed structure–function characterization of proteins at the atomic level (Kim *et al.*, 2003; Eisenberg, 2005). The level of functional understanding derived from experimentally determined structures or from realistic models that are constructed from homologous protein folds (Goldsmith-Fischman and Honig, 2003) can lead to a more complete appreciation of complex biosynthetic pathways. Such information can elucidate the mechanisms of individual biosynthetic reactions (Naismith,

2004) and provides new views at atomic resolution of the temporal and spatial architecture of multi-protein complexes that are vital to metabolic flux and channeling, and this results a practical and rational basis for engineering useful metabolic traits (Whittle and Shanklin, 200; Singh *et al.*, 2005) into medicinally and agriculturally important plants. The fact that *Arabidopsis* has more than one hundred small molecule glucosyltransferases (GSTs) (Bowles *et al.*, 2004) suggests that these enzymes to be relatively promiscuous, at least *in vitro*, presents a challenge in relating *in vitro* biochemistry to *in vivo* function and poses fascinating questions as to why such complex gene families have evolved (Kliebenstein *et al.*, 2005). Studies are currently underway to generate transgenic *A.thaliana* lines that specifically vary in each of these steps to verify their epistatic and phenotypic effect on both glucosinolate structure and herbivores.

I.5 Multiple levels of regulation of plant secondary pathways

Secondary metabolism is an integral part of the developmental program of plants, and accumulation of secondary metabolites often marks the onset of developmental stages. Although this association between plant differentiation and secondary metabolism has long been known, a picture of the molecular mechanisms that connect these two programs is starting to emerge, particularly in the latest findings related to the regulation of flavonoid biosynthesis in *Arabidopsis*. It emphasizes the role played by a common set of transcription factors that control both this pathway and specific aspects of cellular differentiation, and discusses the importance of WD40 proteins in coordinating flavonoid regulation in *Arabidopsis* and other plant species (Broun, 2005). In this respect we have much to learn about the transcription factors, and we need to know more about the post-translational events that control their activity, and their sub-cellular localization and turnover.

I.5.1 Metabolon formation and metabolic channeling in secondary metabolism

Classically, biological membranes such as the endoplasmic reticulum (ER) have been considered as homogenous fluid structures that are composed of lipid bilayers,

which serve as a two-dimensional solvent phase for fully or partly embedded membrane proteins (Singer and Nicolson, 1972). The organization of cooperating enzymes into macromolecular complexes is central feature of cellular metabolism. A major advantage of such spatial organization is the transfer of biosynthetic intermediates between catalytic sites without diffusion into the bulk phase of the cell. This so-called “metabolic channeling” offers unique opportunities for enhancing and regulating cellular biochemistry (Winkel, 2004). The formation of plant secondary metabolites is complex and dynamic process that involves multiple sub-cellular compartments such as the cytosol, endoplasmic reticulum, and the vacuole. The metabolic activities of a plant are highly coordinated at the whole-plant, organ, tissue, cellular, organelle and molecular levels. At the cellular level, channeling of substrates to their target enzymes is facilitated by the compartmentalization of the cell into different organelles and sub-structures. This serves to co-localize and optimize the concentrations of enzymes and their substrates. A limited number of key genes encode the enzymes that are responsible for the synthesis of the pivotal backbone structures that constitute the hallmarks of the different classes of natural products, and progress has been made in the identification of these genes (Kuchan 1995; bak *et al.*, 2003). The subsequent decoration of the backbone structures generates the huge diversity of plant secondary products. The large majority of these decoration processes are mediated by a limited number of enzyme classes, such as glycosyl-, methyl- and acyltransferases, which are all encoded by multi gene families. The positioning of enzymes that have broad substrate specificity downstream of the conserved early pivotal enzymes of plant secondary metabolism opens the possibility of producing new secondary compounds without major re-structuring of the enzyme complement. Metabolic channeling and metabolon formation provide the key to resolving and avoiding potential negative interference in plant natural product formation either by narrowing substrate specificity as a result of conformational changes upon binding or because binding into the metabolon prevents access of unwanted substrates (Jørgensen *et al.*, 2005). A single glycosyl-, methyl- or acyltransferase might possess the ability to bind to different metabolons. In this manner, the possibility of combinatorial defined substrate specificity might explain how the desired substrate specificity is achieved with a minimum number of enzymes (Jørgensen *et al.*, 2005). The latest findings stress the

importance of specific types of transport molecules, and genes encoding various types of multi drug resistance, and ABC transporter proteins. ABC transporters constitute a large protein family that is found in a range of organisms from bacteria to humans. Because of intensive studies on the roles of ABC transporters in multi drug resistance in animal cancer cells, it had long been believed that they exhibit broad substrate specificity (Yazaki 2005). Recent studies have demonstrated that the function of ABC transporters is not restricted to detoxification processes (Martinoia *et al.*). Furthermore, they have been found to be involved in many specific biological activities, such as cell signaling, that have strict substrate specificity, as well as in other divergent physiological functions (Klein *et al.*, 2003; Pighin *et al.*, 2004). It was suggested recently that the ABC transporter family might have evolved according to the need to transport specific substrates in organism, and not as drug efflux pumps (Sheps *et al.*, 2004).

I.5.2 Morphine biosynthesis regulation in *Papaver somniferum*

I.5.2.1 Benzyloisoquinonline alkaloids (BAIs) and morphine biosynthesis

Benzyloisoquinonline alkaloids are large and diverse groups of natural product containing more than 2500 defined structures found mainly in five plant families, including the Papaveracea (Facchini, 2001). BAIs are all based on the elaboration of a simple skeletal structure. Skeletal representation of known stereochemical conformation and functional group substitutions found in major BAI families (D.K. Liscombe *et al.*, 2005). Opium Poppy (*Papaver somniferum* L.) produces a large number of Benzyloisoquinonline alkaloids including morphine and sanguinarine, derived from tyrosine via the Branch -point intermediate (S)-reticuline. Berberine, the first isoquinone alkaloid from an amino acid to have its biosynthetic pathway completely elucidated, which is derived from L-tyrosine via 13 different enzymatic reactions (Sato *et al.*, 2001) Codeine and other morphinan-type alkaloids is centrally involved in the synthesis of many other isoquinonline alkaloid of divergent chemical structure in various plant species (Kutchan, 1996). It is presumed; therefore that morphine biosynthesis proceeds via a common pathway up to (S)-reticuline and that the biosynthetic reactions after this stage constitute the morphine-specific pathway in opium poppy. From morphine- specific

biosynthesis pathway after reticuline, cDNAs of two important genes were cloned i.e. codeinone reductase (Underline *et al.*, 1999) and salutaridinol 7-*O*-acetyltransferase (SalAT) (Grothe *et al.*, 2001). The cell cultures of opium poppy contained these enzymatic activities, although they did not accumulate morphine itself. From the cultured cells, these enzymes were purified to homogeneity and the internal peptide sequences were used to clone their cDNAs taken from a library. The discovery of (salAT) activity catalyzing the acetylation of salutaridinol is an important step. It was not clarified whether the formation of thebaine, (Figure I.1) the first morphinan alkaloid having the pentacyclic ring system is a protein-dependant or it is a non-enzymatic *in vivo* reaction at natural conditions of laticifers in poppy plants

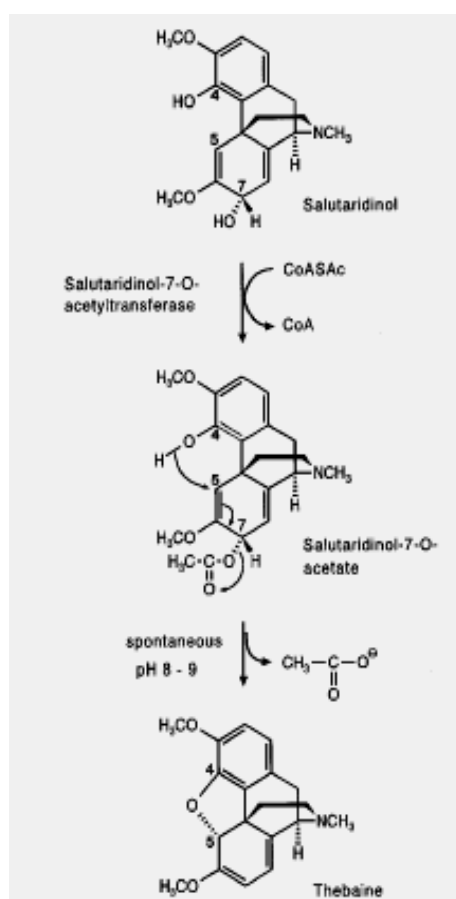


Figure I.1 Proposed reaction Sequence leading from Salutaridinol *via* Salutaridinol-7-*O*-acetate to thebaine (pH 8-9)

The pH value of this novel mechanism in alkaloid biosynthesis is critical for the formation of the phenolate anion that initiates the S_N2 reaction supported by the favored acetate leaving group. In contrast, if the homogeneous Salutaridinol-7-*O*-acetyltransferase was incubated in the presence of its substrates at pH 7 (Figure I.3), hardly any thebaine was formed but rather a completely different reaction product (dibenz [*d,f*]azonine alkaloid) (Lenz and Zenk, 1995).

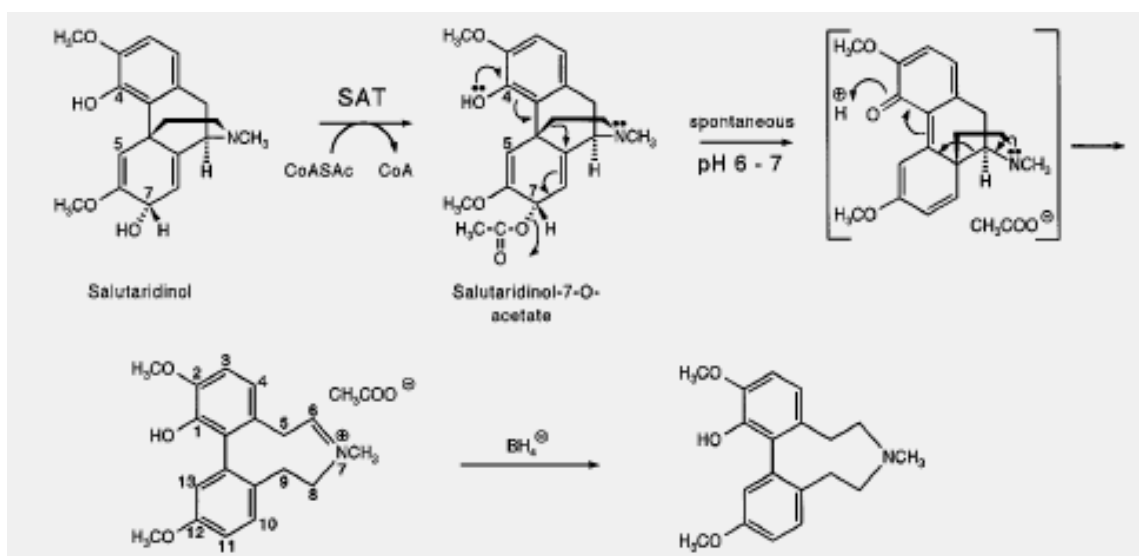


Figure I.2 Proposed reaction Sequence leading from Salutaridinol via Salutaridinol-7-*O*-acetate to [8,9-dihydro-5H-2,12-dimethoxy-1-hydroxy-7-methyl-dibenz[*d,f*]azoninium]acetate (pH 6-7), which was converted chemically to neodihydrothebaine by NaBH₄ reduction

I.5.2.2 Cell-specific localization of morphine biosynthesis key enzymes.

The past decade has provided a lot of new molecular information on the biosynthesis of some of the most complex alkaloids, including the description of all the individual steps in the conversion of tyrosine into berberine and the elucidation of most of the steps in morphine biosynthesis (Qunaron *et al.*, 2003). The alkaloid (S)-reticuline constitutes an important branch point in alkaloid synthesis because several different subclasses of isoquinoline alkaloids can be formed from this compound, depending on the subsequent regio- or stereo specific transformations that take place (Qunaron *et al.*, 2003) The cell-specific localization of five key enzymes in the metabolic grid has been

determined in the capsule, stem, and root tissues (Figure I.4). It appears that the early stages of morphine biosynthesis, starting with the decarboxylation of amino acid L-tyrosine occur in the parenchyma cells surrounding laticifers. In contrast, the later stages of morphine biosynthesis occur in the laticifer, which is the storage site of morphine alkaloids thebaine, codeine and morphine. (Kutchan, 2005). This outstanding example of channeling at the cellular level is provided by the different spatial organizations of the key enzymes in the metabolic enzyme grid that results in the synthesis of different morphinans suggest many questions about the involvement of diverse organelles in plant natural product biosynthesis in addition to the simple diffusion transport. Furthermore the interaction of macromolecular biosynthetic enzyme complexes with metabolite transporters might also be a consideration (Kutchan, 2005).

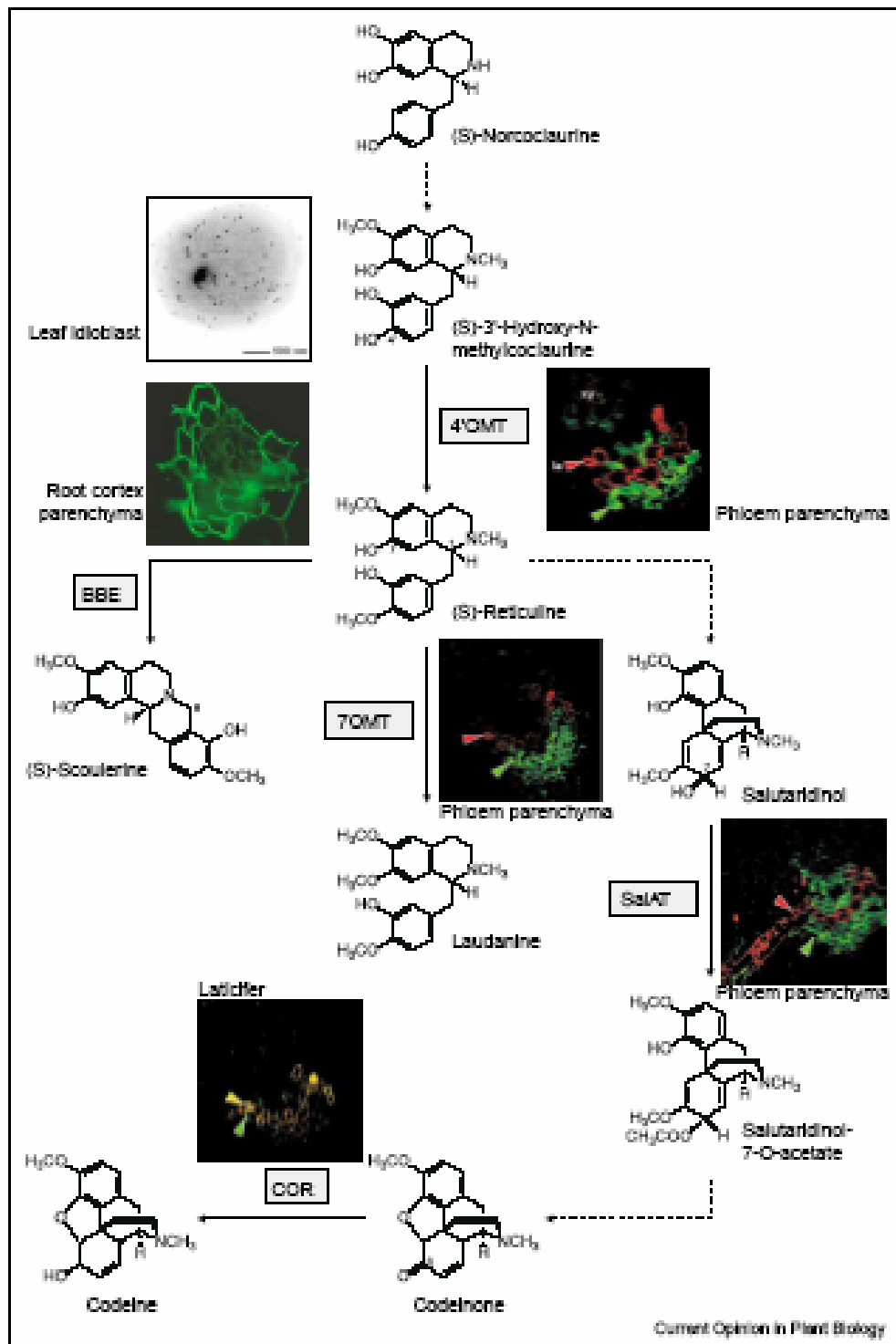


Figure I.3 Schematic of the biosynthetic pathway leading to tetrahydrobenzylisoquinoline-derived alkaloids in opium poppy. In the capsule and stem, 4'OMT, 7'OMT and SalAT are found predominantly in phloem parenchyma cells and codeinone reductase is localized to laticifers. These are the site of morphinan alkaloid accumulation, as determined by fluorescence immunocytochemical localization. The berberine bridge enzyme has been localized to vesicles in idioblasts of young shoot and parenchyma cells of the root cortex (by fluorescence immunocytochemical labeling; image reproduced). Major latex proteins are represented by red arrowheads, biosynthetic enzymes by green arrowheads and the co-localization of major latex proteins and biosynthetic enzymes by yellow arrowheads. laticifer; MLP 15, major latex protein 15; Xy, xylem.

I.6 yeast two-hybrid system and Protein-protein interactions detection

All biological processes depend on interactions formed between proteins and the mapping of such interactions on a global scale is providing interesting functional insights. One of the techniques that have proved itself invaluable in the mapping of protein-protein interactions is the yeast two-hybrid system. The yeast two-hybrid screen is a powerful artificial transcription-based assay which provides a rapid and straight forward mechanism to identify proteins that interact *in vivo* in a yeast model system. A significant issue in the use of two-hybrid system is the degree to which interacting proteins distinguish their biological partner from evolutionarily conserved related proteins and the degree to which observed interactions are specific (Causier and Davies, 2002). A number of variants of the two-hybrid system have been developed for library screening one of them is the Cyto Trap two-hybrid system (Figure I.4).

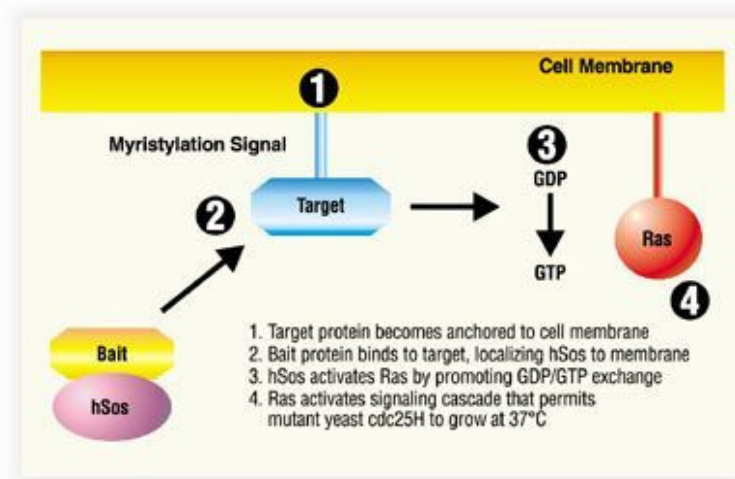


Figure I.4 Cyto Trap two-hybrid system: CytoTrap two-hybrid system restores the Ras signal transduction pathway as opposed to transcriptional activation of a reporter gene.

The system is able to detect protein-protein interactions in the yeast cytoplasm instead of in the nucleus.

Cyto Trap two-hybrid system restores the Ras signal transduction pathways opposed to the transcriptional activation of reporter gene in the traditional systems which rely on transcriptional factors LexA or GAL4. Cyto Trap assay uses an exclusive yeast strain (*cdc25H*) that harbors a temperature-sensitive mutant of the *cdc25* gene, the yeast homologue for hSos. This kind of mutation allows the yeast cells to grow only at room

temperature (25 °C) but not at 37 °C. The Ras rescue depends on the unique design of the bait and target vectors in Cyto Trap system. To use the system target gene or cDNA library should be inserted into the pMyr vector which fuses the target gene to the myristylation factor that anchors the protein to the cell membrane. Bait gene or protein of interest must be cloned into the pSos vector which fuses the bait to hSos. If the bait and target interact, hSos will be recruited to the cellular membrane, and the Ras pathway can be stored, as a result, yeast cells could be assayed for growth at 37 °C. Along the biosynthetic pathway that leads to morphine, salutaridinol is acetylated by salutaridinol 7-*O*-acetyltransferase to salutaridinol- 7-*O*- acetate. The oxide ring is closed and acetate is eliminated to form thebaine, the first morphinan alkaloid with the complete pentacyclic ring system (Figure III.20). The current study will focus on the molecular characterization and further *in vitro* biochemical analysis of the hypothetical “thebaine synthase” from opium poppy *Papaver somniferum* using the yeast two-hybrid assay.

II. Materials and Methods

II.1 Materials

II.1.1 Organisms

II.1.1.1 Plant system

- *Papaver somniferum* plants were grown outdoors in the field at the Leibniz-Institute of Plant Biochemistry, Halle, Germany.
- *Papaver somniferum* seedlings were grown in the greenhouse or a growth chamber at 24°C, 50 % relative humidity under a photoperiod of 16 hours light/8 hours dark cycle with a light intensity of 85 $\mu\text{mol sec}^{-1} \text{m}^{-2}$ per μA .
- *Papaver somniferum* (paso paris) cell suspension cultures were provided by our cell culture laboratory in the in the department of Natural Product Biotechnology. A specific strain of *Papaver somniferum* not capable of producing alkaloids in culture. The suspended cells were grown in 1-liter Erlenmeyer flaks at 23 °C on rotating shaker (100 rpm). Sub culturing was done every 7th day. Tissue was harvested by suction filtration, shock-frozen in liquid nitrogen and stored at -80°C

II.1.1.2 Bacteria

<i>Escherichia coli</i> DH5 α	<i>deoR endA1 gyrA96 hsdR17(r_km_k⁺) recA1 relA1 supE44 thi1</i> $\Delta(lacZYAargF) \phi 80lacZ\Delta M15F$ (Clontech)
<i>Escherichia coli</i> BL21 (DE3)	<i>FompT hsdSB (r_Bm_B) gal dcm</i> (DE3) (Novagen)
<i>Escherichia coli</i> XL1 Blue	Chemically competent cells were prepared according to the protocol described by Sambrook et al., 1988 (Stratagene)
<i>Escherichia coli</i> . XL10 Gold	Chemically ultracompetent cells. (Stratagene)
<i>Escherichia coli</i> TOP10	Chemically ultracompetent cells. (Invitrogen)

II.1.1.3 Yeast

<i>Saccharomyces cerevisiae</i> cdc25H(α)	(Stratagene) MAT α ura352 his3 200 ade2 101 lys2801 trp1901 leu2 3 112 cdc25 2 Gal ⁺
<i>Saccharomyces cerevisiae</i> cdc25H(<i>a</i>)	(Stratagene) MAT a ura352 his3 200 ade2 101 lys2 801 trp1 901 leu2 3 112 cdc25 2 Gal ⁺

II.1.2 DNA

II.1.2.1 Vectors and control plasmids

pSos vector	Supercoiled (Stratagene)
pMyr Xp vector	Digested with EcoRI-XhoI and treated with (CIAP) (Stratagene)
pSos MAFB	Positive control plasmid (Stratagene)
pMyr MAFB	Positive control plasmid (Stratagene)
pSos Col	Negative control plasmid (Stratagene)
pMyr Lamin C	Negative control plasmid (Stratagene)
pMyr SB	Positive control plasmid (Stratagene)
neapUC18	Control plasmid. (Stratagene)
PbluescriptSK-2	Cloning vector (Stratagene)
pCR®T7/NT TOPO®	Expression vector (Invitrogen)
pGEM®-T Easy	Cloning vector (Promega)
pCR2.1	Cloning vector (Invitrogen)
pQE30	Expression vector Qiagen

II.1.2.2 Primers

Primer	Sequence	Annealing temp (° C)
SalAT2	5'-CTTTGGATCCATGGCAACATGTATAGTGCT-3'	57.2
SalAT2R	5'-ATTAGCGGCCGCTCAAATCAATTCAAGGATTTAC-3'	67.5
Myr 5`primer	5'-ACTACTAGCAGCTGTAATAC-3'	55.3
Myr 3`primer	5'-CGTGAATGTAAGCGTGACAT-3'	53.9
Sos 5`primer	5'-CCAAGACCAGGTACCATG-3'	55.7
Sos 3`primer	5'-GCCAGGGTTTTCCAGT-3'	52.6
Oligo dT20VN	5'-TTTTTTTTTTTTTTTTTTTTTTVN-3'	55.1
6OMT 1f	5'-CAGCTAAAGTGTCTAAACAGAG-3'	56.5
6OMT 2f	5'-CTA CCA CGC AGA AAT ACT CAT TAG-3'	59.5
6OMT 3f	5'-CAG TGA TGG AAT CAG TAC AC-3'	55.2
6OMT 4f	5'-AAGGTGGCAAAGTTATTATCGTG-3'	57.1
pMyr-16B1- EcoRI	5'-CAGAATTCATGCCTGAAACATGTCC-3'	54.6
pMyr-16B1-XhoI	5'-CACTCGAGATAACTCAAATGCAGATAGTTCTG-3'	63.7
6OMT-GSP-(as)	5'-GCGCGCTACGTATTAATAAGGGTAAGCCTCAATTAC-3'	56.5
6OMT-GSP-(s)	5'-GCGCGCTACGTAATGGAAACATAAGCAAGATTGAT-3'	55.8
CNMT- GSP(Start)	5'-ATGCAGCTAAAGGCAAAGGAA-3'	56.7
CNMT-GSP(Stop)	5'-TCATTTTTTCTTGAAGAGAAGATG-3'	55.5
pSos-CNMT-NcoI	5'-ATCCATGGATGCAGCTAAAGGCAAAGGAA-3'	65.3
pSosCNMT-NotI	5'-ATATGCGGCCGCTCATTTTTTCTTGAAGAG-3'	65.4
pMyr-6OMT- EcoRI	5'-CAGAATTCATGGAAACAGTAAGCAGATTGATCAAC-3'	66.0
pMyr-6OMT- XhoI	5'-CACTCGAGTTAATAAGGGTAAGCCTCAATTAC-3'	65.5

II.1.3 Chemicals

All analytical-grade chemicals were purchased from Biomol (Heidelberg-Germany), Fluka (Seelze- Germany), Merck (Darmstadt-Germany, Pharmacia-(Phizer-USA), Roche (Basel-Switzerland), Roth (Karlsruhe-Germany), Serva (Heidelberg-Germany), and Sigma Aldrich (Seelze-Germany).

II.1.4 Molecular kits and enzymes

The regular suppliers of molecular biological kits and enzymes were Stratagene, Bio-Rad, Clontech, Invitrogen, Life Technologies, New England BioLabs, Promega, and QIAGEN.

II.1.5 Equipment

PCR:

PCR system 9700, PE Applied Biosystems

Thermal Cycler GeneAmp PCR 9700 (PE Applied Biosystems, CA, USA).

PTC 200, peltier Thermal Cycler, Gradient cycler

Electrophoresis:

Horizontal gel electrophoresis apparatus (Biometra, Göttingen, Germany)

Gel Doc Gene Genius, Bio Imaging system, (Bio-Rad, CA, USA)

Digital Graphic printer UP-D895 (Bio-Rad, CA, USA)

Nucleotide sequencing:

DNA Sequencer 3100 Avant Genetic Analyzer, (Applied Biosystems, CA, USA)

Radioactivity detection:

TLC scanner model Rita Star (Raytest, Straubenhardt, Germany)

Liquid scintillation counter model LS6000TA (Beckman, CA, USA)

Phosphorimager Storm 860 (Molecular Dynamics, Amersham Pharmacia

Biotech, Uppsala, Sweden)

Chromatographic separation:

HPLC system series 1100 (Hewlett Packard, Waldbronn, Germany)

LC-MS (SepServa, Berlin, Germany)

HPLC-electrospray (ESI) Selected Reaction Monitoring (SRM)

Centrifugation:

Centrifuge Sorvall RC 26 Plus (DuPont, USA)

Centrifuge Sorvall RC 28S (DuPont, USA)

Centrifuge model 4K 10 (Sigma, Osterode, Germany)

Centrifuge model 5415C (Eppendorf, Hamburg, Germany)

Miscellaneous:

Cross-linker UV Stratalinker (Stratagene, CA, USA)

pH-Meter model pH526 (WTW, Weilheim, Germany)

Precise Balance model A200S (Sartorius, Göttingen, Germany)

Sterile bench laminar flow work station (MDH, Andover Hants, UK)

Vacuum concentrator (Bechofer, Reutigen, Germany)

Themomixer 5436 (Eppendorf Hamburg, Germany)

MilliQ synthesis (Millipore, Germany)

SPD speed Vac, Thermo Savant (Germany)

Rota Vapor, R114 (Germany)

Ultrospec 3000, UV visible spectrophotometer (Pharmacia Biotech, Germany)

II.2 Methods

II.2.1 Subcloning

II.2.1.1 Polymerase chain reaction (PCR)

The standard PCR The reaction was subjected to 30 cycles of PCR, each incorporating 30 sec of denaturation at 94 °C, 30 sec of annealing at 55 °C and 1.5 min of polymerization at 72 °C. After 30 cycles, 10 min of polymerization at 72 °C was carried out before cooling to 4 °C. The PCR mixture consists of:

- Template DNA 100 ng
- 20 µM sense primer 1 µl
- 20 µM anti sense primer 1 µl
- 2.5 mM dNTP mix 1 µl
- 25 mM MgCl₂ 1 µl
- Taq DNA polymerase 1.5 U
- 10 x PCR buffer 2 µl
- Double-distilled water added to 20 µl

II.2.1.2 Gel electrophoresis

II.2.1.2.1 Agarose gel electrophoresis of DNA

The DNA samples were mixed with the corresponding volume of 6x loading buffer, and the samples were applied to the wells. The gel was run in 1% 1xTAE at 100 V until the separation was optimal. The separation of DNA was observed using Gel Doc Gene Genius, Bio Imaging system, (Bio-Rad, CA, USA).

II.2.1.2.2 Formaldehyde agarose (FA) gel electrophoresis of RNA

1-volume of 5 x loading buffer (QIAGEN) was added to 4-volumes of RNA sample. The mixture was incubated at 65 °C for 5 min before chilled in ice. The RNA

was resolved in 1.2% formaldehyde agarose (FA); running buffer was 1x FA. The RNA was visualized using Gel Doc Gene Genius, Bio Imaging system, (Bio-Rad, CA, USA).

II.2.1.2 Isolation of DNA fragments from agarose gels

The DNA fragment band was excised from the agarose gel. A QIAquick Gel Extraction kit (QIAGEN) was used to isolate the DNA fragment. The agarose gel was melted in a chaotropic salt buffer at 55 °C for 10 min. DNA was then bound to a membrane and eluted with low salt buffer according to the manufactures instructions

II.2.1.3 Ligation

The ligation reaction was as below. The mixture was incubated at 12°C overnight.

- Prepared vector 0.1 µg/µl
- Prepared insert 0.1 µg/µl
- T4 DNA ligase 0.5 µl
- 10 x T4 DNA ligase buffer 1 µl
- 10 mM rATP (PH7.0) 1 µ
- Double-distilled water added to 10 µl

II.2.1.4 DNA transformation using frozen competent cells

2-5 µl of ligation mixture were subsequently added to the competent cells, and incubated on ice for 30 min. The cells then heat shocked for 30 sec at 42 °C in a water path. At the end of heat shock 400 µl of recovery LB medium was added and the tube was further incubated for 30 min at 37 °C. Aliquots of cells were plated on selective LB agar plates containing appropriate antibiotic. The plates were incubated over night at 37 °C.

II.2.1.5 Isolation of plasmid DNA

The preparation of plasmid DNA was carried out by using a QIAprep miniprep kit (QIAGEN) according to the supplier's instructions. The protocol was designed for purification of up to 20 µg high-copy plasmid DNA from 1-5 ml overnight culture of *E. coli* in LB medium.

II.2.1.6 Identification of insert size (digestion)

Positive clones from transformed cells were characterized as to the size of the insert. The isolated plasmids were digested with restriction endonuclease for two hours at 37 °C. The digestion reaction consisted of:

- DNA 1-10 µg
- Restriction endonuclease 1 U/ µg DNA
- 10 x reaction buffer 2 µl
- Double-distilled water added to 20 µl

Reaction was analyzed using an agarose gel electrophoresis.

II.2.1.7 Sequencing analysis

Sequencing reactions were run after excess dye removal on the ABI Prism 3100 Avant Sequencer facility in Leibniz-Institute of Plant Biochemistry. Sequences were clustered, assembled and analyzed using the SeqManII Software. (DNASTAR Inc.). Sequencing reactions were as following

- Big Dye premix (for 1:1 diluted BigDye)
 - 2 µl BigDye terminator
 - 1 µl 5x dilution buffer
 - 1 µlH₂O
- 1µl primer (3.2-5 pmol)

- 1-5 μ l plasmid (600ng plasmids; 20 ng PCR product)
- 0-5 μ l H₂O.

Total volume for each reaction was 10 μ l

II.2.2 cDNA library construction

cDNA synthesis kit (Cyto Trap® XR Library construction) (Stratagene) provided all the reagents required to convert mRNA to cDNA inserts prior to unidirectional insertion into the pMyr XR vector.

II.2.2.1 Isolation of total RNA

Total RNA isolation was based on Sambrook et al. (1989). Plants were frozen in liquid nitrogen and ground to a fine powder. 5 g of powder were transferred to an SS34 tube containing extraction buffer and mixed well, 5 ml of TLE-saturated phenol were then added and the mixture homogenized with an Ultraturrax. 5 ml of chloroform were added and again homogenized with an Ultraturrax. The homogenate was incubated in a water bath at 50 °C for 20 min. Plant debris was removed by centrifugation (8000 x g, 15 min, and room temperature). The aqueous phase was transferred into a new SS34 tube and re-extracted with 10 ml chloroform. After centrifugation (8000 x g, 15 min, room temperature), the aqueous phase was transferred into a new SS34 tube. RNA was precipitated by adding 1/3 volume of 8 M LiCl. After incubation at 4 °C overnight, RNA was collected by centrifugation (8000 x g, 20 min, 4 °C). RNA pellets were washed with 5 ml of 2 M LiCl and dissolved in 600 μ l sterile water. The RNA was precipitated again by adding 200 μ l of 8 M LiCl, incubation at 4°C for 2 hours, and centrifugation (14000 x g, 15 min, 4 °C). The pellet was washed with 500 μ l of 2 M LiCl and dissolved in 200 μ l sterile water. The RNA was finally precipitated by adding 20 μ l of 3 M NaOAc pH 5.2 and 550 μ l of absolute ethanol cooled down to -80 °C for 1 hour, RNA was obtained by centrifugation (14000 x g, 15 min, and 4 °C). Total RNA was dissolved in 100-200 μ l of sterile water.

II.2.2.2 Isolation of poly (A)⁺ RNA

Poly (A)⁺ RNA (mRNA) was isolated from total RNA using an Oligotex[™] kit (QIAGEN). Poly (A)⁺ RNA was isolated according to the supplier's instructions. Both mRNA and total RNA were analyzed using Formaldehyde Agarose (FA) gel electrophoresis.

II.2.2.3 First-strand synthesis of cDNA.

First strand-synthesis was primed with the linker-primer and was reverse transcribed using StraScript reverse transcriptase (StraScript RT) (Stratagene). The standard reaction for First strand-synthesis was

- 5 µl of 10x first-strand buffer
- 3 µl of first –strand methyl nucleotide mixture
- 2 µl of linker-primer (1.4 µg/µl).
- X µl of DEPC-treated water
- 1 µl of RNase Block Ribonuclease Inhibitor (40 U/µl)
- X µl of (A)⁺ RNA pRNA (5µg).

The final volume of the First strand-synthesis reaction was 50 µl

II.2.2.4 Second-strand synthesis of cDNA.

The second-strand nucleotide mixture has been supplemented with dCTP to reduce the probability of 5-methyl-dCTP becoming incorporated in the second strand.

The standard reaction for second-strand synthesis was

- 20 µl of 10x second-strand buffer
- 6 µl of second –strand dNTP mixture
- 114 µl of sterile dH₂O

- 2 μ l of DNA [α -³²P] (800Ci/mmol).
- 2 μ l of RNase H (1.5 U/ μ l).
- 11 μ l of DNA polymerase I (9.0 U/ μ l)
- 23 μ l blunting dNTP mix
- 2 μ l of cloned *Pfu* DNA polymerase.

The final volume of the second strand-synthesis reaction was 180 μ l.

II.2.3 CytoTrap yeast two-hybrid system

II.2.3.1 Preparation of yeast host strain

A frozen glycerol stocks of the temperature-sensitive phenotype of *cdc25H* host strain were prepared to minimize the number of generations between retrieval from the freezer stock and final two-hybrid interaction assays.

II.2.3.2 Preparation of yeast competent cells

4-5 independent preparations were generated of yeast competent cells derived from independent colonies, due to the ability of the host strain to revert during growth. A number of strategies, specialized media, and reagents were carried out by using the supplier's instructions.

II.2.3.3 Library screening

II.2.3.3.1 Co-transformation.

Transformation mixture was incubated at room temperature for 30 min, and then was heat shocked for 20 min at 42 °C before chilling the reaction suspension in ice for 3 min. Transformed cells were collected by centrifuging (14,000 rpm, room temperature). At the end 500 μ l of recovery 1M sorbitol medium was added. Aliquots of cells were plated on selective agar plates containing SD/glucose based medium. The plates were incubated over night at room temperature.

The yeast transformation standard mixture was as the following

- Target Plasmid (cDNA construct) 100 ng.
- Bait Plasmid 100 ng.
- 1.4 M β -mercaptoethanol 2 μ l

II.2.3.3.2 Identification of “putative positive” interactors

The pMyr cDNA and Library bait construct co-transformants colonies were selected at permissive temperature, and then candidate interactors were identified by transferring the co-transformants to 37 °C. “Putative positive” were identified among the candidates by two rounds of testing for galactose-dependent growth at 37 °C. The putative positives were subjected to further analysis to verify the interaction. Verification strategy includes co-transformation of naive yeast host with purified plasmid DNA from the putative positive colony and the bait plasmid.

II.2.3.3.3 Isolating of library plasmid from yeast cells

5 ml of overnight yeast cultures in SD/glucose (-UL) medium were pelleted down and were resuspended in 1 ml of H₂O twice. Cells were resuspended in 1 ml of rescue buffer before pelleted once again and resuspended in 25 μ l of lysis solution. The tubes were vortexed and incubated for 1 hour at 37 °C. As the result of lysis, yeast coagulates into a white precipitate. 10% SDS were added and the cultures were gently mixed to completely disperse the precipitates. 100 μ l of 7.5 M ammonium acetate was added, and the samples were incubated for 15 min at -80 °C. After freezing, the cultures were collected for 15 min at 3000 g at 4 °C. 100-150 μ l of the resulting clear supernatants were transferred to a fresh tube where 100 μ l of isopropanol were added. The pellets were washed with (500 μ l) 70% cold ethanol, evaporated and resuspended in 20 μ l TE buffer.

II.2.4 Alkaloid analysis (HPLC & HPLC-MS)

Different plant parts were frozen in liquid nitrogen and ground to a fine powder. The Plant tissues were subjected to two extractions the first with 70% ethanol and the second was with ethyl acetate. After centrifugation (14,000 rpm, room temperature), 15 min evaporation using a speed vac concentrator the residue was resuspended in methanol for HPLC and LC-HPLC analysis.

II.2.5 Protein over-expression and purification

II.2.5.1 Bacteria as an expression system.

50 ml of *E. coli* culture containing appropriate antibiotic was prepared into 250-ml Erlenmeyer flasks then incubated at 37 °C overnight with orbital shaking (~ 250 rpm). Next day, culture was diluted in 1000-ml LB culture to (OD₆₀₀ 0.2) and allowed to grow until (OD₆₀₀ between 0.5-0.7). Induction was started by adding 0.5 M IPTG from the 20% stock to the 1000 ml culture to a final concentration of 0.2%. The cultures were then grown for an additional 12 hours at 28 °C. Bacterial cells were pelleted by centrifugation at 4 °C, for 20 minutes in large screw cup bottles. Pellets were resuspended in His-tag lysis buffer (HLB) for purification.

II.2.5.2 Protein purification

(Immobilized Metal Affinity Chromatography) IMAC

The principle of IMAC is based on the reversible interaction between immobilized metal ions and various protein side chains (Porath et al., 1975). TALON resins are cobalt-based IMAC resins developed to enhance polyhistidine tagged binding capacity and allow protein purification under native conditions. For Resin Preparation 1 ml of TALON[®] resin was washed twice with 10 ml of His-tag wash buffer (HWB). The resin was collected by centrifugation (700 x g, 2 min, and 4 °C). To 25 ml of the solution containing the polyhistidine-tagged protein was added 0.73 g of NaCl, 2.5 ml of glycerol, 50 µl of β-mercaptoethanol. The pH 7.0 was adjusted. The TALON[®] resin and protein solution were mixed and gently shaken at 4 °C for 30 min. After centrifugation (700 x g, 2min, 4 °C), the supernatant was discarded. The resin was washed with 15 ml of HWB.

Again the resin was collected by centrifugation (700 x g, 2 min, and 4 °C) and resuspended in 2 ml of HWB. The suspension was transferred to a gravity flow column (TALONspin™ column) and was allowed to settle before being washed with 3 ml of HWB. The bound protein was eluted from the resin with 3 ml of His-tag elution buffer (HEB). To remove NaCl and imidazole, 2.5 ml of protein-containing HEB were applied to a PD-10 desalting column (Amersham) that had been previously equilibrated in enzyme storage buffer. The purified protein was eluted by using 3 ml of enzyme storage buffer. The protein amount was determined using Bradford reagent SDS-PAGE was used to determine protein purity.

II.2.5.3 Protein concentration assay

100 µl of protein samples were mixed with 900 µl of Bradford reagent (Bradford, 1976) and left at room temperature for 30 min. The UV absorption at 595 nm was then measured, using water or His-tag elution buffer for the blank reaction.

II.2.5.4 SDS-PAGE electrophoresis

The resolving gel mixture was poured to the two glass plate sandwiches. This was immediately overlaid with water-saturated n-butanol to exclude oxygen from the surface. After polymerization, the n-butanol was drained off and the gel surface rinsed with distilled water. Similarly, the stacking gel overlaid on the resolving gel up to the brim of the glass plate sandwich. A 10 slot comb was inserted such that approximately ten 30 µl wells were left on the stacking gel. The monomer was then left to polymerize. The polymerized gel slab-glass plate's sandwich was removed from the casting stand and transferred to the buffer chamber, properly covered in buffer before the combs were carefully pulled out. Samples were then heated in a thermo mixer for 5 minutes to denature the proteins then micro centrifuged for 1 min at 12, 000 rpm. Desired amounts of the protein samples or pre-stained SDS-PAGE molecular weight standard markers were

loaded into each lane. The gel run at a constant current at 40mA per gel until the dye front reached the end of the gel. SDS-PAGE components were the following

Stock solutions	Stacking gel, solution 4% gel 0.125 M Tris, pH6.8	Separating gel, solution 0.375 M Tris, pH8.8			
		7%	10%	12%	15%
Double-distilled water	3.075 ml	5.1 ml	4.1 ml	3.4 ml	2.4 ml
0.37M Tris, pH8.8	-----	2.5 ml	2.5 ml	2.5 ml	2.5 ml
20% SDS (w/v)	25 µl	50 µl	50 µl	50 µl	50 µl
Acrylamid/Bis-acrylamid	670 µl	2.3 ml	3.3 ml	4 ml	5 ml
10% APS	25 µl	50 µl	50 µl	50 µl	50 µl
TEMED	5 µl	5 µl	5 µl	5 µl	5 µl
4% gel 0.125 M Tris, pH6.8	1.25 ml	-----	-----	-----	-----
Total monomer	5.05 ml	10.00 ml	10.00 ml	10.00 ml	10.00 ml

Table II.2.1 Components of SDS-PAGE gel solution

II.2.5.5 Gel Staining/Destaining

Coomasie brilliant blue staining solution was used to stain separation gels. Gels were stained for 2-3 hours and then destained in destaining solution till bands were clearly visible.

II.2.6 Macroarrays analysis.

II.2.6.1 cDNA preparation.

Using a vector-specific primer adjacent to the MCS, cDNAs were amplified for membrane spotting. PCR reactions were purified and re-concentrated by filtration through NucleoFast 96 PCR (Machery-Nagel).

II.2.6.2 Membrane spotting

cDNA were spotted in quadruplicate with a 384 pin replica (Biodyne membranes) (PALL Corporation) using the Microgrid II spotter (BioRobotics). Spotted cDNAs were chemically denatured, neutralized and finally treated with 5 x SSC buffer. The arrayed DNA was immobilized via UV cross-linking using a Stratalinker 1800 (Stratagene).

II.2.6.3 Random- prime cDNA labelling and northern hybridisation

Total RNA was used as a template for reverse transcription using oligodT primers. After purification using the Probe Quant G-50 Micro columns (Amersham Biosciences), cDNAs were labelled with [α 32 P]-dATP using the Megaprime DNA Labelling System (Amersham Biosciences). Membranes were Pre-hybridised for at least 4 hours at 65 °C. The over night hybridisation was performed at 65 °C by addition of labelled cDNAs to the pre-hybridisation solution. Next day, the membranes were washed three times for 15 min with 2x SSC, 0.1% SDS at 65 °C and exposed to Storage phospho screen for 2-3 days. The signals were developed with a STORM 860 Gel and Blot Imaging System (Amersham Biosciences).

II.2.6.4 Array analysis

AIDA Image Analyzer software (Raytest) was used for Array determination and Spot intensity evaluation. The features of Array module including the import of names tables, automatic positioning of measurement dots, background subtraction, and normalization allow us to evaluate arrays.

II.2.7 Enzymes activity assays

The standard enzyme assay reaction consists of:

- 2 μ l [3 H]-Salutaridinol, Spezifische Aktivität 7.2 mCi/mmol

- 2µl 10mM Salutaridinol (20 nmol)
- 6µl 10mM Acetylc-CoA (60nmol)
- 8µl 1M K₂PO₄ + 1M H₂PO₄, PH6.5
- 20µl Pure SalAT solution.
- 20µl MLP 146 solution.

Time	Control Reactions	SalAT Reactions	SalAT + MPL146 Reactions	↑MLP Reactions
0min	T0	T0S	T0SM	5µl
5min	T5	T5S	T5SM	10µl
10min	T10	T10S	T10SM	20µl
20min	T20	T20S	T20SM	40µl
40min	T40	T40S	T40SM	80µl
60min	T60	T60S	T60SM	160µl

Table II.2.2 The enzymatic assay reactions [T: time (min), S: SalAT, M: MLP 146, “0” min: reactions were incubated in ice].

The reaction assay was modified form (Lenz & Zenk, 1995a). The mixture was incubated at 47 °C for 0, 5, 10, 20, 40, and 60 min. The reaction was terminated by adding 10 µl of ethylacetate. Enzymatic products were extracted twice using 100 µl ethylacetate before evaporating the ethylacetate phase and finally resuspend the product in 50µl Methanol.

II.2.7.1 Enzymatic products analysis

The enzymatic product was detected with The HPLC-electrospray (ESI) Selected Reaction Monitoring (SRM) data were obtained from a Finnigan MAT TSQ Quantum Ultra AM system equipped with a hot ESI source (HESI, electrospray voltage 3.0 kV, sheath gas: nitrogen; vaporizer temperature: 50 ° C; capillary temperature: 250 ° C; collision gas: argon; collision pressure: 1.5 mTorr). The MS system is coupled with a

Surveyor Plus micro-HPLC (Thermo Electron) and equipped with an Ultrasep ES RP18E-column (5 μm , 1x100 mm, SepServ).). For the HPLC a gradient system was used starting from $\text{H}_2\text{O}:\text{CH}_3\text{CN}$ 85:15 (each contains 0.2% HOAc) to 10:90 within 15 min followed by a 15 min isocratic period and a flow rate of 50 $\mu\text{l min}^{-1}$. The used software was Xcalibur™ (version 1.4). For the selected reaction monitoring (SRM) measurements the MS1 (Q1) is selected for a precursor mass, the MS2 (Q3) for a prominent key ion to monitor a specific CID (“collision induced dissociation”) reaction of the corresponding compound. Thebaine ($[\text{M}+\text{H}]^+$ at m/z 312), salutaridinol acetate ($[\text{M}+\text{H}]^+$ at m/z 372), and salutaridinol ($[\text{M}+\text{H}]^+$ at m/z 330) were detected during the HPLC run by performing the following SRM measurements with the collision energies (CE) listed below:

Compound	RT (min)	CE (eV)	Selected Reaction Monitoring (SRM)
Thebaine	13.00	-18	m/z 312 ($[\text{M}+\text{H}]^+$) \rightarrow m/z 58 (base peak ion)
		-18	m/z 312 ($[\text{M}+\text{H}]^+$) \rightarrow m/z 249
		-18	m/z 312 ($[\text{M}+\text{H}]^+$) \rightarrow m/z 266
Salutaridinolacetate	6.30	-30	m/z 372 ($[\text{M}+\text{H}]^+$) \rightarrow m/z 221 (base peak ion)
Salutaridinol	4.90	-30	m/z 330 ($[\text{M}+\text{H}]^+$) \rightarrow m/z 181 (base peak ion)

Table II.2.3 collision energies (CE): SRM measurements with the collision energies (CE) of thebaine ($[\text{M}+\text{H}]^+$ at m/z 312), salutaridinol acetate ($[\text{M}+\text{H}]^+$ at m/z 372), and salutaridinol ($[\text{M}+\text{H}]^+$ at m/z 330) were detected during the HPLC run by performing SRM measurements with several collision energies

The measured peak areas of the transition m/z 312 \rightarrow m/z 58 were used for an estimation of the thebaine content in the enzyme assays.

III Results

III.1 Bait plasmid construction

III.1.1 Cloning of salutaridinol 7-*O*-acetyltransferase (SalAT) from *P. somniferum*.

DNA encoding the Bait Protein salutaridinol 7-*O*-acetyltransferase (SalAT) was prepared and inserted into the pSos vector (Stratagene) MCS, generating a fusion protein of the yeast homologue of the human Sos (hSos) and SalAT protein (Figure III.1a) by standard PCR amplification. Yeast homologue for hSos remains essential for activation of the Ras pathway, and, ultimately, the survival and growth of yeast cells. (II.2.1.1). The two oligodeoxynucleotide gene specific primers are as follows

SalAT2F (sense primer) 5`-CTTTGGATCCATGGCAACATGTATAGTGCT-3`

NcoI

SalAT2R (anti-sense primer) 5`-ATTAGCGGCCGCTCAAATCAATTCAAGGATTTTCAC3`

NotI

DNA encoding the protein of interest (SalAT) was cloned so that the bait protein is expressed in same reading frame as the hSos protein (Figure III.1a). A band of the expected size (~1400 bp) was exhibited on agarose gel electrophoresis (Figure III.1b) after performing an enzyme-restriction analysis with NotI and NcoI restriction enzymes, which cleave at the beginning and the end of the Bait clone insert respectively. The bait hybrid of SalAT-Sos fusion was expressed in the *cdc25H* yeast strain (Figure III.2)

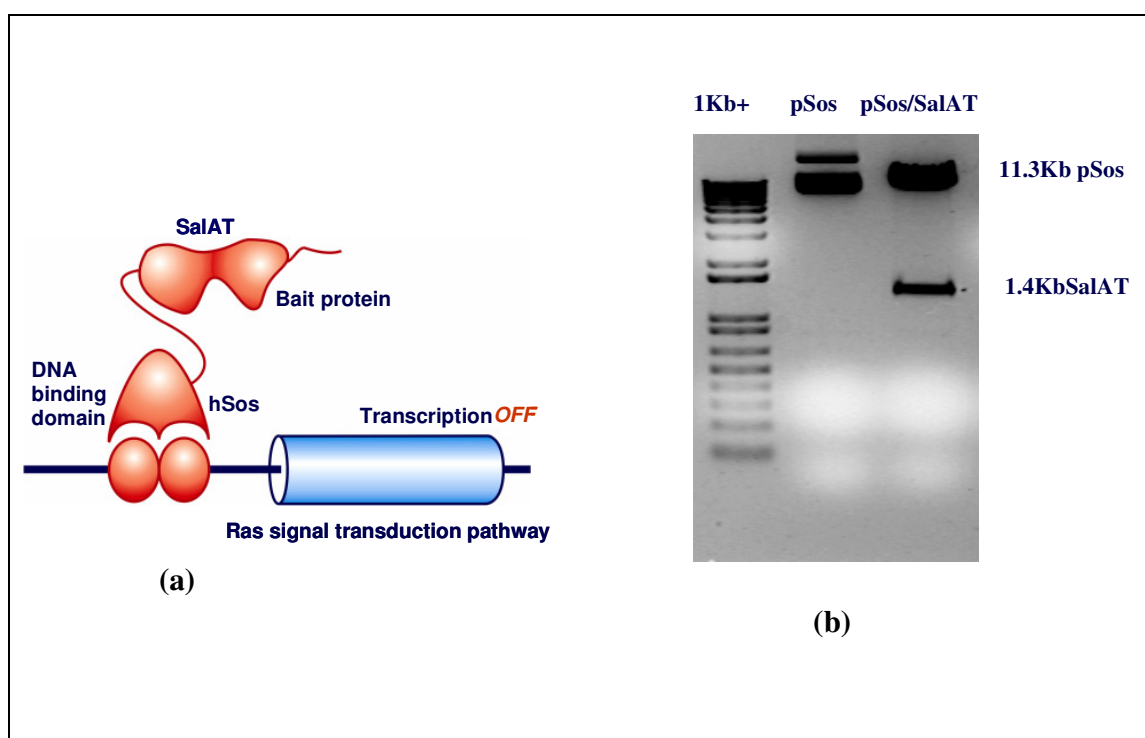


Figure III.1 SalAT insert cloning into pSos vector (Bait): A salutaridinol 7-*O*-acetyltransferase “Bait”, fusion was generated so that the bait protein is expressed in same reading frame as the hSos protein (a). A (~1400 bp) band was put on display on agarose gel electrophoresis after performing an enzyme-restriction analysis using NotI /NcoI restriction endonucleases for the bait construct (b).

III.1.2 Verifying expression and interaction specificity of bait protein for target proteins

The nucleotide sequence of cloning junctions and DNA insert were determined by sequence analysis to verify that the bait protein will be expressed in frame with the Sos domain. Expression of the bait protein was verified by co transformation of pMyr SB plasmid (positive control) (Stratagene) and pSos bait plasmid followed by patching on galactose-containing medium and assaying for growth at 37 °C (Figure III.2C). Yeast transformants with pSos/SalAT + pMyr/SB clones show positive growth on SD/galactose (-UL) at 37 °C, in the meantime, it shows negative growth on glucose based media at the same temperature which means that bait and target protein interact in

respect to the temperature-sensitive mutation at the *cdc25* gene of the yeast strain. Protein interactions (A) and (B) are represent positive and negative controls respectively.

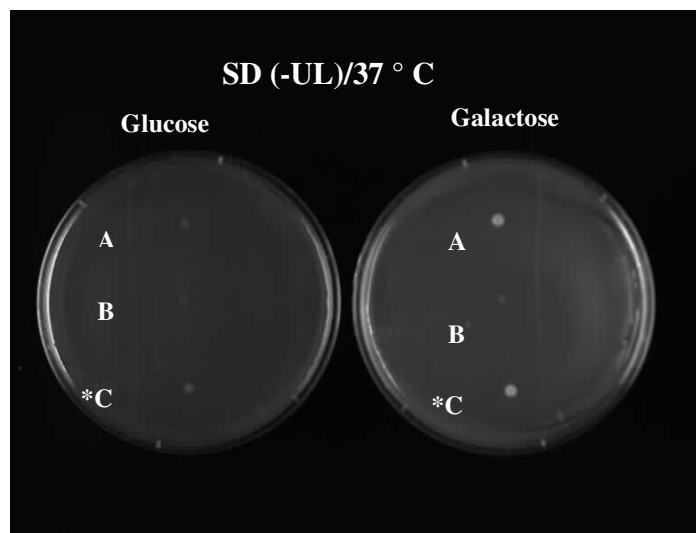


Figure III.2 Verifying bait expression: * the combination of “no growth” on glucose and “growth” on galactose at 37 ° C is a confirmation of the protein-protein interaction (C). pSos/MAFB + pMyr/SB serve as a positive control (A). pSos/MAFB + pMyr/Lamin C serves as a negative control (B)

III.2 pMyr target vector construction

III.2.1 cDNA synthesis from *P. somniferum*.

An accurate quantitation of the synthesized cDNA sample was obtained by UV visualization on ethidium bromide agarose plate (Figure III.3). Seven DNA standard samples of known concentration to cover the range from 200 to 10 ng/ μ l were prepared for the use as comparative standards in this assay. Spotted cDNA was estimated to be 50-60 ng/ μ l when it was compared to the known concentrations of the standards.

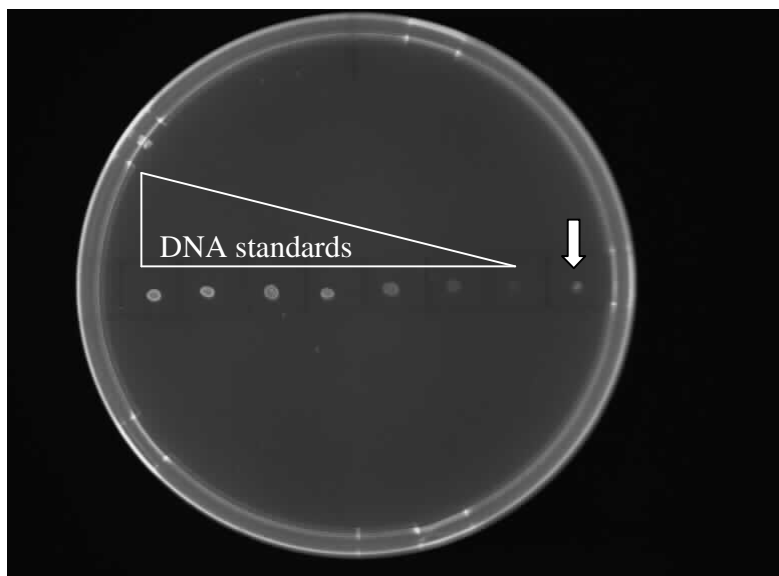


Figure III.3 Quantitation of cDNA: Ethidium bromide plate assay for quantitation of cDNA from *P. somniferum*. DNA standard (200, 150, 100, 75, 50, 25, and 10 ng/ μ l) were prepared in 100 mM EDTA. cDNA spot (under arrow) exhibit a concentration of 50-60 ng/ μ l on the Ethidium bromide plate.

III.2.2 Cloning of cDNA library from *P. somniferum* into pMyr target vector

For the target clone to be expressed in yeast, DNA encoding an expression cDNA library (~250,000 *cfu*) from the stems of *P. somniferum* was unidirectional inserted into pMyr XR vector MCS and expressed as a fusion protein with a myristylation sequence that anchor the fusion protein to the plasma membrane of the *cdc25H* yeast strain (Figure III.4a).

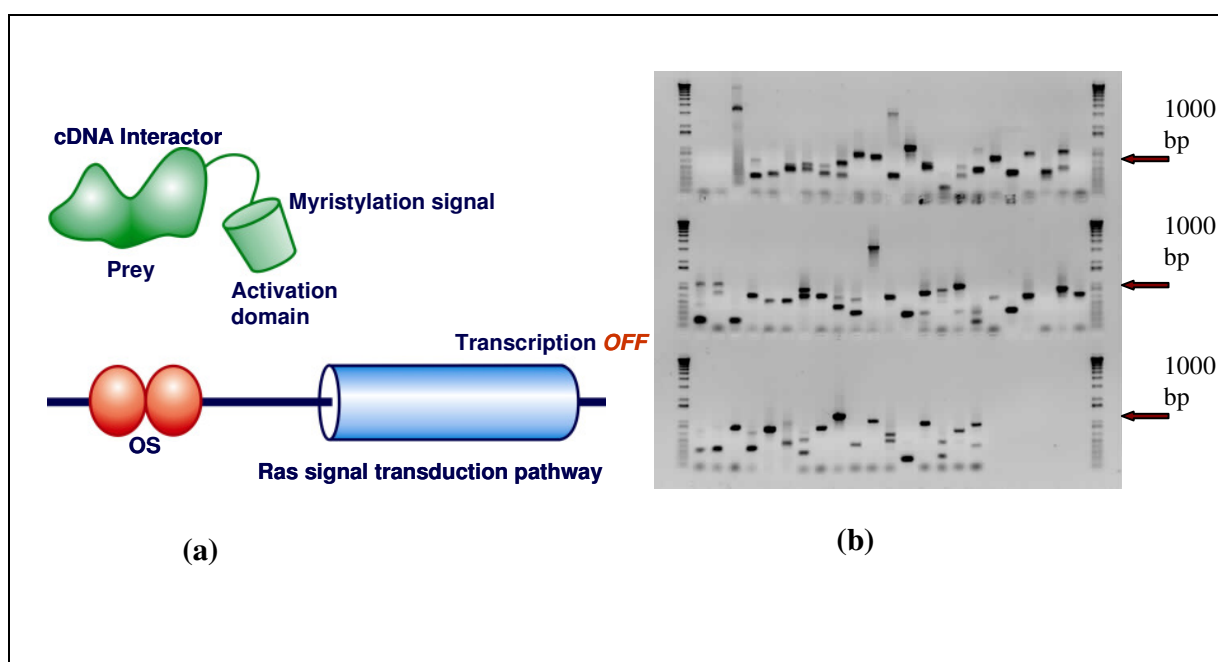


Figure III.4 pMyr target vector construction: DNA encoding the target protein was inserted into the pMyr vector so that the target protein is expressed in the same reading frame as the Myr coding sequences (a). Direct colony PCR amplification with Myr-specific primers was performed to verify the insert percentage and size (b)

III.2.3 Verifying the insert percentage and size

Determination of cDNA inserts, percentage and size were performed after amplification cDNA library once using the semi-solid amplification method to produce a large and stable quality of library followed by colony PCR (Figure III.4b) amplification with Myr-specific Primers. The percentage of vectors with insert was more than 97% which indicates the efficiency of insert cloning in the pMyr target vector (Figure III.5b). The vast majority of insert clones size was between 500 and 1500 bp which are recommended by supplier of molecular biological kit (Stratagene), very few of them were less than 500 bp and the rest is more than 1500 bp (Figure III.5b). The PCR primer for colony PCR was a 20-base oligonucleotide each with the following sequence

Myr 5` Sense primer 5` -ACTACTAGCAGCTGTAATAC-3`
 Myr 3` (anti-sense primer) 5` -CGTGAATGTAAGCGTGACAT-3`

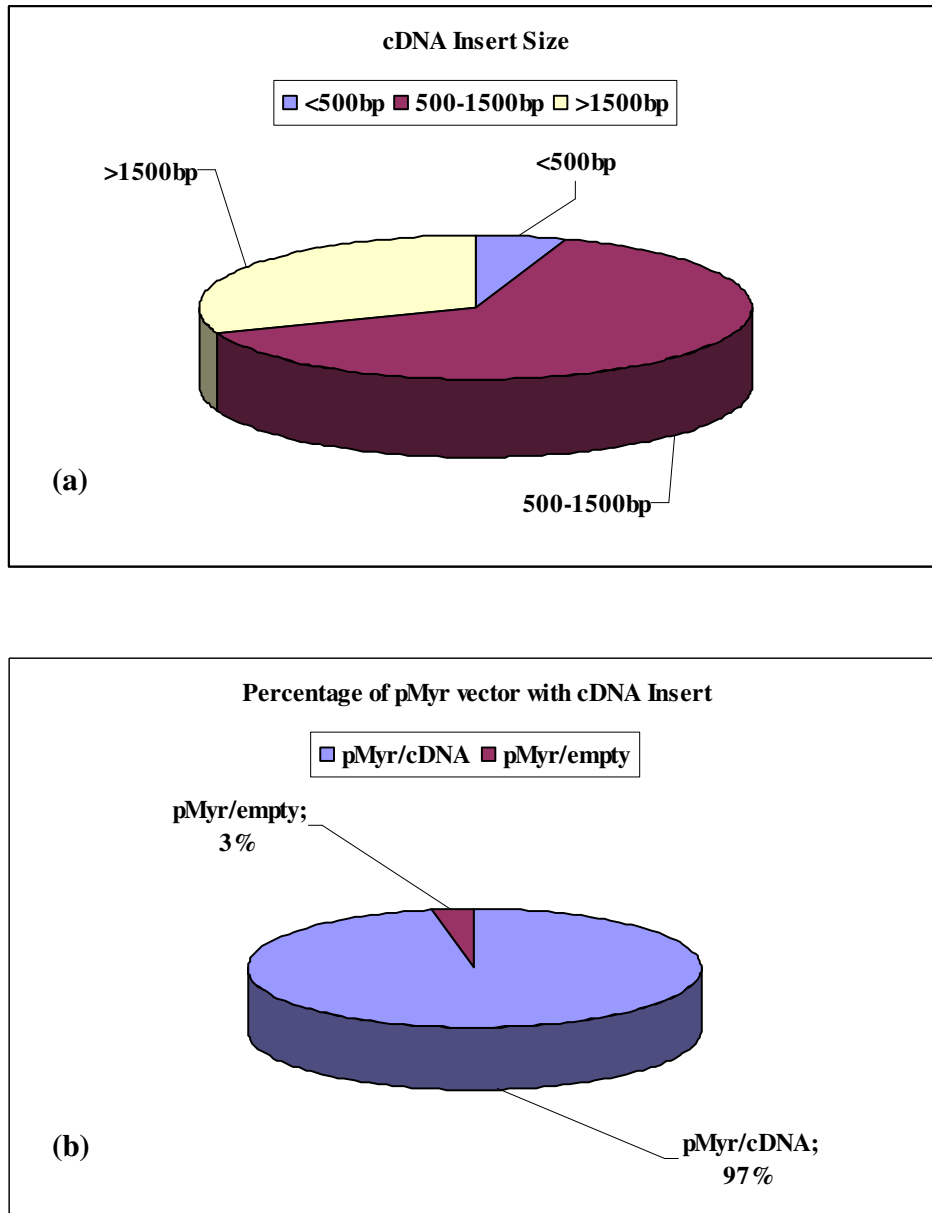


Figure III.5 cDNA insert, percentage and size: Individual colonies were used to determine the percentage of vectors with inserts and average insert size by PCR directly from colonies with pMyr-specific primers.

III.3 Yeast transformation

III.3.1 Preparation of *cdc25H* yeast competent cells

The temperature-sensitive phenotype of *cdc25H* host yeast strain (II.2.3.1) was prepared from both mating types (α and α) (II.1.1.3) for bait and target clones co transformation and subsequently to screen for possible interactions. All necessary precautions and recommendations by the supplier's instructions were strictly applied and carried out when yeast competent cells assayed to grow on YPAD agar plates at 37 °C to reduce the number of revertant colonies (less than 30 colonies for each preparation) due to the ability of the *cdc25H* strain to produce revertants of the temperature-sensitive phenotype during growth. A small number (3-5) of revertant colonies appear on each plate (Figure III.6) which is not supposed to affect the reliability of library screening and identification of "putative positive" interactions.

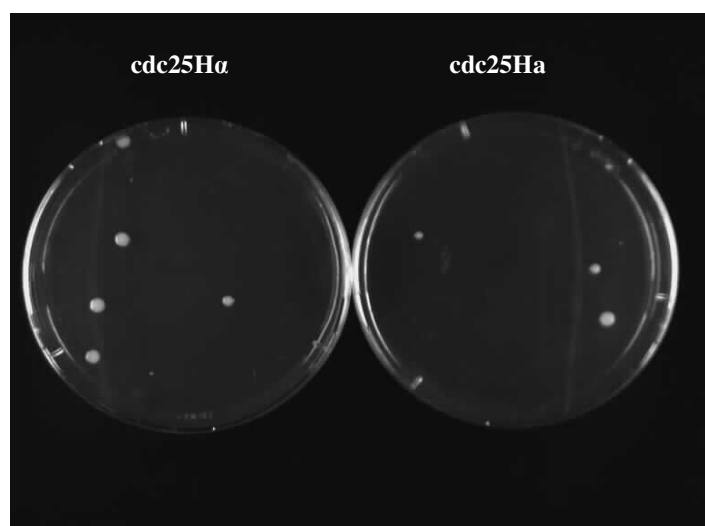


Figure III.6 *cdc25H* yeast host strain: Approximately 1×10^6 cells of each plate were plated on YPAD agar plates, incubated at 37 °C, and observed daily for 4-6 days, checking for temperature-sensitive revertants. If up to the sixth day of incubation, more than 30 colonies appear on plate, the yeast competent cells preparation will be unreliable for further work.

III.3.2 Transformation of control plasmids

Control plasmids (Stratagene) were introduced into the host *cdc25H* yeast by co-transformation (II.2.3.3.1).

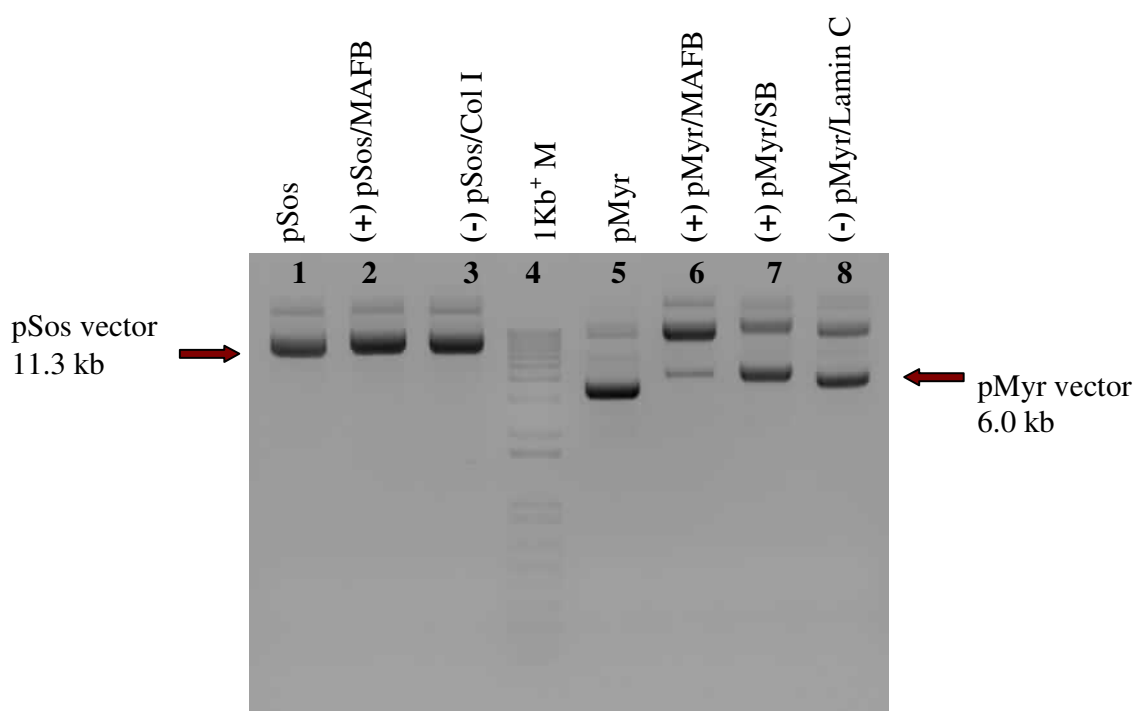


Figure III.7 Control plasmids: The cytoTrap system includes two negative control plasmids (lane 3, and 8) and three positive (Lane 2, 6, and 7). The pSos/Collagenase I (pSos Col I) (lane 3) control plasmid expresses the Sos protein and amino acids 148–357 of murine 72-kDa type IV collagenase. The pMyr/Lamin C (lane 8) control plasmid expresses the myristylation signal fused to human lamin C (aa 67–230). pSos/MAFB (lane 2) expresses the Sos protein and full-length MAFB as a hybrid protein. The pMyr/MAFB (lane 6) control plasmid expresses a hybrid protein that contains the myristylation signal fused to full-length MAFB. The pMyr/SB (lane 7) control plasmid expresses the myristylation signal fused to a Sos-binding protein. pSos represents the bait hybrid (lane 1). pMyr represents the target hybrid (lane 5).

Positive and negative controls (Figure III.7) was carried out in parallel with each bait and target plasmid transformation as indicator of growth levels in the presence and absence of interacting protein. These transformations (Table III.1) confirm the integrity of pSos vector and the ability of the bait protein (pSos/SalAT) to interact with target protein in order to rescue yeast growth at 37 °C when plated on galactose based medium.

Table III.1 Control plasmids transformation: Both fusion proteins were co-expressed in the cdc25H yeast strain, and the yeast cells were incubated at the restrictive temperature of 37 °C. Only the co-transformations were spotted and grown at 37 °C. (+): Full growth (-): no growth NA: not assayed to grow at the temperature of 37 °C.

No	Plasmid Transformed	SD/Glu,Gala(25 °C)	SD/Glu /Gala(37 °C) after spotting	
			Glucose	Galactose
1	pSos + pMyr	+	N.A.	N.A.
2	pSos/MAFB	+	N.A.	N.A.
3	pMyr/SB	+	N.A.	N.A.
4	pMyr/Lamin C	+	N.A.	N.A.
5	pSos/MAFB + pMyr/MAFB	+	-	-
6	pSos/MAFB + pMyr/Lamin C	+	-	-
7	pSos/Col I+ pMyr/MAFB	+	-	-
8	pSos/MAFB+ pMyr/SB	+	-	+
9	pSos/SalAT	+	N.A.	N.A.
10	pSos/SalAT+ pMyr/Lamin C	+	-	-
11	pSos/SalAT+ pMyr/SB	+	-	+

III.3.3 Library screening & identification of “putative positive” interactions

Protein expression was controlled by the GAL1 promoter which is induced in the presence of galactose but repressed in the presence of glucose. The bait and a number of target proteins were physically interacted (Figure III.8D), consequently, the hSos protein was recruited to the membrane, thereby activating the Ras-signaling pathway and allowing the *cdc25H* yeast strain to grow at 37°C. To screen for the putative positive interactions, fusion proteins (pSos/SalAT + pMyr/cDNA target proteins from *P. somniferum*) were selected at permissive temperature (25°C) for glucose dependent growth (Figure III.8A); afterward candidate interactors “putative positive” were identified among the candidates by two rounds of testing for galactose dependent growth at 37 °C (Figure III.8B1, B2).

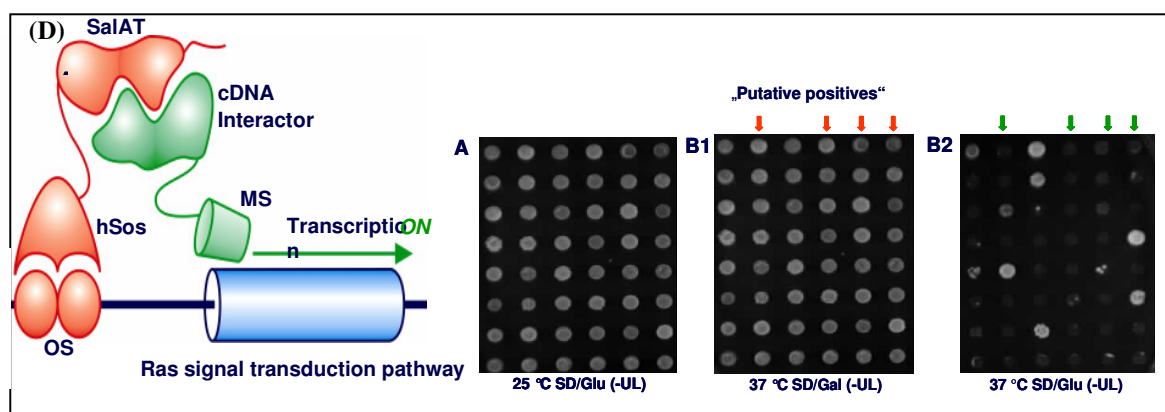


Figure III.8 SalAT interactor candidate: Initially the pMyr cDNA library and pSos co-transformant colonies were selected at permissive temperature at 25°C (A). „Interactor candidates “were identified by transferring the candidates by two rounds of testing for galactose dependent growth at 37°C (B1, B2).

Positive yeast host colonies that passed the primary and secondary specificity test were grown in liquid cultures in SD/glucose (-U), which selects only for the presence of the library plasmid. Plasmid DNA was isolated and digested with EcoRI and XhoI restriction enzymes, which cleave at the beginning and the end of the cDNA insert respectively. In this way approximately 400 putative positive clones have been isolated. The estimated

sizes SalAT interactors were mostly variable (Figure III.8C) which indicated the presence of multiple interacting proteins

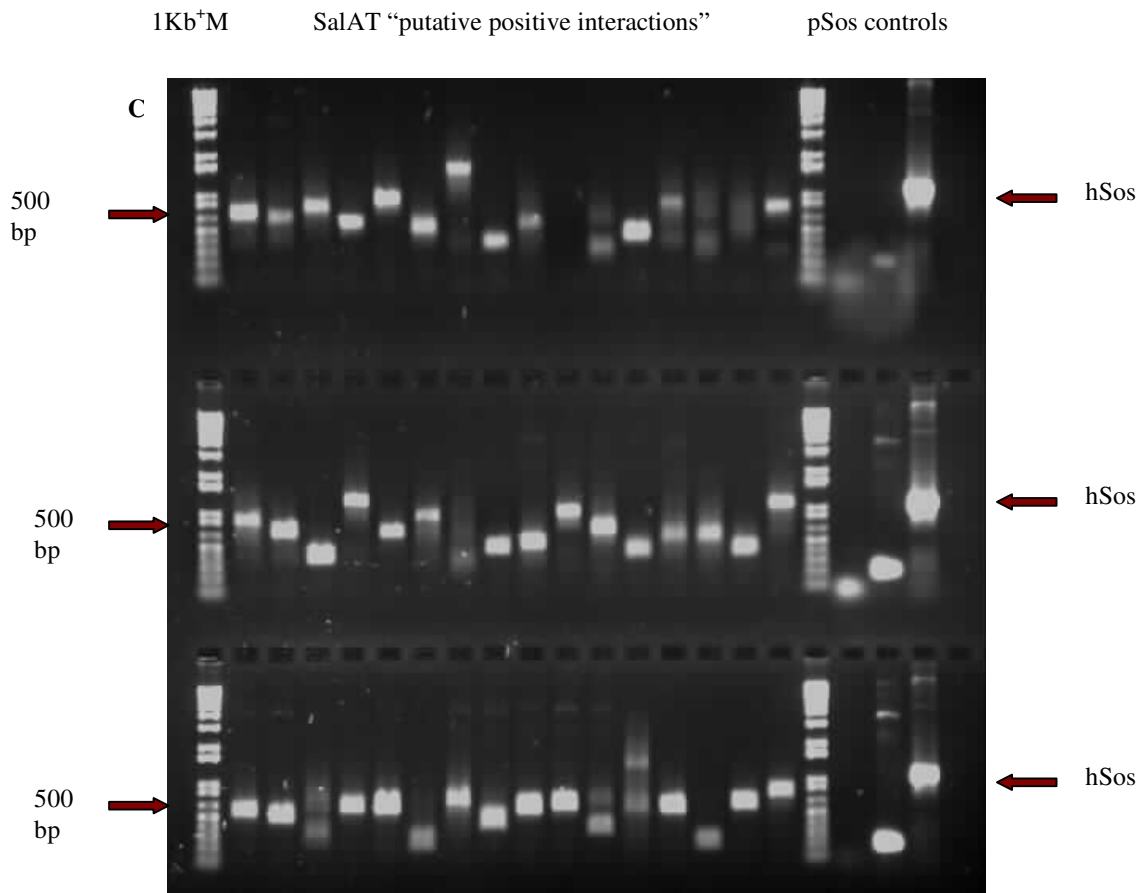


Figure III.8C SalAT interactor candidate: Agarose gel electrophoresis shows "Putative positives" of different sizes after they were subjected to yeast plasmid DNA purification and PCR analysis.

III.4 Interactions of SalAT through morphine biosynthesis pathway

III.4.1 Cloning of salutaridine reductase (SalR) and norclaurine 6-O-methyltransferase (6OMT) from *P. somniferum* into pMyr target vector.

In order to confirm the physical association of adjacent proteins or enzymes in the morphinan biosynthesis and consequently to demonstrate the ability of SalAT to interact with a possible consecutive thebaine synthase, DNA encoding the neighboring Salutaridine reductase (SalR) and the distant Norclaurine 6-O- methyl transferase (6OMT) as a negative control were generated by standard PCR reaction (Figure III.9A, B). Subsequently, SalR and 6OMT were cut using EcoRI and XhoI restriction enzymes before unidirectional inserted into pMyr XR vector MCS as target proteins.

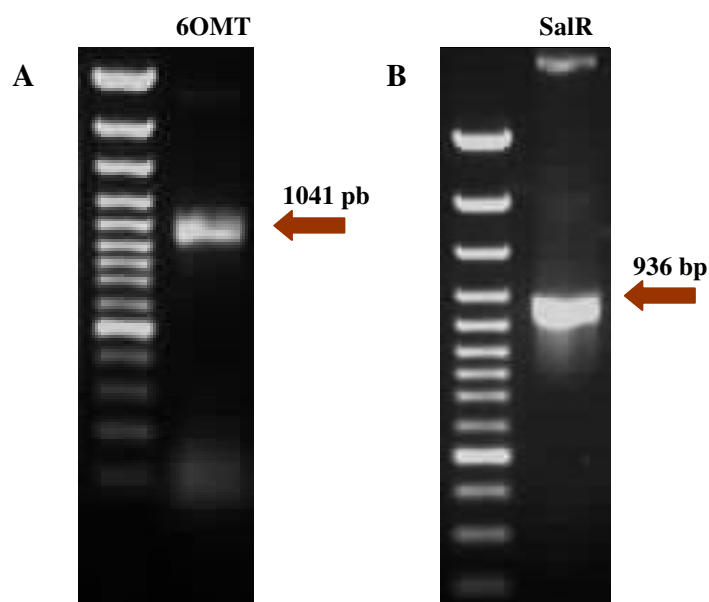


Figure III.9 pMyr XR/target clone construction: Agarose gel electrophoresis analysis of (6OMT) (A) and SalR (B) PCR amplification using gene specific primers.

Two bands of the expected size were displayed on agarose gels electrophoresis (A) and (B) (Figure IV.24). Salutaridine reductase (SalR) gene specific primers were with the following sequence



pMyr-16B1-XhoI 5`-CACTCGAGATAACTCAAAATGCAGATAGTTCTG-3`
XhoI

Norclaurine 6-*O*- methyl transferase (6OMT) gene specific primers were with the following sequence

pMyr-6OMT-EcoRI 5`-CAGAAATTCATGGAAACAGTAAGCAAGATTGATCAAC-3`
EcoRI

pMyr-6OMT-XhoI 5`-CACTCGAGTTAATAAGGGTAAGCCTCAATTAC-3`
XhoI

III.4.2 Yeast Transformation and Detection of Protein-protein interaction

Both target clones (pMyr XR/SalR and (pMyr XR/6OMT) were independently introduced into *cdc25Hα* yeast competent cells by co-transformation (II.2.3.3.1) with bait plasmid construction pSos/SalAT. Each transformation mixture were plated on 100-mm SD/glucose (-UL) plates and incubated at room temperature (25 °C) (Figure III.10).

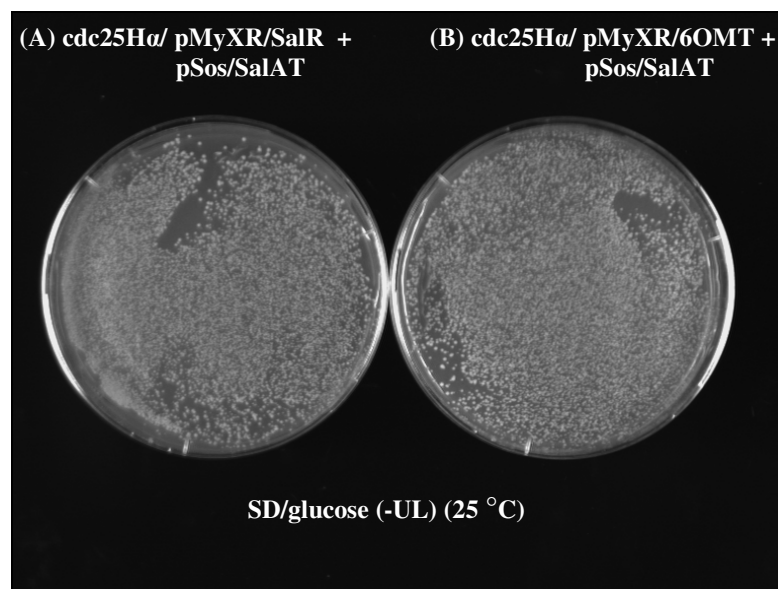


Figure III. 24 Yeast transformation: *cdc25Hα* competent yeast cells harboring the bait clone and target clones pMyr XR/SalR+pSos/SalAT (A) and pMyr XR/6OMT+pSos/SalAT (B) were plated on SD/glucose (-UL) plates and incubated at (24 °C) for 48 hours.

Following a series of replica plating for co-transformants clones on galactose based media at 37 °C for “interactor candidate” and on glucose dependent media for GAL1 promoter repression. “Interactor candidates” were subjected to two serial interaction tests (Primary and secondary) on galactose dependent plates at 37 °C to verify the interaction for 48 hours each. Colonies which were capable to grow at 37 °C on SD/galactose (-UL) plates, but not on SD/glucose (-UL) plates were re-patched from the re-patching source plate (SD/glucose (-UL)) for the secondary test to confirm the ability of these proteins to interact. Accordingly, it was clear that SalAT and SalR do have the ability to interact however; SalAT and 6OMT do not (Figure III.11).

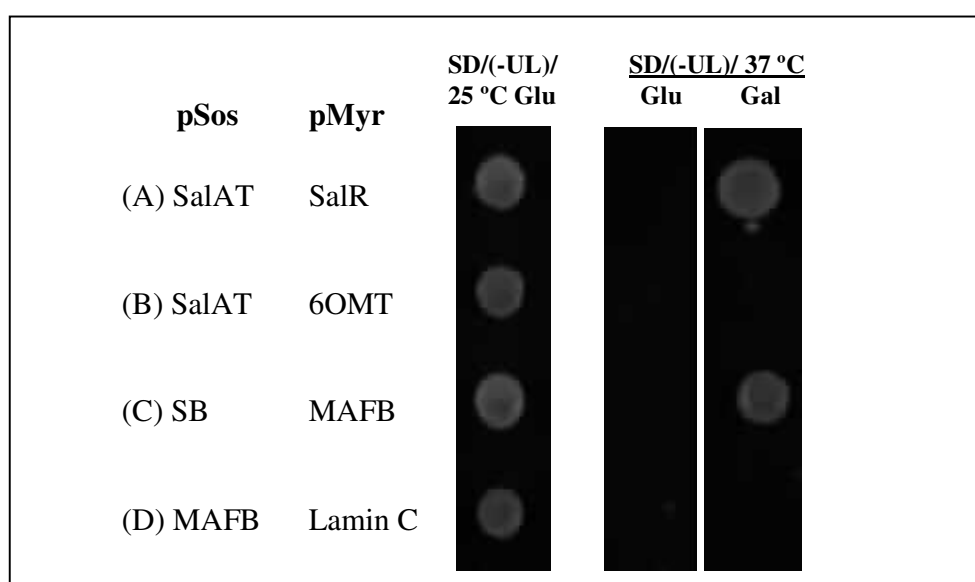


Figure III.11 Detection of protein-protein interaction by Cyto Trap system: Cyto Trap system figures demonstrate a combination of growth on galactose dependent media at 37 °C and no growth on glucose dependent media at 37 °C as a result of the physical interaction of SalAT and SalR proteins (A), meanwhile there was no growth at 37 °C for colonies harboring SalAT and 6OMT clones which means that the two proteins failed to interact (B). SB and MAFB represent positive control (C), MAFB and Lamin C represents negative control (D).

III.5 Analysis of SalAT protein interactors from *Papaver somniferum*.

Unexpectedly, a large number of positive colonies (400) were obtained after the second interaction conformation test. Following the daily observation of some colonies growth, the fastest (3-4 days) were frequently considered the strongest interactors

(Golemis and Brent, 1992) to minimize the number of library isolates. In order to evaluate further SalAT protein interactors various analytical approaches were carried out, starting with sequence analysis of each interactor to gene expression and alkaloid profiling and finally performing enzymatic assays reactions that catalyzed by recombinant salutaridinol 7-*O*-acetyltransferase (SalAT) and a hypothetical “thebaine synthase” from *opium* poppy.

III.5.1 Sequencing of library plasmids

Toward identifying the protein encoded by the target DNA, the nucleotide sequence of the target DNA was determined by sequencing analysis (II.2.1.6) and compared to protein and nucleotide sequence databases (NCBI-BLAST) to identify related or homologous proteins. Finally 345 were sequenced (Appendix VI.1.1, VI.1.2, VI.1.3, VI.1.4, VI.1.5) sequenced known homologue isolates of proteins with related functions could be categorized as proteins associated with metabolism, cell cycle, DNA processing and protein synthesis, defense and environmental interaction, cellular development and others

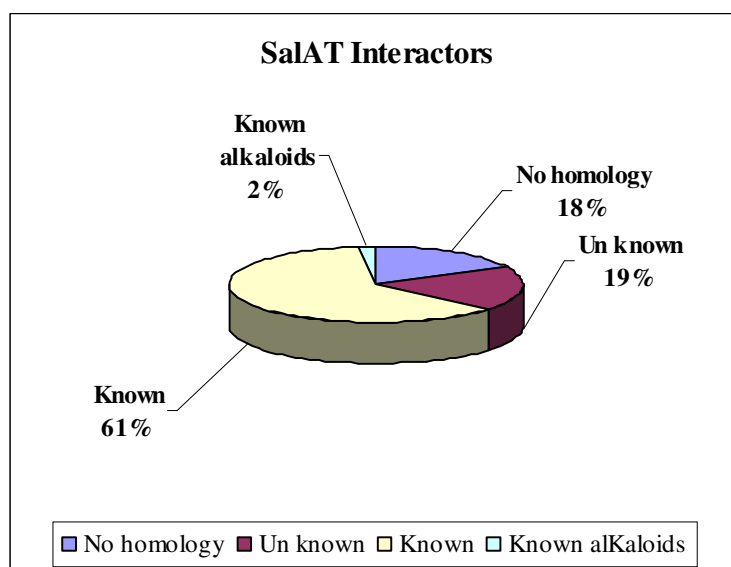


Figure III.12 sequencing analysis: Approximately 400 of SalAT interactors were sequenced, analyzed, and compared to protein and nucleotide sequence databases (NCBI-BLAST)

Sequences were clustered, assembled and analyzed using the SeqManII Software. (DNASTAR Inc.). Sequencing analysis of all interactors shows that only 2% of them are correlated to the alkaloid biosynthesis (Figure III.12). From a set of 345 sequenced isolates the following grouping of proteins (Table II.2) with related functions can be inferred two independent partial sequences of cytochrome P450s ;Cytochrome P450-3 [Musa acuminata] (P4F2), and Cytochrome P450 monooxygenase (P4C2); one *O*-methyltransferase, *O*-methyltransferase [Mentha x piperita] (P5C6); and four different partial clones for major latex proteins (MLPs). Major latex protein146 [Opium poppy] (P1A8), major latex protein 15 (P3G4), major latex-like protein [Plantago major] (P3E7), and Major latex-like protein [Arabidopsis] (P5C1) were among the isolates.

Table III.2 **SalAT interactorts:** Selected hits of the SalAT interactors, two partial sequences of Cytochrome P450s (P4C2, P4C2), one *O*-methyltransferase (P5C6), and four different partial clones for major latex proteins (MLPs) (P1A8, P3G4, P1D4, P5C1), a random e-value of $1e^{-10}$ has been imposed

Interactor	Gene	Size/ pb	Score	Expect	Identity	Similarity
P4F2	Cytochrome P450-3 [Musa acuminata]	600	70	9.00E-12	94.40%	97.20%
P4C2	Cytochrome P450 monooxygenase	500	66	2.00E-10	74.40%	87.29%
P5C6	<i>O</i> -methyltransferase [Mentha x piperita]	350	56	2.00E-09	51%	70.60%
P1A8	Major latex protein MLP146 - opium poppy	650	87	1.00E-16	35%	54%
P3G4	Major latex-like protein 1 [Plantago major]	450	56	1.00E-10	77.40%	87.10%
P1D4	Major latex protein MLP146 opium poppy	850	190	7.00E-48	63.30%	77.50%
P5C1	Major latex-like protein [Arabidopsis thaliana]	500	42	2.00E-11	42.30%	61.50%

III.5.2 Comparative microarrays analysis of SalAT interactors

With the intention of optimally correlate the gene expression profile for each SalAT interactor and alkaloid profile of poppy plants at deferent growing stages; microarrays and alkaloid content analysis were performed. Total RNA was isolated from stems from *Papaver somniferum* plants (4 months), *P. somniferum* seedlings (30 days), *P. somniferum* (paso paris) cell suspension cultures. The purified total RNA was used as a template for reverse transcription using oligodT primer. cDNAs were amplified using pMyr vector specific primers (Figure III.13) and subsequently spotted in quadruplicate. The oligonucleotide primer was with the following sequence.

Myr 5` Sense primer 5` -ACTACTAGCAGCTGTAATAC-3`
Myr 3` (anti-sense primer) 5` -CGTGAATGTAAGCGTGACAT-3`

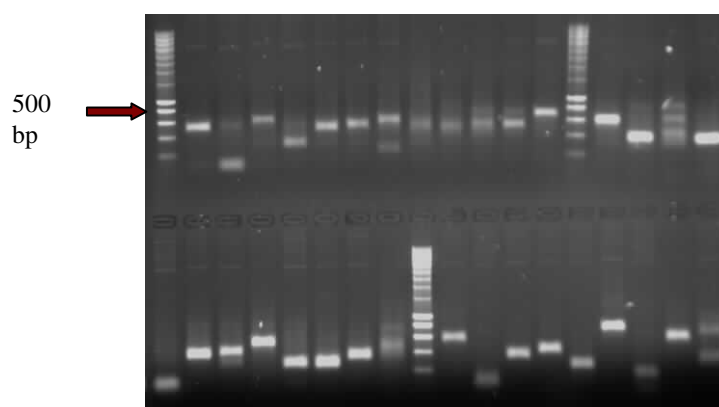


Figure III 13 SalAT interactors: PCR reactions were purified and re-concentrated by filtration through NucleoFast 96 PCR (Machery-Nagel) to at least 100 ng/ μ l.

Labelled cDNAs signals were developed with Gel and Blot Imaging System (Figure III.14a) (Figure III.15a) (Figure III.116a).

SalAT interactors /Stems arrays

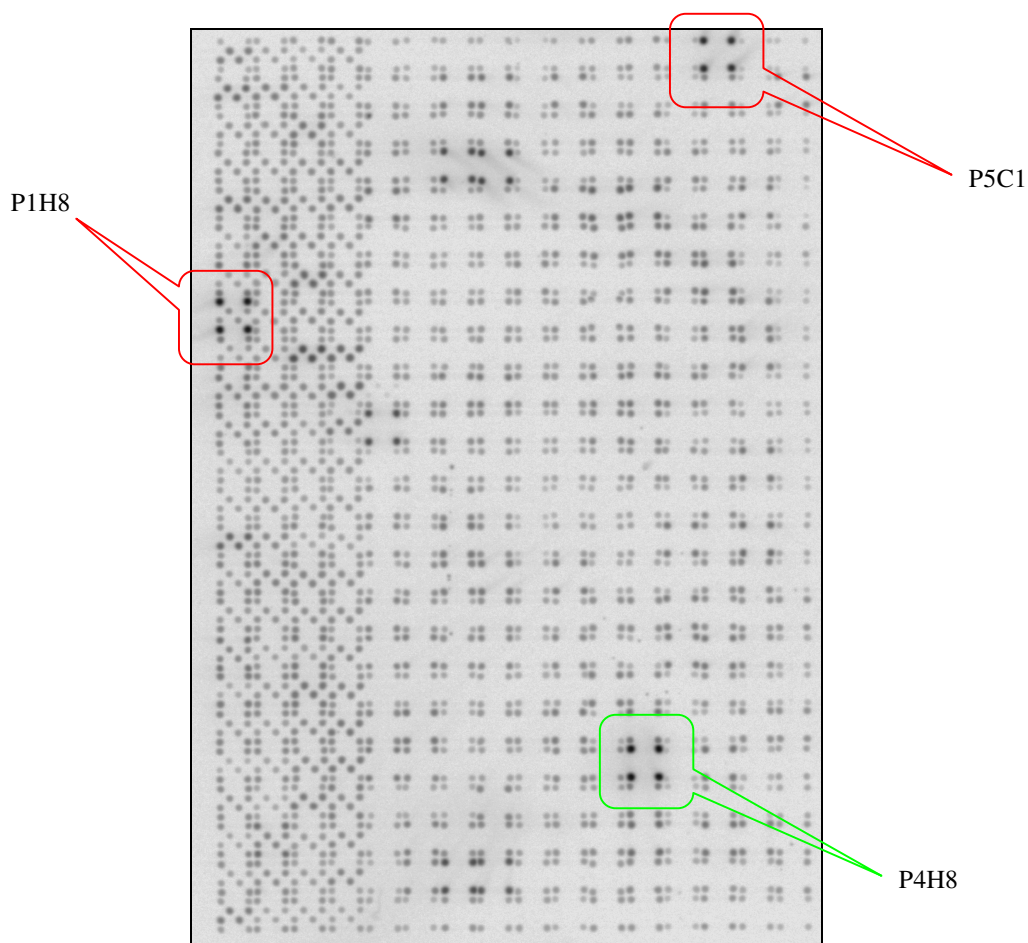


Figure III 14a Macroarrays /stems: Macroarrays consisting of 400 cDNA SalAT interactors. MLP146 [opium poppy] interactor P1H8 and Major latex-like protein [Arabidopsis thaliana] interactor P5C1 (red boxes) are the most highly expressed genes. Total RNA was isolated from plant stems (4 months), reverse transcribed, labelled with [α 33P]-dATP and hybridised

SalAT interactors /Seedlings arrays

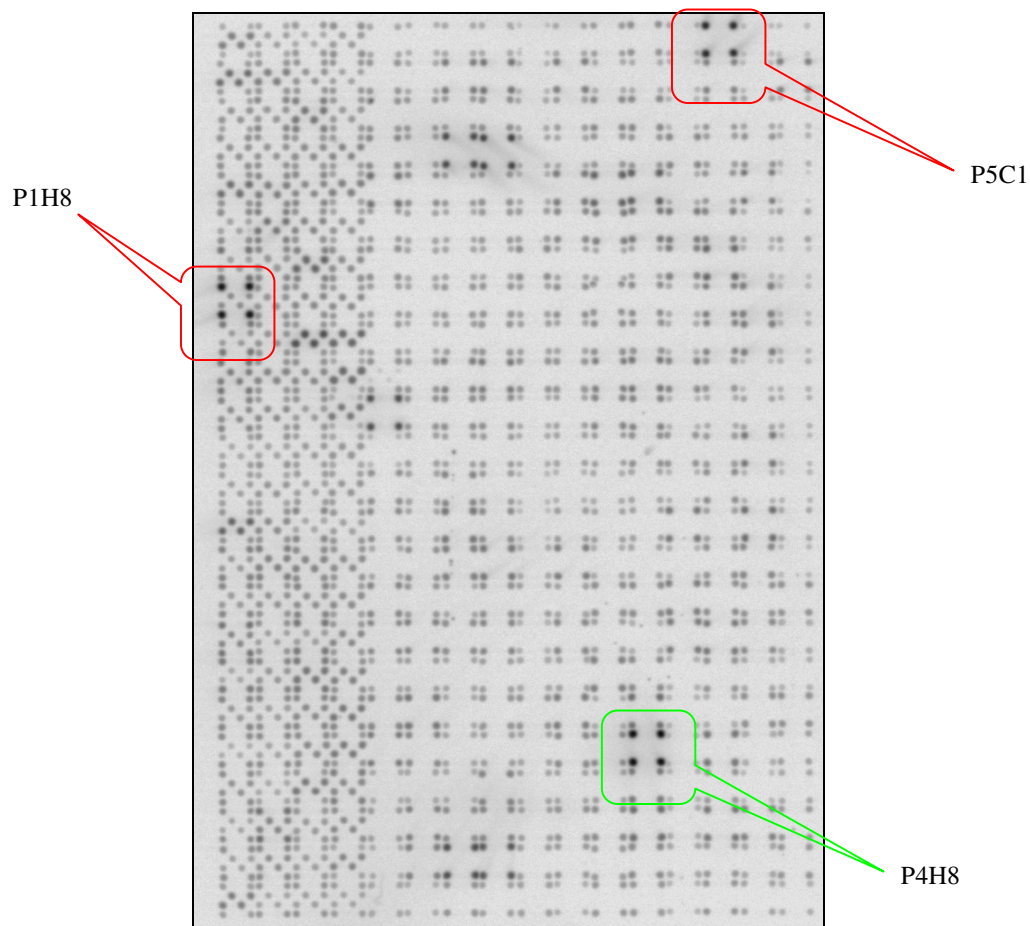


Figure III 15a Macroarrays /Seedling: Macroarrays consisting of 400 cDNA SalAT interactors. MLP146 [opium poppy] interactor P1H8 and Major latex-like protein [Arabidopsis thaliana] interactor P5C1 (red boxes) are the most highly expressed genes Total RNA was isolated from Paso paris cell suspension culture, reverse transcribed, labelled with [α 33P]-dATP and hybridised

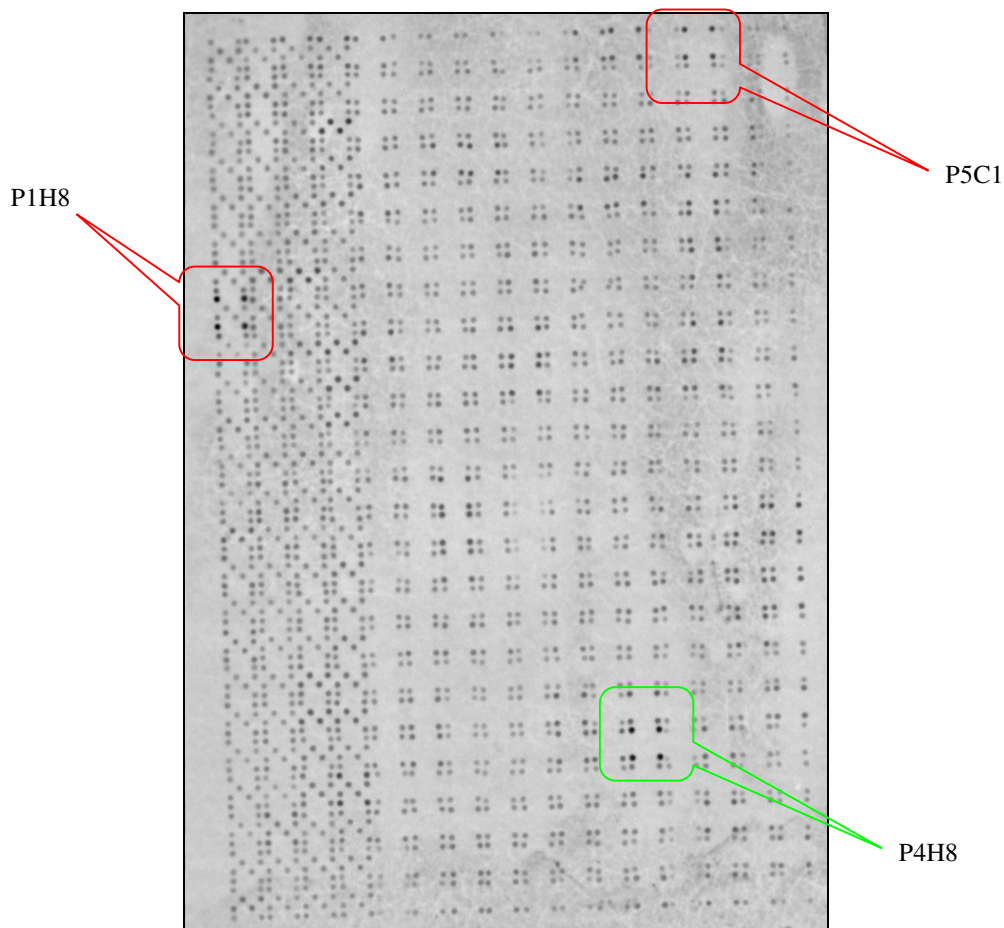
**SalAT interactors /Paso paris cell
suspension culture arrays**

Figure III 16a Macroarrays / Paso paris cell suspension culture arrays: Macroarrays consisting of 400 cDNA SalAT interactors. MLP146 [opium poppy] interactor P1H8 and Major latex-like protein [Arabidopsis thaliana] interactor P5C1 (red boxes) are the most highly expressed genes Total RNA was isolated from seedlings (30 days), reverse transcribed, labelled with [α 33P]-dATP and hybridised

AIDA image analyzer software (Raytest) was used for array determination and spot intensity evaluation. The features of Array module including the import of names tables, automatic positioning of measurement dots, background subtraction, and normalization allow us to evaluate arrays. Beside the image and the table of array results a schematic display (Figure III.14b) (Figure III.15b) (Figure III.16b) was performed. This display shows on the level of array data a schematic drawing of the array in colors. The data range was set to be in 7 colors ranging from the lowest level of array (dark blue) to the highest (red) which reflects the gene expression profile for each interactor. Comparative evaluation of spot intensity for all interactors show that most genes have a tendency to down regulate as the plants grow; the number of highly expressed genes in cell suspension culture and Seedlings arrays are much more what in stems of fully developed plants (Figure III.14b) (Figure III.15b) (Figure III.16b). Nevertheless, some of these genes are keeping active or even intensify their activity during growing (Table III.3). Gene expression data shows that (MLPs) Major latex protein146 from opium poppy (P1A8) and Major latex-like protein from *Arabidopsis thaliana* (P5C1) together with interactor which NAD kinase, which enhances the activity of ferric reductase (Fre1p); Utr1p in *Saccharomyces cerevisiae* (P4H8) are the most highly expressed among the sequenced clones in the three arrays.

Table II.3 SalAT interactors: Highly expressed genes of the SalAT interactors, two partial sequences of major latex protein homology (MLPs) (P1A8, P5C1) and one NAD Kinase (P4H8) show a very high expression level in all arrays.

Num	SalAT Interactor	Gene	Expression level	Accession number
1	P1A8	Major latex protein MLP146 - opium poppy	+++	NP_177245.1
2	P2B2	Hypothetical protein F36H2.2 - caenorhabditis elegans	+	pirllT21887
3	P2E3	No matching sequences reported	+	
4	P2G9	Predicted: non-tyrosine protein kinase.	++	XP_425696.1
5	P2E7	No matching sequences reported	+	
6	P3A11	EST AU065533(C2174)	++	NP_910543.1
7	P3E4	Protein v-src	++	prfll0903255A
8	P3F11	EST AU065533(C2174)	++	NP_910543.1
9	P3G4	Major latex-like protein 1 [Plantago major]	++	CAH59440.1
10	P3H11	Metallothionein-like protein	+	CAA07565.1
11	P4E5	60S ribosomal protein L24	+	
12	P4G5	No matching sequences reported	+	
13	P4H8	NAD kinase, active as a hexamer; enhances the activity of ferric reductase	+++	NP_012583.1
14	P5C1	Major latex-like protein - [Arabidopsis thaliana]	+++	CAC83579.1

Schematic display of SalAT interactors
/Stems arrays

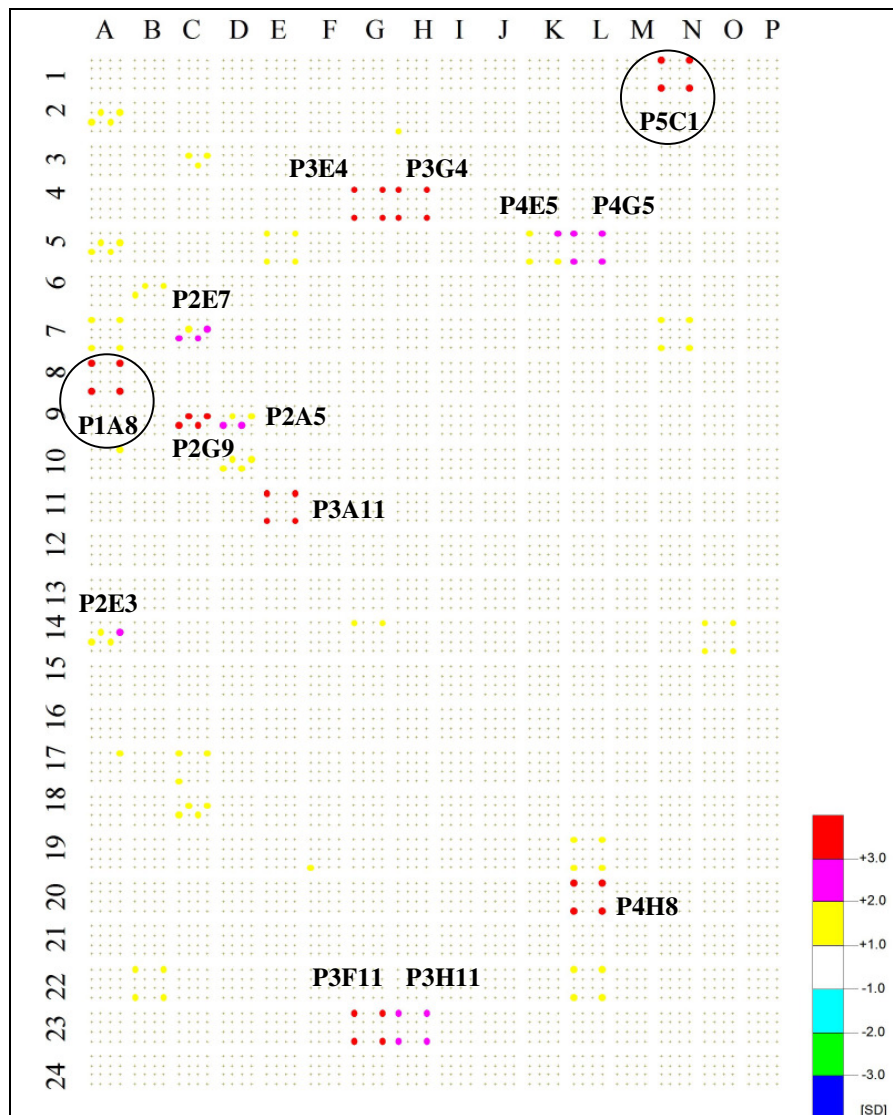


Figure III 14b A schematic display /stems: Gene expression profile for SalAT interactors was set to be represented in 7 colors ranging from the lowest level of array (dark blue) to the highest (red).

**Schematic display of SalAT
interactors /Seedlings arrays**

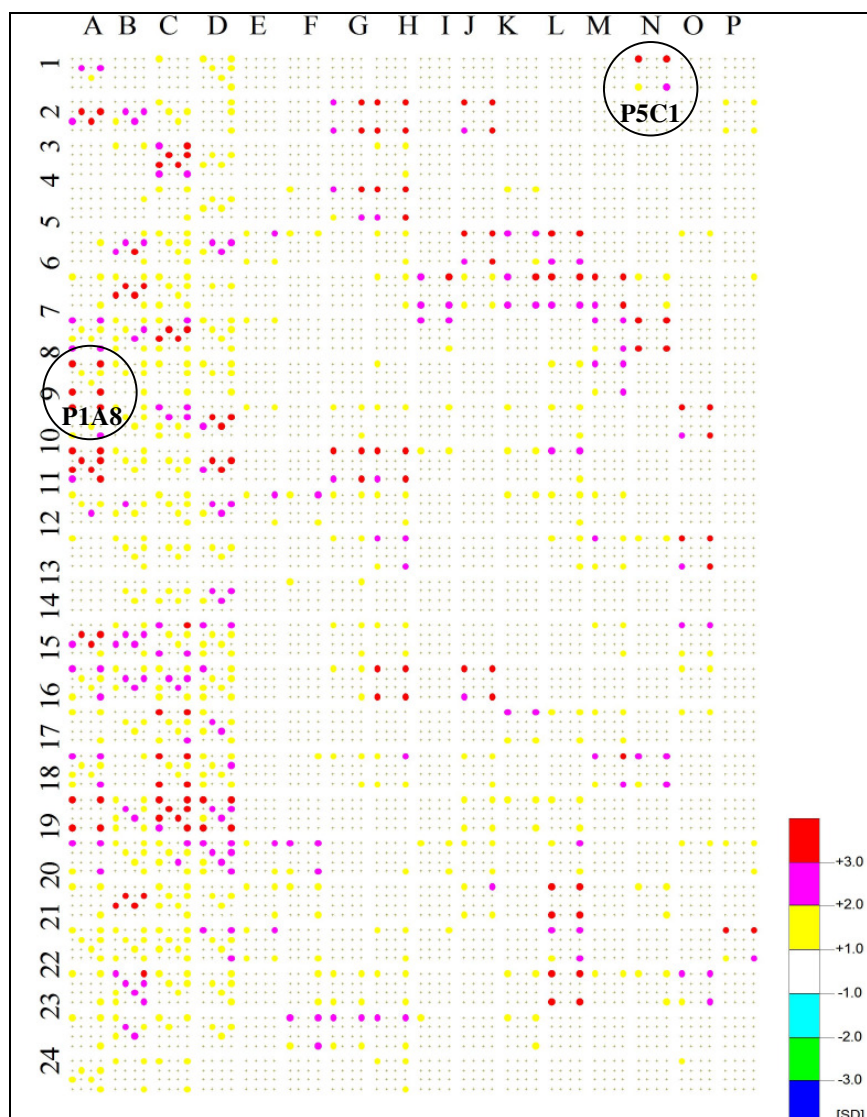


Figure III 15b A schematic display /Seedlings: Gene expression profile for SalAT interactors was set to be represented in 7 colors ranging from the lowest level of array (dark blue) to the highest (red).

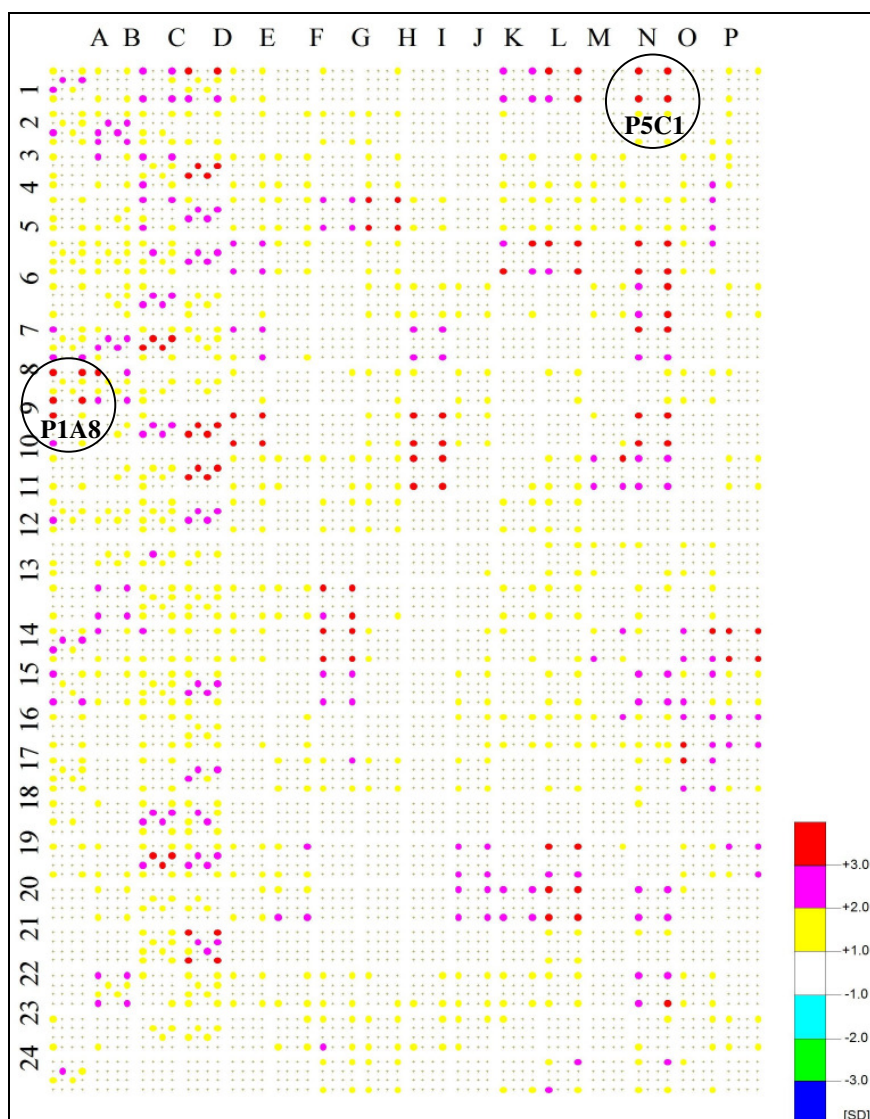


Figure III 16b a schematic display / Pasoparis cell suspension culture arrays: Gene expression profile for SalAT interactors was set to be represented in 7 colors ranging from the lowest level of array (dark blue) to the highest (red).

III.6 Alkaloid analysis in *P.somniferum* L.

The distribution of major alkaloids in stems and latex (Figure III.17) have a similar pattern with respect to the differences in quantity, morphine almost comprises 45%-50% of the alkaloid's content; the second major alkaloid was the thebaine with a percentage of more than 30%; the remaining alkaloids may reach 20% of the total content. Comparative and quantitative HPLC and LC-MS analysis of 4 months old plants showed that alkaloid content was accumulated mainly in latex and stems as second storage site (Figure III.18D, C). *P. somniferum* plant cell suspension culture (paso paris) showed no alkaloids at all (Figure III.18B). Morphine, thebaine, codeine and oripavine were shown to be the main constituents of alkaloids in latex and stems, with morphine as the major alkaloid followed by thebaine.

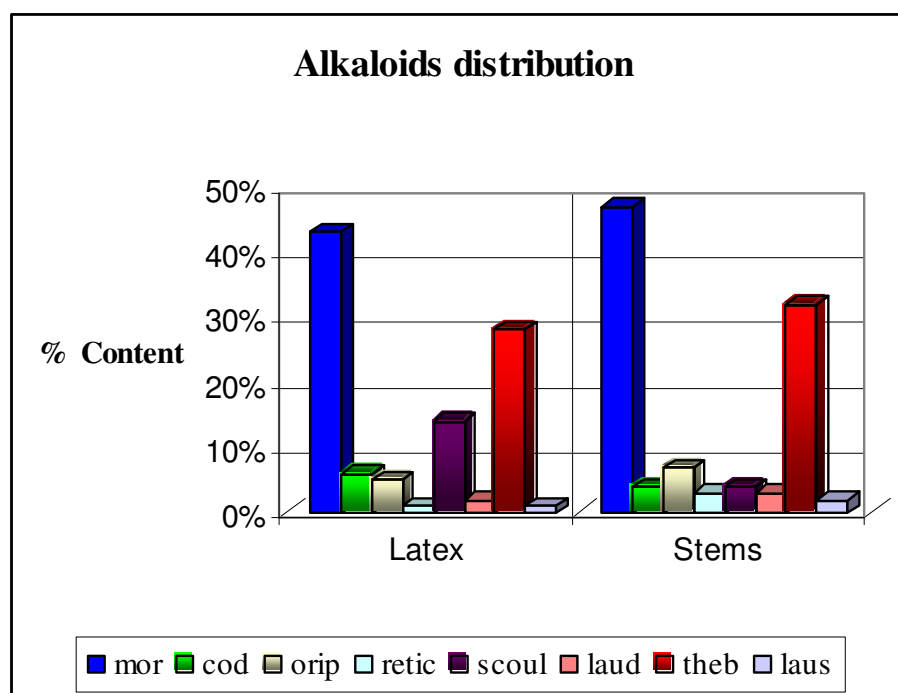


Figure III.17 Alkaloid distribution: HPLC and LC-MS analysis of 4 months old poppy plants.

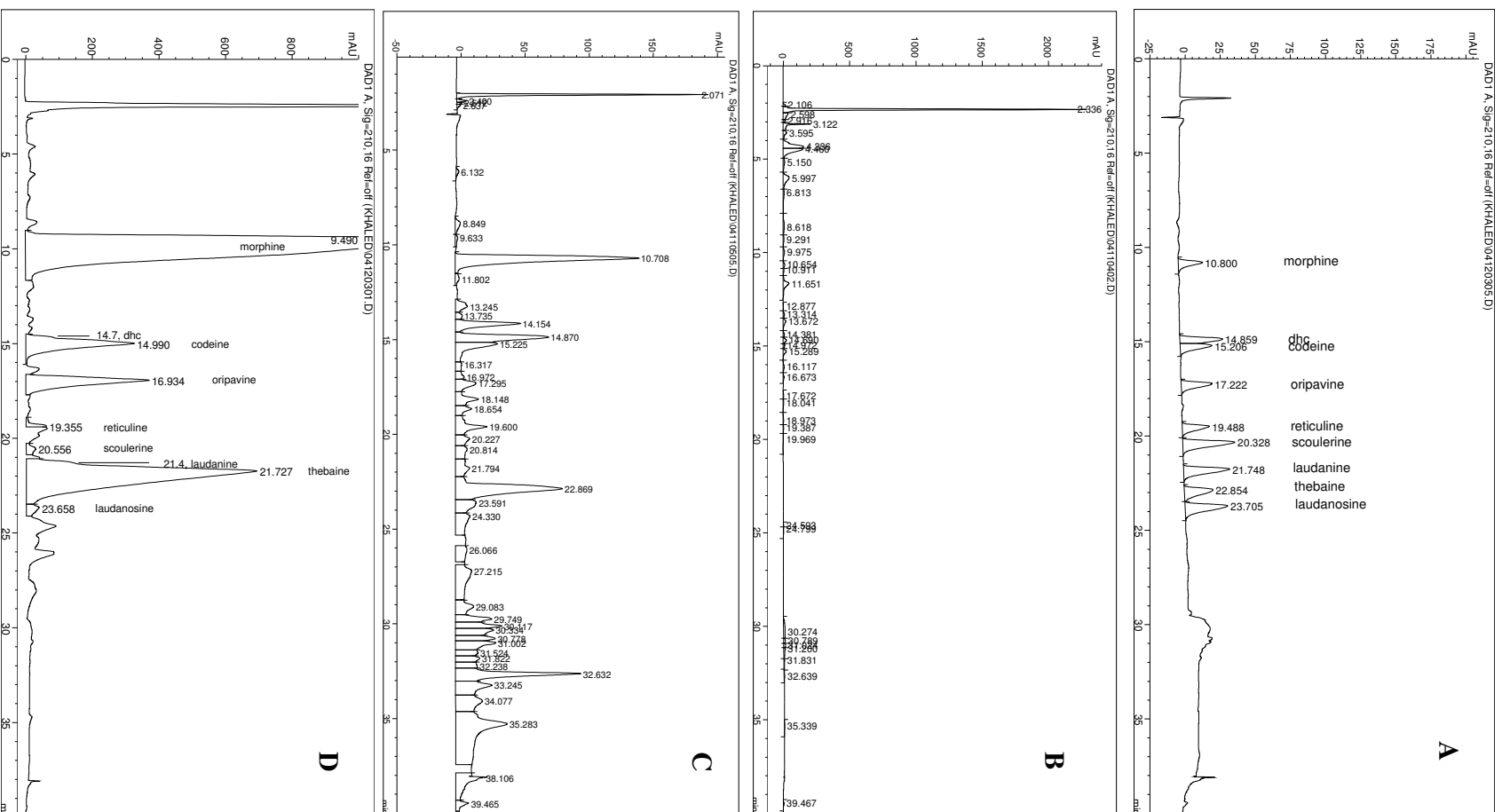


Figure III.18 HPLC analysis: HPLC quantitative analysis of alkaloids accumulation in *P. somniferum* Latex (D), and stems (C). Authentic alkaloids serve as positive control (A). No alkaloids detected in paso paris cell cultures which serve as negative control (B).

III.6.1 Accumulation of alkaloids in *P.somniferum* seedlings

The accumulation of the major alkaloids (codeine, morphine, thebaine, reticuline, papaverine, sanguinarine, laudanine and laudanosine) was determined by HPLC and HPLC-MS (Appendix VI.2). In this experiment, whole single plant was used for each measurement, samples of *P.somniferum* seedlings were collected every 4 days over two month's period. Codeine was detected 12 days after germination (2.2 µg/100 mg fresh weights). Approximately the same amount of morphine was detected at day 20 (Figure III.19A), and then the level increased with time. The level of major alkaloids seems to reach a peak after 30-40 days. The highest level of codeine and thebaine was 4.9 and 3.8 µg/100 mg fresh weight, respectively at day 32. The levels of morphine and papaverine at day 32 were 8.90 and 7.0 µg/100 mg fresh weights respectively. The morphine levels continue to increase to reach at day 60 about 12.5 µg/100 mg fresh weights. The remaining alkaloids mainly sanguinarine, laudanine and laudanosine did not show up before day 48 in minor levels (Figure III.19B).

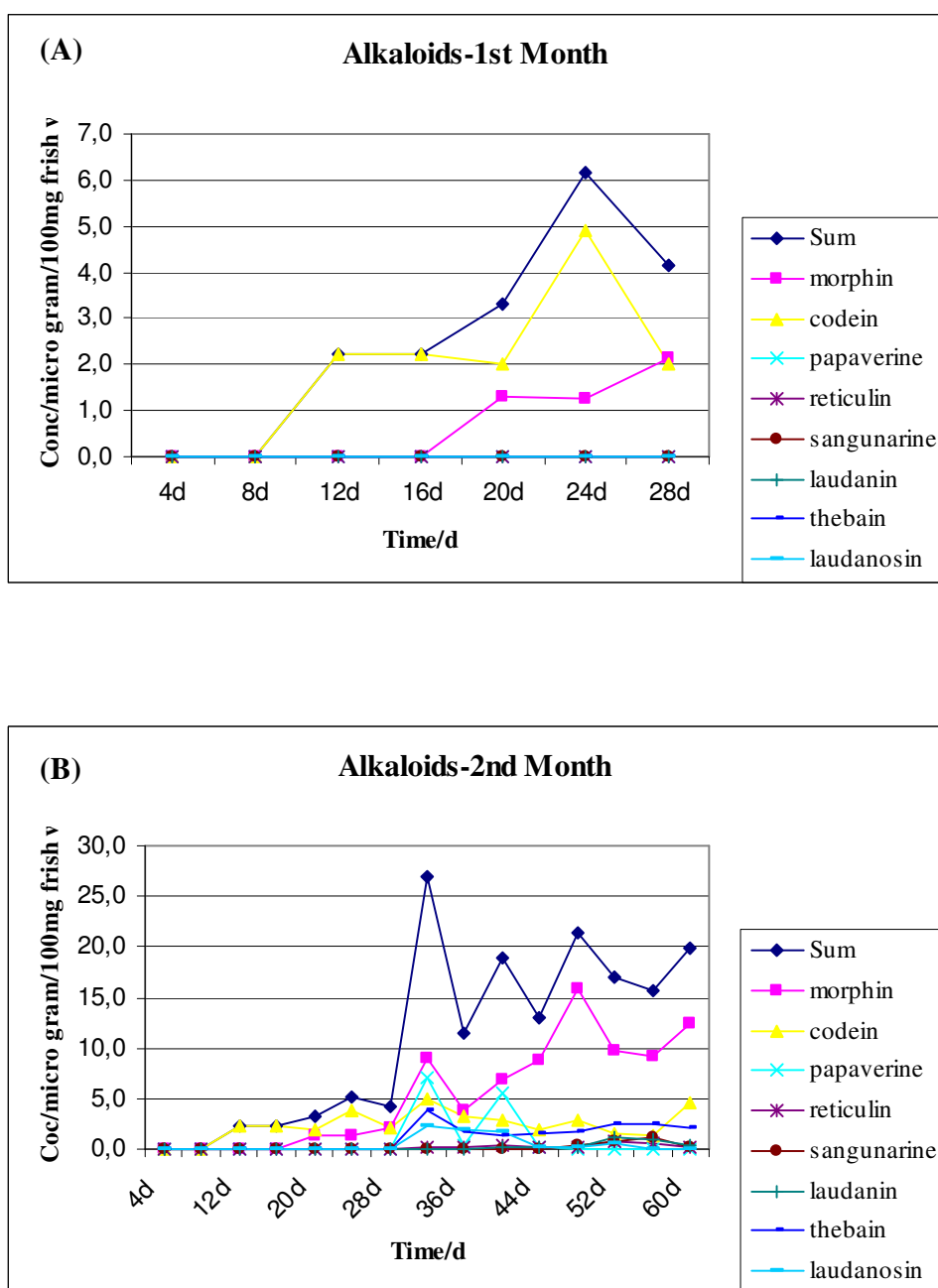


Figure III.19 Alkaloid time course analysis of *Papaver somniferum* L. seedlings: HPLC and HPLC-MS analysis show that only codeine (12 days) and morphine (20 days) were detectable in the first month of growing for seedlings (A). Alkaloids accumulation continue by time; by the end of day 50 almost all alkaloids were detectable (B)

III.7 Bacteriology and gene expression

Putative SalAT interactor P1A8 (major latex protein 146 homologue) has been selected for bacterial over expression and subsequently purification along with SalAT for enzymatic activity assay. Major latex protein 146 (MLP146) which shares a considerable homology with many other interactors (Table.II.2), was one of the first interactors to be isolated by the Cyto-Trap two-hybrid system which represents relatively a strong interaction. Macroarrays analysis also shows that MLP 146 gene is a very highly expressed gene in poppy plants in all growing phases.

III.7.1 Over-expression and purification of recombinant salutaridinol 7-O-acetyltransferase (SalAT) from *P. somniferum* L.

The over-expressed recombinant protein was isolated from *E.coli* and displayed in Figure III.20 with a yield of 2.1 mg/L cell culture and a relative molecular mass of ~ 55kDa as determined by SDS-PAGE.

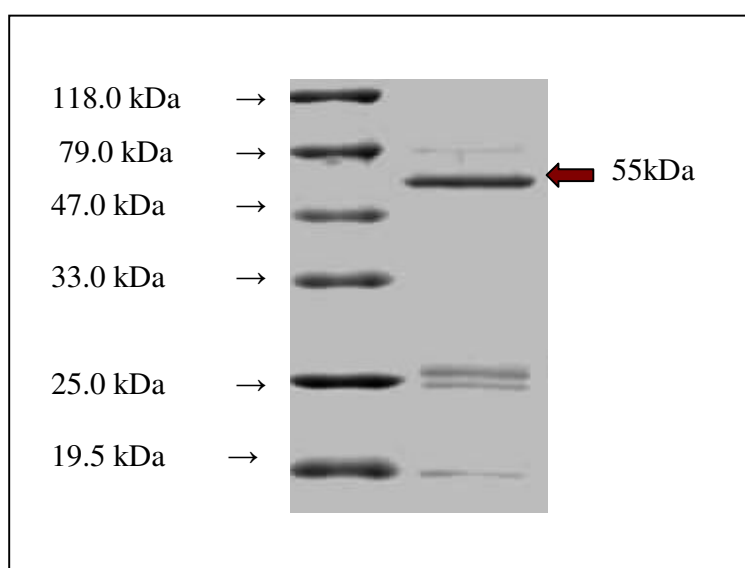


Figure III.20 SalAT over-expression and Purification: Analysis of one- step protein purification. Pure recombinant SalAT exhibit about 55 kDa on 15% SDS-PAGE

The predicted and calculated size of salutaridinol 7-*O*-acetyltransferase (SalAT) is 52.6 kDa without the fused tag, which corresponds to 1425 nucleotides and 474 amino acids, (Grothe et al., 2001); the exhibited size in SDS-PAGE is in good agreement with the literature.

III.7.2 Over-expression and purification of recombinant major latex protein 146 (MLP 146) from *P. somniferum* L.

A full length sequence of MLP 146 was cloned in the expression vector pHIS8-3 (Jez et al) controlled by T7/SP6 promoter and containing six histidines as an N-terminal tag to facilitate over-expression in *E.coli* strain BL21 DE3 and the purification by Immobilized Metal Affinity Chromatography after protein dialysis to eliminate urea, imidazole and the other detergent. The LB-^{kan} cultures were then grown for an additional 12 hours at 28 °C. SDS-PAGE analysis of the purified protein shows a band with a molecular weight close to 25 kDa (Figure III.18) which matches the predicted size of the MLP family (Decker et al, 2000). MLP 146 protein turns out to be a non-soluble protein; therefore, 8 M Urea was used for inclusion disruption and subsequent purification from *E.coli*.

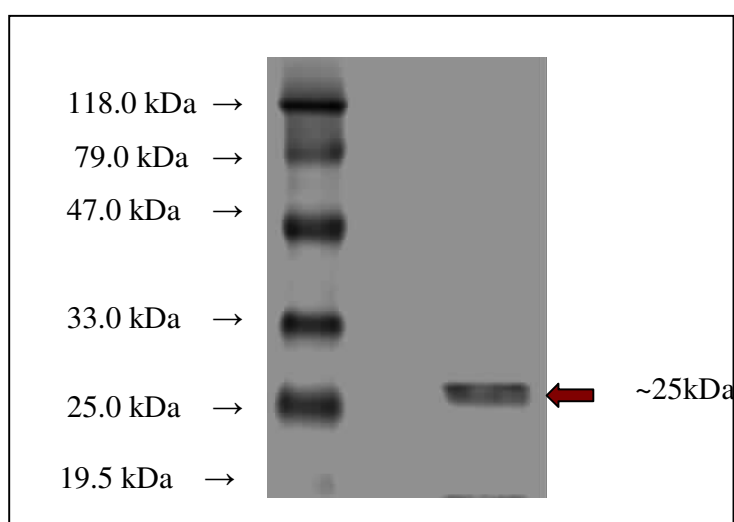


Figure III.21 MLP 146 over-expression and purification: Analysis of one-step protein purification. MLP 146 exhibits about 25 kDa on 15% SDS-PAGE. Pellet was resuspended with 0.5-1 ml of 8M Urea buffer (1L culture ~50 ml Urea buffer), and sonicated with ultrasonic probe for 2x 30sec.

Final yield for the recombinant purified protein was 2.5 mg/L cell culture. The monomer enzyme was stored at -80 °C in 50 mM HEPES (pH 7.0), 5 mM DTT, 10% glycerol

III.8 Enzymatic activity assays

III.8.1 Recombinant salutaridinol 7-*O*-acetyltransferase (SalAT) activity.

Recombinant salutaridinol 7-*O*-acetyltransferase was incubated in the presence of substrate salutaridinol and co-substrate acetyl co-enzyme A at pH 6.5. The mixture of SalAT reactions (T0S, T5S, T10S, T20S, T40S, and T60S) together with control reactions (T0, T5, T10, T20, T40, and T60) (Table II.2.2) were incubated at 47 °C for 0, 5, 10, 20, 40, and 60 min.

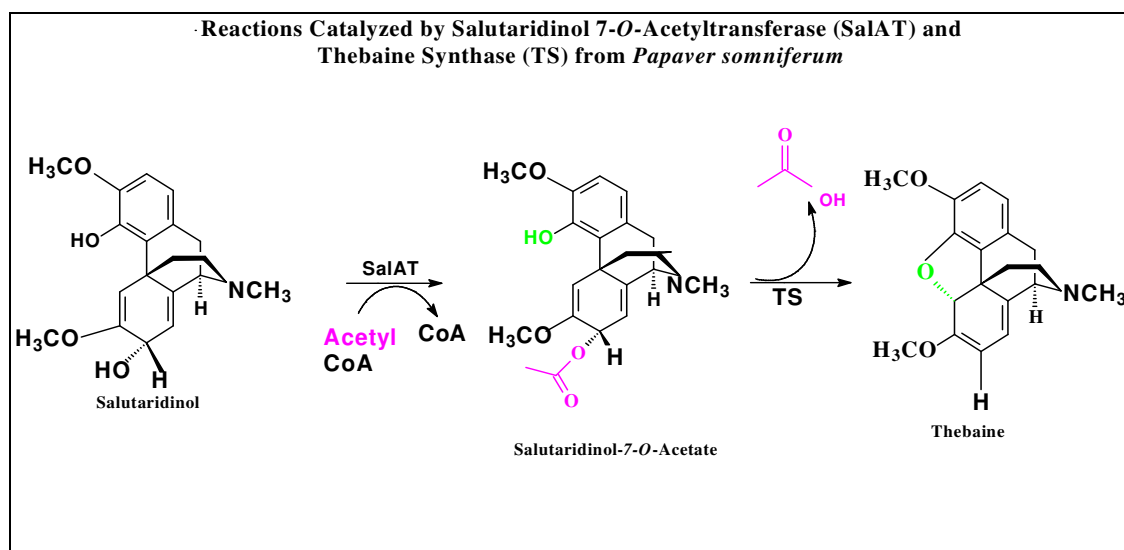


Figure III.22 Reactions catalyzed by salutaridinol 7-*O*-acetyltransferase (SalAT) and thebaine synthase (TS) from *Papaver somniferum*. The oxide ring is closed and acetate is eliminated to form the pentacyclic morphinan ring system of thebaine.

The products were analyzed using the LC-MS/ESI (electro spray ionization) with Selected Reaction Monitoring (SRM) technique. Activity assay (II.2.7) of pure

recombinant SalAT enzyme was prepared using salutaridinol as substrate results in very prompt and active conversion into thebaine (signals at m/z 312 ($[M+H]^+$) characteristic fragments at m/z 58, m/z 249 and 266 with RT of ≈ 12.5) and Salutaridinol-7-*O*-acetate (Signal m/z 372($[M+H]^+$) at RT of ≈ 6.3 min) and (Figure 23B,C). The amount of thebaine was 7.35 ng/ μ l (Appendix 3); in the meantime salutaridinol acetate was not detectable (Appendix 3). Control assay show signals for salutaridinol only at (m/z 330 ($[M+H]^+$) and characteristic fragments at m/z 58, m/z 249 and m/z 266 with RT of ~ 4.9 min. (Figure 23A). This reaction (thebaine formation) takes place in alkaline, neutral, and acidic conditions as well.

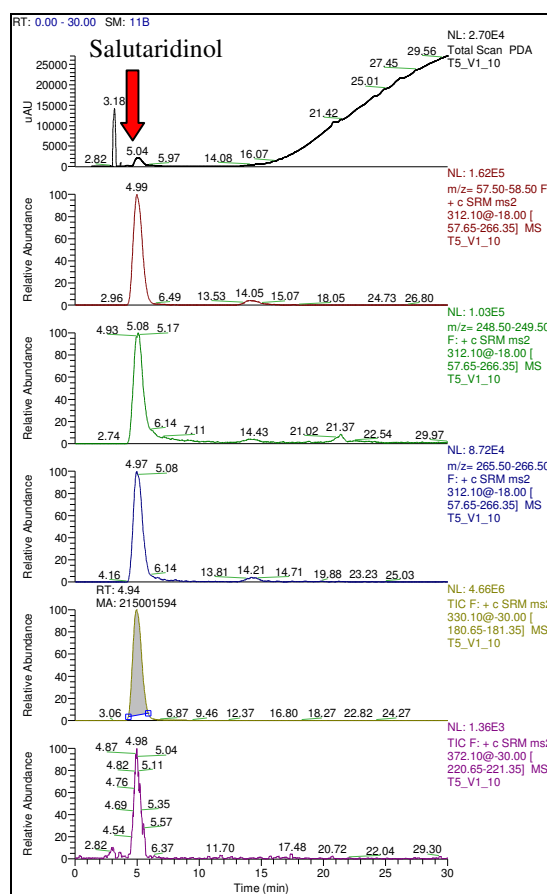


Figure III.23A LC-MS (SRM) analysis of control assay (T5): SRM data show signals for salutaridinol at (m/z 330 ($[M+H]^+$) and characteristic fragments at m/z 58, m/z 249 and m/z 266 with RT of ~ 4.9 min. Control assay did not show any signals for thebaine and salutaridinol-7-*O*- acetate.

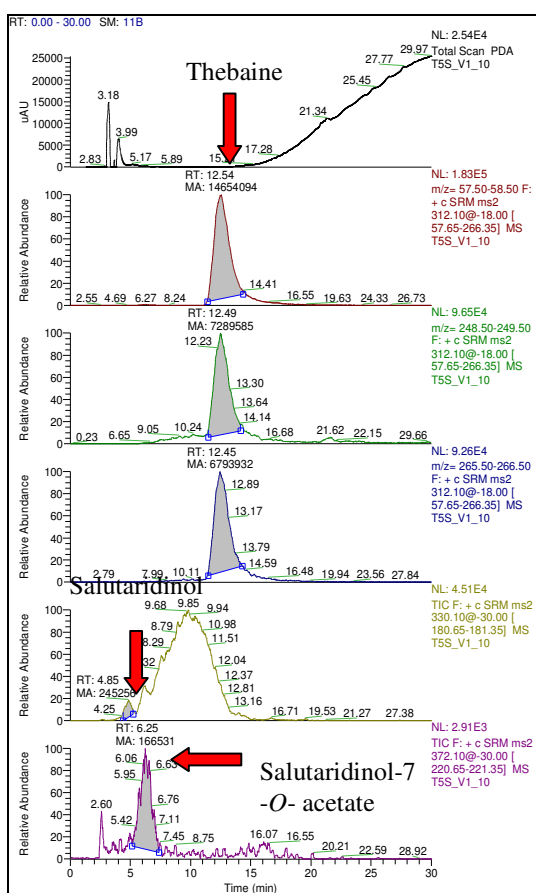


Figure III.23B LC-MS (SRM) analysis of enzyme assay (T5S): SRM data show signals for thebaine at m/z 312 ($[M+H]^+$) and characteristic fragments at m/z 58, m/z 249 and 266 with RT of \square 12.5. Enzymatic assay showed traces of salutaridinol at RT of \square 4.9 min and salutaridinol-7-*O*- acetate m/z 372 ($[M+H]^+$) at RT of \square 6.3 min.

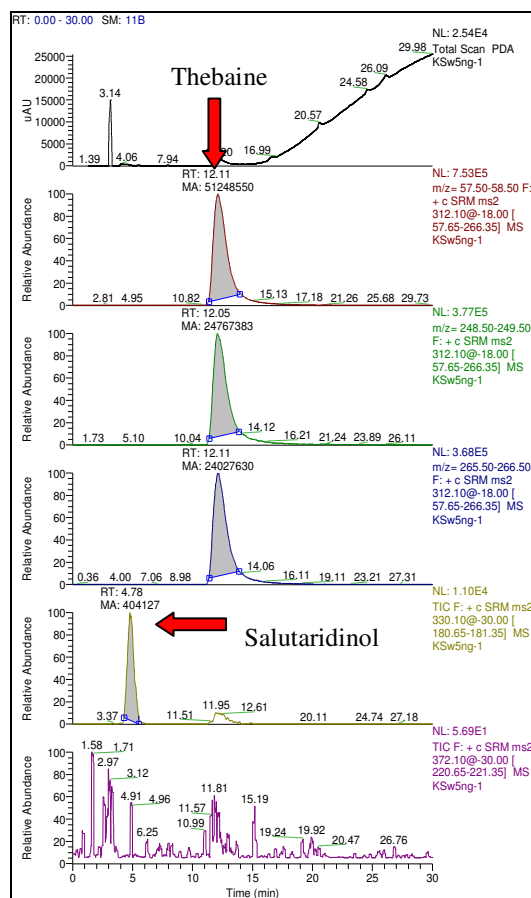


Figure III.23C LC-MS (SRM) analysis of authentic thebaine and Salutaridinol: SRM data show signals for thebaine at m/z 312 ($[M+H]^+$) and characteristic fragments at m/z 58, m/z 249 and 266 with RT of \square 12.1 min. And for salutaridinol at m/z 330 ($[M+H]^+$) at RT of \square 4.8 min and no signal for salutaridinol-7-*O*- acetate at m/z 372 ($[M+H]^+$).

III.8.2 Salutaridinol 7-*O*-acetyltransferase (SalAT) and Major Latex protein 146 coupled activity assay.

A dramatic 50% drop of thebaine content was observed directly after adding pure recombinant (MLP 146) to the SalAT activity assay (SalAT + MLP146 Reactions) (Table II.2.2) in all reactions (T0SM, T5SM, T10SM, T20SM, T40SM, and T60SM) salutaridinol-7*O*-acetate was not detectable in any of the reaction the reactions. The concentration of thebaine was 2.95 ng/ μ l (Appendix 3); 5 min after the reaction have been started (Figure III.24A). A gradual increase (5 μ l-160 μ l) of MLP 146 levels showed no significant effect in thebaine formation compared to the coupled assay reactions (Figure III.24B) (Appendix 3).

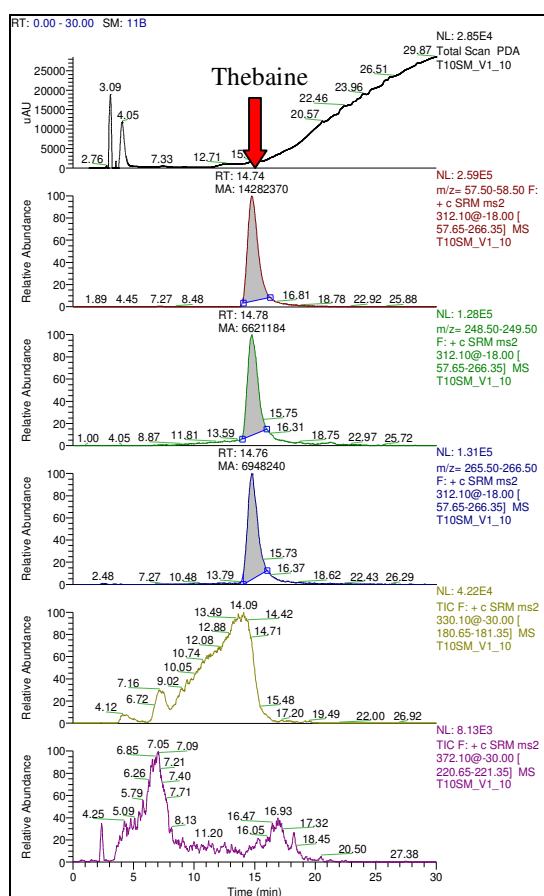


Figure III.24A LC-MS (SRM) analysis of SalAT - MLP 146 coupled assay (T10SM): SRM data show signals for thebaine at m/z 312 ($[M+H]^+$) and characteristic fragments at m/z 58, m/z 249 and 266 with RT of \square 14.7 min. Signals for salutaridinol and salutaridinol-7-*O*- acetate were not detectable.

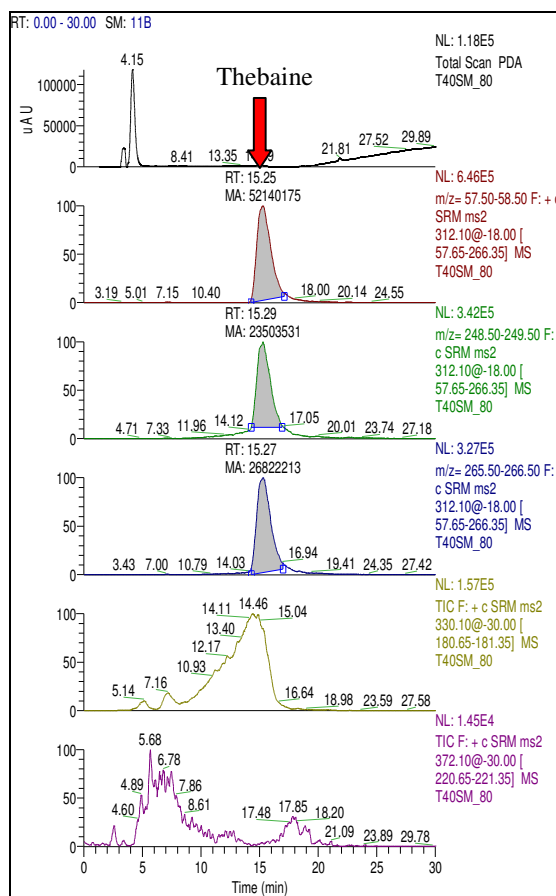


Figure III.24B LC-MS (SRM) analysis of SalAT - MLP 146 coupled assay (T40SM_80): Thebaine was still detectable after increasing MLP 146 solution (80 μ l). Signals for salutaridinol and salutaridinol-7-*O*- acetate were not detectable.

The MS data obtained did not show signals characterizing by-product such as neodihydrothebaine at m/z 314 ($[M+H]^+$), nudaurine at m/z 328, and [8,9-dihydro-5H-2,12-dimethoxy-1-hydroxy-7-methyl-dibenz[*d,f*]azonium]acetate at m/z 312 (Figure III.25A). Furthermore, the assay T10SM was analyzed by LC-MS concerning reticuline as possible product. The SRM data exhibited no significant signal for the benzyloquinoline alkaloid, because the typical isoquinolinium ion at m/z 192 was not detectable (Figure III.25B). Nevertheless, MS/MS spectrum shows a molecular ion ($[M+H]^+$) at m/z 332 and fragments which can not related it to the structure of the unknown compound (Figure III.26A, B)

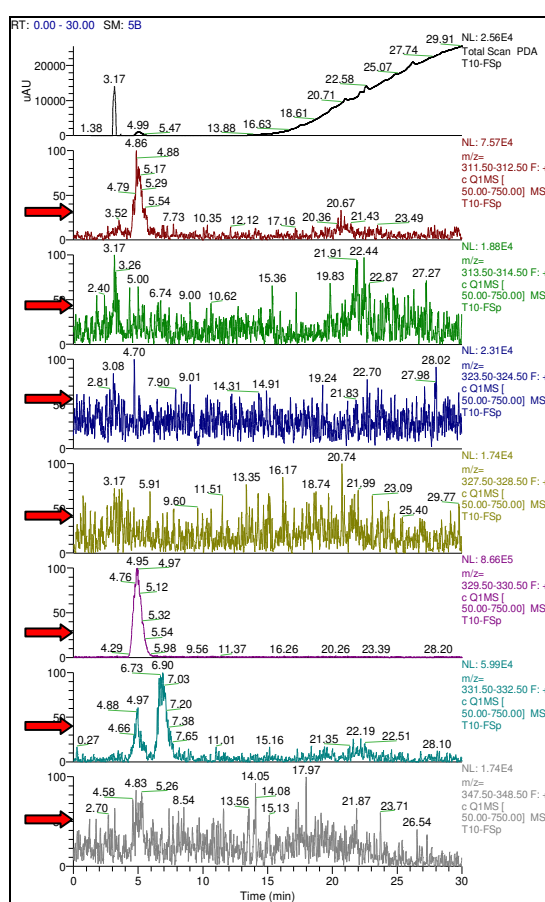


Figure IV.25A LC-MS (SRM) analysis of by-products(T10): Full scan data show no signals for neodihydrothebaine at m/z 314 ($[M+H]^+$), nudaurine at m/z 328, and [8,9-dihydro-5H-2,12-dimethoxy-1-hydroxy-7-methyl-dibenz[*d,f*]azonium]acetate at m/z 312.

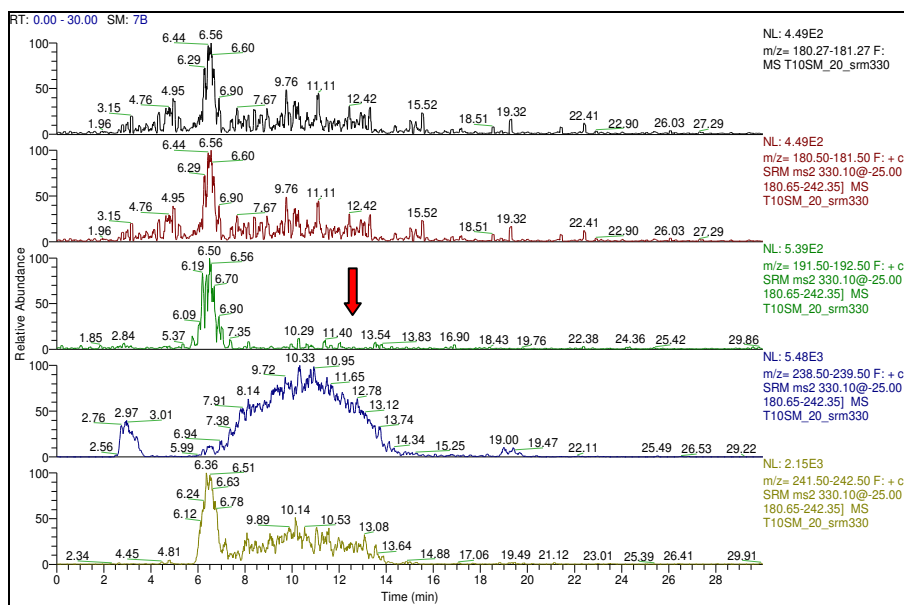


Figure III.25B LC-MS (SRM) analysis of assay T10SM: The characteristic fragment ion for the by-product reticuline at m/z 192 (middle lane) was not detected.

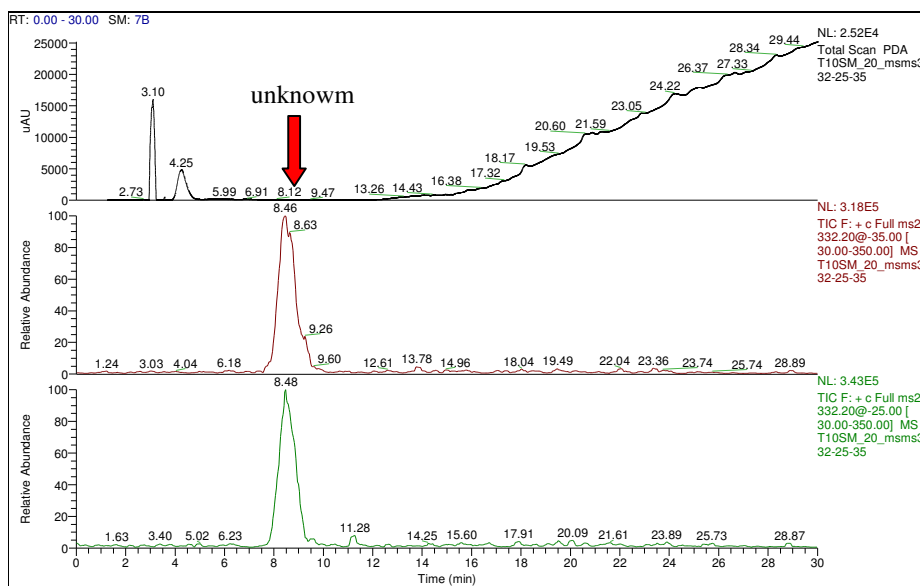


Figure III.26A MS full scan: The ion chromatogram shows molecular ion at m/z 332 ($[M+H]^+$) using different energies (35eV, 25eV),

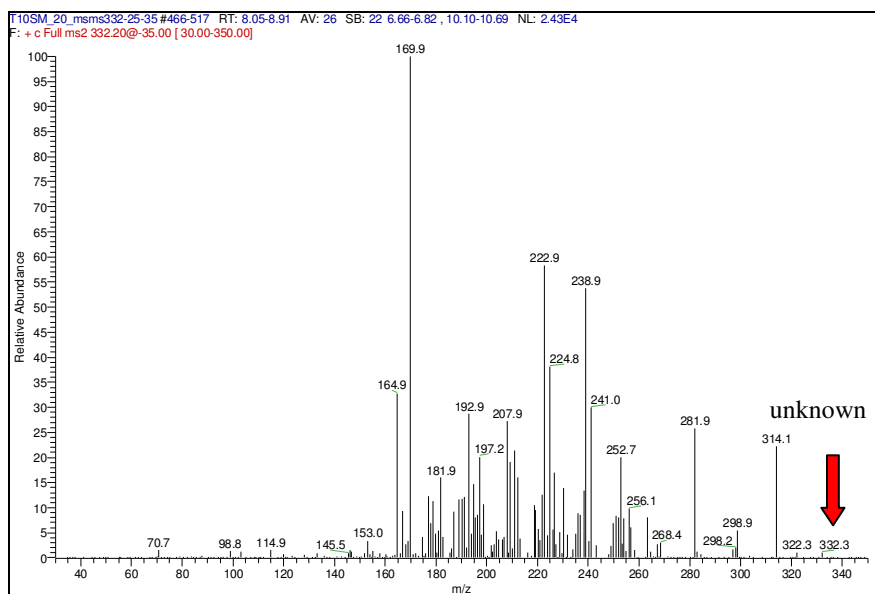


Figure III.26B MS/MS spectrum: MS/MS data illustrate the molecular ion at m/z 332 ($[M+H]^+$) and fragmentation pattern of the unknown compound .

Finally it is also valuable to mention that salutaridinol acetate and thebaine were immediately formed the moment that salutaridinol 7-*O*-acetyltransferase was put in the assay even when the reaction tube placed in ice (TOS reaction) (Figure III.25). The formation of thebaine continues to build up during the first 5 min (7.35 ng/ μ l) of the reaction before it began to gradually decrease. Salutaridinol and salutaridinol acetate were almost not detectable after 5 min of the reaction.

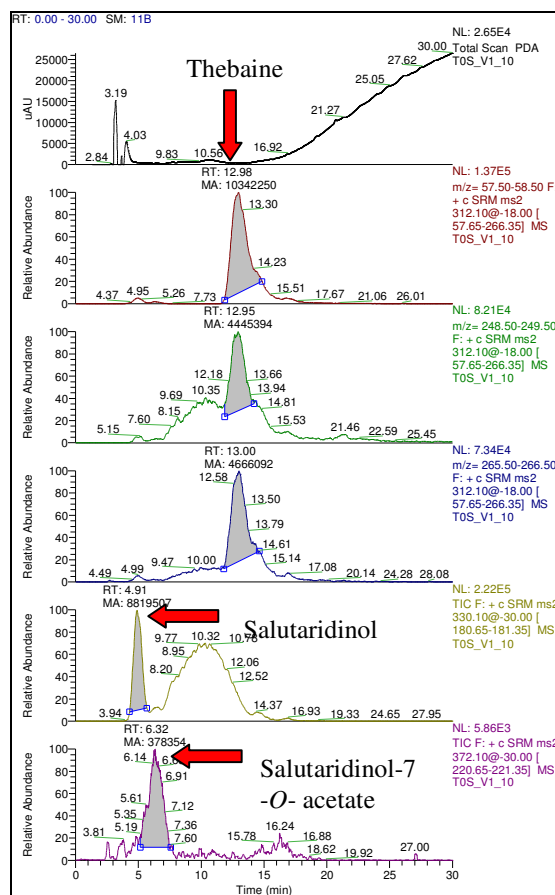


Figure III.25 LC-MS (SRM) analysis of enzyme assay (T0S): SRM data show signals for thebaine at m/z 312 ($[M+H]^+$) and characteristic fragments at m/z 58, m/z 249 and 266 with RT of \square 12.5. Enzymatic assay showed of salutaridinol at m/z 330($[M+H]^+$) at RT of \square 4.9 min and salutaridinol-7-*O*- acetate at m/z 372 ($[M+H]^+$) at RT of \square 6.3 min.

IV Discussion

In this study we have attempted to identify a cDNA encoding thebaine synthase involved in morphine biosynthesis from opium poppy *Papaver somniferum* derived from L-tyrosine. Based upon the assumption by Lenz and Zenk (1995a) that acetylating and subsequent allelic elimination is a new enzymatic mechanism in alkaloid biosynthesis (Lenz and Zenk, 1995a), Based on this assumption, Poppy plants may transform one precursor into completely different alkaloid biosynthetic pathways depending on the reaction pH value; suggests that this elimination possibly is a protein- dependent process and that this “thebaine synthase” should be physically associated with Salutaridinol 7-*O*-acetyltransferase. The yeast two-hybrid system was used in an attempt to isolate a cDNA that encodes thebaine synthase. In this schema, a salutaridinol 7-*O*-acetyltransferase - human gene product (hSos), “Bait“, fusion was generated and screened against a *P. somniferum* cDNA library cloned into the activation domain vector pMyr “Target”.

IV.1 CytoTrap yeast two-hybrid system and identification of “putative positive” interactors

Analyzing protein-protein interactions with the Cyto Trap yeast two-hybrid system draw attention to two main issues. Although by performing the functionally screening for the SalAT interacting proteins, 345 interacting cDNAs were isolated and sequenced. Alkaloid biosynthesis enzymes homologues were rare. Therefore, it was not possible to directly correlate any of SalAT interactor proteins that we obtain to one of the identified enzymes in alkaloid biosynthesis. The physical interaction between the consecutive salutaridinol 7-*O*-acetyltransferase and salutaridine reductase (SalR) (Figure IV.2) demonstrate the increasing possibility of the cross-talking between adjacent enzymes in the same biosynthetic pathway which is not the case for salutaridinol 7-*O*-acetyltransferase and norclaurine 6-*O* methyl transferase (6OMT) (Figure IV.1). Consequently, the theoretical “thebaine synthase” was expected to show a significant interaction level with salutaridinol 7-*O*-acetyltransferase if thebaine formation is actually a protein-dependent process. Those two particular assumptions favor the possibility of an

unprompted and spontaneous removal of acetate group from salutaridinol- 7-*O*- acetate to yield thebaine. On the other hand, there are a number of problems with this particular yeast two-hybrid system should be taken in consideration. In our experience the *cdc25* yeast strain reverts (i.e. is able to grow at the restrictive temperature regardless of the plasmids it carries. This means that the yeast strain must be tested for temperature sensitivity both before and after transformation, prior to any assays for protein-protein interaction. Secondly, the detection of protein-protein interactions relies solely on the growth of the yeast at the restrictive temperature; there is no other marker to confirm an interaction. The problem of reversion of the yeast strain and the lack of additional markers for protein-protein interactions suggests that the hSos/Ras recruitment system may not be the best to library screening (Causier and Davies, 2002).

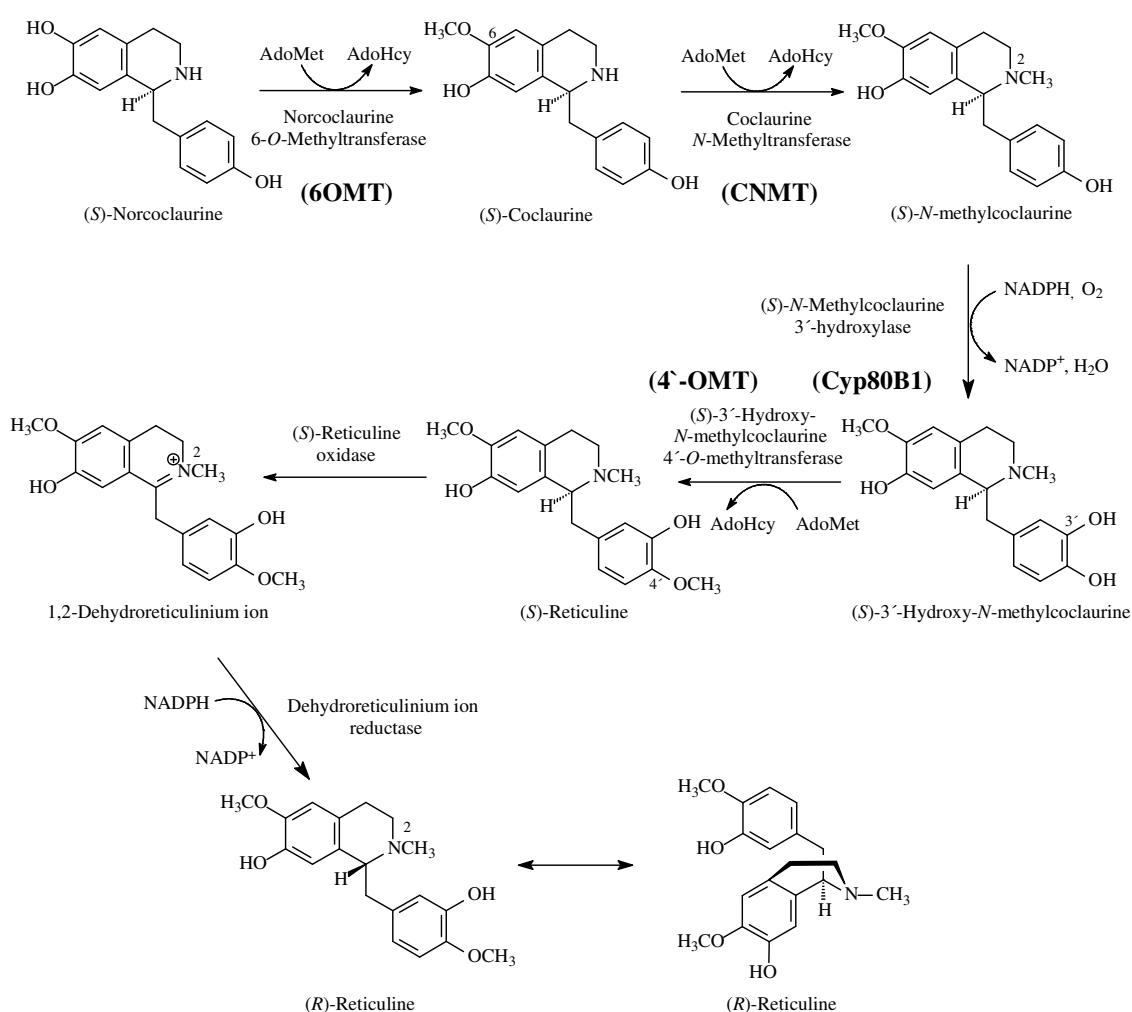


Figure IV.1 The morphine biosynthetic pathway: from (S)-norcoclaurine to (R)-reticuline.

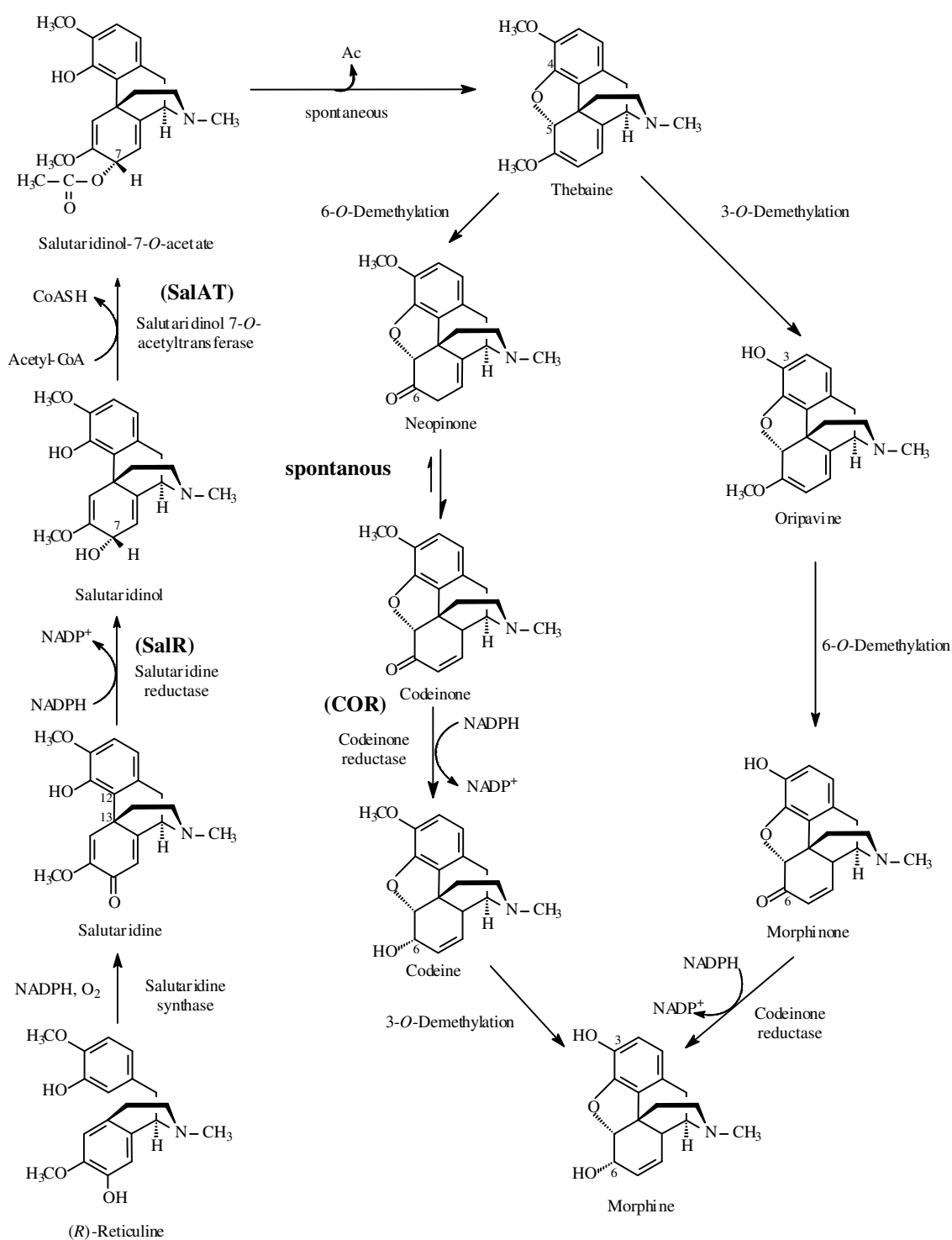


Figure IV.2 The morphine biosynthesis pathway: from *(R)*-reticuline to morphine via either neopinone or oripavine.

IV.2 Macroarrays analysis and alkaloid profiling

The macroarrays analysis of SalAT interactor cDNAs and alkaloid analysis in *Papaver somniferum* did not show a significant correlation between the gene expression profile and alkaloid profile, for instance, the alkaloid free paso paris cell suspension cultures and the one month old seedlings showed very similar gene expression profile, even though a down regulation or non expression of alkaloid specific genes was expected in paso paris cell suspension cultures compared to the same genes in the one month old seedlings or even to the 4-months old. Only a few of the SalAT interactors show a considerable association between alkaloids formation and level of gene expression. One of these isolates is interactor P1A8 which represents major latex protein 146 homologue from opium poppy. MLP146 shares substantial homology with three (P3G4, P1D4, P5C1) other MLPs interacting with SalAT protein (Table.III.2). MLPs are a group of laticifer-specific, low-molecular-weight polypeptides, coded by nine genes that can be divided into two distinct sub-families (Nessler, 1994). Although the role of MLPs in laticifer function is not yet clear, their abundance restricted distribution make them convenient markers for studying laticifer-specific genes (Nessler, 1988). The fact that late stages, possibly at the level either salutaridinol-7-*O*-acetate or thebaine of the morphine biosynthesis occurred in laticifers (Weid et al., 2004) which is the storage site for the alkaloid and MLPs suggested a potential regulatory role for the MLPs morphinans accumulation. Ultra-structural immunolocalization shows that MLPs accumulate early in laticifer development and remain sequestered in a subset of membrane-bound latex vesicles in mature cells (Griffing and Nessler, 1989). Genes MLP146 and MLP149 are 83.9% identical in their nucleotides sequences (Figure IV.3), a similar level of nucleotides sequences identity with exists between MLP15 (Nessler et al., 1990) and MLP146 (82.1%) and MLP149 (81.1%). Slightly less identity is scored between MLP22 (Nessler and Burnett, 1992) and MLP146 (78.1%) and MLP149 (80.1%) which suggests that MLP146 and MLP149 belonged to the MLP15 gene subfamily (Nessler, 1994).

```

*           20           *           40           *           60
MLP1492.se : ATGGCTCATACTCCTGGTATTTTCAGGTCTAGTTGGGAACTTGTATGGAAACGGAGGTTAACTG : 65
MLP146mw.s : ATGGCTCAACATCATACCATTTTCAGGTCTTATTGGGAACTTGTGACCGAATCAGAAGTTAAATG : 65
ATGGCTCA TC T ATTTTCAGGTCT TTGGGAA CTTGT A GAA C GA GTTAA TG

*           80           *           100          *           120          *
MLP1492.se : CAACGGCTGACAAGTATTACCAAAATATAAAGCACCATGAAGATCTTCCAAGCGCAATCCCTCATA : 130
MLP146mw.s : CCATGCTGAAAAATATTACAAAATAATAAAGCACCACGAAGATGTACCTAATGCAACCCCTTATG : 130
C A GCTGA AA TATTAC AAATA TAAGCACCA GAAGAT T CC A GCAA CCCT AT

140           *           160           *           180           *
MLP1492.se : TTGTCACTAGCGCCAAAGCTGTGTGAGGGACATGGAACACTACTTCTGGTTGCGTCAAGGAGTGGGGC : 195
MLP146mw.s : TTTCCGAT---GTCAAAGTTACTGAAGGACATGGTACCCTTCGGGTTGTGTCAAGCAATGGAAC : 192
TT C T G CAAAG T TGA GGACATGG AC ACTTC GGTTG GTCAAG A TGG C

200           *           220           *           240           *           260
MLP1492.se : TATATGCATGAGGGT-AAAACACTTACTTGCAAGGAGAAAACACTACCTATAACGATGAAACAAGGA : 259
MLP146mw.s : TTTGTTGTTGCGGGTCCAAACGAATATGTCCTTGAA-AAAACAACATACAATGATGAAACAAGGA : 256
T T T TG GGGT AAAC TA T C G A AAAAC AC TA AA GATGAAACAAGGA

*           280           *           300           *           320
MLP1492.se : CCATATGTCATAGCATATCTGAAGGAGACTTGATGATGATACAGAAGTTGATGCAACACTT : 324
MLP146mw.s : CAATATGTCACAGTGACTTTGAAGGAGACCTGATGAAGAAATACAAGAAGTTGATGCAATCCTT : 321
C ATATGTCA AG T TGAAGGAGAC TGATGAA A TACAAGAAGTT GATGCAA CTT

*           340           *           360           *           380           *
MLP1492.se : GTCGTTGATCCAAGGATAATGGACATGGAAGCATTGTGAAGTATATTTTAGATTATGAGAAGAT : 389
MLP146mw.s : GTAGTTAAGCCAAGGATAATGGACATGGTAGTAATGTGAGATGGACTATTGAACATGAGAAGAA : 386
GT GTT A CCAAAGGATAATGGACATGG AG A TGTGA T A T T GA ATGAGAAGA

400           *           420           *           440           *
MLP1492.se : AAATGAGGATTCTCCGGTTCCATTATCTAGCTCTGTGCAATCAAGCCACCGAAGACTTGA : 454
MLP146mw.s : TAACGAGGATTCTCCGGTTCCAATTGATTATCTAGCTTCTTCCAATCGTTAATCGATGACTTGA : 451
AA GAGGATTCTCCGGTTCC ATT ATTATCTAG T T T C A A CGA GACTTGA

460           *           480
MLP1492.se : ACACTTACCTTTGTGCTTCTGTCTAA : 480
MLP146mw.s : ACTCTCATCTTTGCTCCTCT---TAA : 474
AC CT A CTTTG C TCT TAA

```

Figure IV.3 MLP Sequence association: Sequence comparison of opium poppy major latex protein encoding genes MLP 149 (top) and MLP 146 (bottom). *Black boxes* indicate identical residues, *dashes* are gaps. MLP146 and MLP149 share 83.9% identity in their nucleotides sequences, and they both belong to the MLP 15 gene subfamily (Nessler, 1994).

IV.3 The enzymatic activity assays for SalAT and MLP 146

The data obtained from the Salutaridinol 7-*O*-acetyltransferase activity assay, without any doubt confirm that salutaridinol was acetylated enzymatically by SalAT at the hydroxyl group of C-7 followed by a subsequent allelic elimination of acetate yielding the penta cycle thebaine at pH 6.5. Thebaine accumulation took place without any involvement of recombinant MLP 146 or any other protein. Alternatively, our data may suggest that MLP 146 is one reason for a staged drop in thebaine content under acidic conditions; this acidic environment may affect the regulatory features of major latex proteins which in its turn decline thebaine contents. A slightly alkaline pH is known to prevail in certain plants organelles (Amann et al., 1988) this may also concern organelles in of *Papaver somniferum* including laticifers, the site of morphinan alkaloid accumulation (Weid et al., 2004). Salutaridinol and salutaridinol acetate were virtually not detectable after 5 min of the reaction because enzymatically formed salutaridinol acetate was transformed to thebaine. This reaction could be also spontaneously under alkaline conditions (Grothe, 2002). Another explanation may be the fact that salutaridinol acetate is relatively unstable in aqueous solution depending on pH value (Lenz and Zenk, 1995a). The instability of the acetate can be one reason for formation of “wrong” products, e.g. epi-salutaridinol at m/z 330 ($[M+H]^+$), neodyhydrothebaine at m/z 314 ($[M+H]^+$), nudaurine at m/z 328 ($[M+H]^+$), or an alkaloid compound with dibenzaonium structure at m/z 312 ($[M+H]^+$) therefore the assays were analyzed by LC-MS.

IV.4 Spontaneous reactions in the biosynthesis of secondary compounds

The involvement of non-enzymatic steps in the biosynthesis of secondary compounds is observed rarely; for example, Michael-type addition of (*S*)-kynurenine to *N*- β -alanyldopamine quinone methide leads to papiliochrome II, a yellow pigment of butterflies (Saul and Sugumaran, 1991); intermolecular cyclisation of γ -methylaminobutyraldehyde to *N*methyl pyrrolinium cation, and its coupling with acetoacetic acid giving hygrine (Endo *et al.*, 1998); and hydration at the 6-position of protein-bound dopaquinone to form 6-hydroxy-dopa (Topa), the precursor of topaquinone

that was identified as an essential co-factor of copper amine oxidase (Mure and Tanizawa, 1997). An additional spontaneous reaction in the morphine biosynthesis is the transformation of neopinone to codeinone (Gollwitzer et al., 1993) (Figure IV.2). In benzylisoquinoline biosynthesis, the reaction of an amine with an aldehyde is an enzyme catalyzed step (dopamine with 4-hydroxyphenylacetaldehyde or 3,4-dihydroxyphenylacetaldehyde), which leads to the cyclical intermediates norcoclaurine and noraudanosoline, respectively (Rueffer and Zenk, 1987). Similarly, the condensation of dopamine with the aldehyde secologanin was found to be catalyzed by cell-free extracts of *Alangium lamarckii* (De-Eknamkul et al., 1997). This cyclisation proceeded, in contrast to the betaxanthin formation, directly to tetrahydroisoquinoline derivatives (*R*- and *S*-form), which spontaneously cyclical further in lactam formation. The first reaction steps can also proceed non-enzymatically at pH 5.0 (Itoh et al., 1995).

IV.5 Thebaine as the major product for Salutaridinol 7-*O*-acetyltransferase

The instability of enzymatic synthesized salutaridinol acetate as a reaction product demonstrates thebaine as the only *in vivo* major product of acetylating salutaridinol in morphine biosynthesis by salutaridinol 7-*O*-acetyltransferase, SalAT from *Papaver somniferum* together with putative acyltransferase from (*Capsicum annuum*) and the terminal *O*-acyltransferases from *R. serpentine* involved in the vindoline biosynthesis define one subfamily with clade III include BAHD acyltransferases that are involved in the modification of alkaloid compounds (Figure IV.4). The BAHD acyltransferases family (D'Auria, 2006) was named according to the first letter of each of the four biochemically characterized enzymes of this family. The majority of BAHD members with clade III (Table IV.2) accept a diverse range of alcohol substrates, although the vast majority of these enzymes utilize acetyl-CoA as major acyl donor. In contrast, only salutaridinol and nudaurine acted as substrates for SalAT (Lenz and Zenk, 1995a), which makes it one of the most highly substrate-specific acyltransferases in alkaloid biosynthesis.

Table IV.2 Genetically or biochemical Characterized BAHD acyltransferases of Clade III (D'Auria, 2006). Abbreviations: SalAT, salutaridinol 7-O-acetyltransferase; Pun1, acyltransferase (*Capsicum annuum*); DAT, deacetylvindoline 4-O-acetyltransferase; MAT, minovincinine 19-hydroxy-O-acetyltransferase; Ss5MaT2, anthocyanin 5-O-glucoside-4"-O-malonyltransferase; CbBEAT, acetyl CoA: benzylalcohol acetyltransferase; BEAT; CmAAT4, putative alcohol acyl-transferases; RHAAT1, acetyl CoA geraniol/citronellol acetyltransferase; SAAT, alcohol acyltransferase; VAAT, unnamed protein product. Clade number is based on the phylogenetic tree presented in Figure IV.5

Acytransferase name	NCBI Genebank protein ID number	Major acyl CoA donor	Major products formed	Species
SalAT	AAK73661	Acetyl	Thebaine	<i>Papaver somniferum</i>
Pun1	AAV66311	Unknown	Capsaicin pathway	<i>Capsicum annuum</i>
DAT	AACA99311	Acetyl	Vindoline	<i>C. roseus</i>
MAT	AAO13736	Acetyl	Minovincinine	<i>C. roseus</i>
Vinorine synthase	CAD89104	Acetyl	Vinorine	<i>R. serpentine</i>
Ss5MaT2	AAR26385	Malonyl	Antocyanins	<i>S. splendens</i>
CbBEAT	AAC18062	Acetyl	Benzyl acetate	<i>C. breweri</i>
CmAAT4	AAW51126	Medium-chain aliphatic	Medium-chain and hydroxycinnamoyl acylesters	<i>C. melo</i>
RHAAT1	AAW31948	Acetyl	General acetate and other volatile esters	<i>Rosa hybrid cultivar</i>
SAAT	AAG13130	Acetyl	Medium-chain aliphatic and benzyl esters	<i>Fragaria x ananassa</i>
VAAT	CAC09062	Acetyl	Small - to medium-chain aliphatic esters	<i>Fragaria vesca</i>

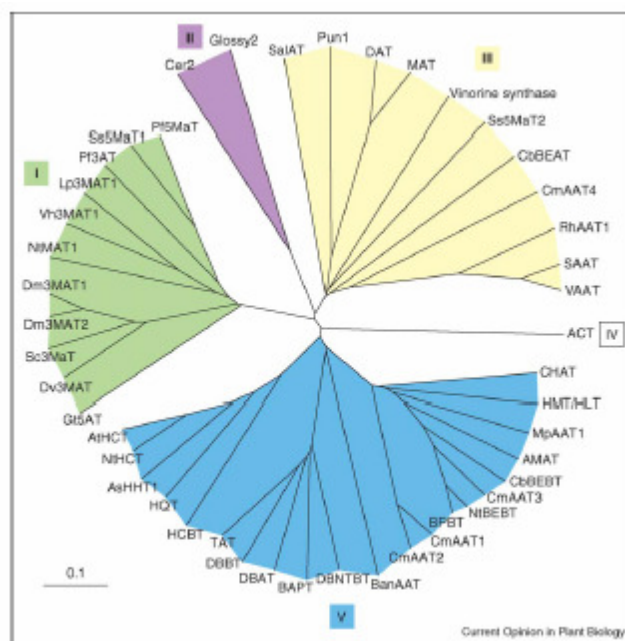


Figure IV.4 BAHD acyltransferases family: Phylogenetic tree of the plant BAHD family of functionally characterized by either genetic mutant screening or biochemical assay acyltransferases (D'Auria, 2006)

All previous results suggest that salutaridinol 7-*O*-acetyltransferase exhibit a very fast acetylation of salutaridinol into salutaridinol acetate; however, our results did not show this step as a pH controlled intersection between morphine biosynthetic pathway and other alkaloid pathways. On the other hand the very sharp drop in the thebaine content by adding the recombinant MLP 146 to the salutaridinol 7-*O*-acetyltransferase activity assay reactions suggests a further step in complexity for the regulatory architectures of thebaine and morphinans profiling. Recently, cDNAs encoding 10 enzymes of alkaloid biosynthesis in *Papaver somniferum* have been isolated and characterized (Weid *et al.*, 2004) on the pathway leading from L-tyrosine to morphine. SalAT was the only acetyltransferase occurring between (R) - reticuline and morphine which was followed by extremely rare spontaneous non-enzyme-catalyzed reactions in natural product synthesis. Further genes and the corresponding proteins still need to be isolated to achieve the long-standing goal of chemically, enzymatically, and biotechnologically synthesis of morphinan alkaloids.

V. Summary

Benzylisoquinoline alkaloids represent a group of about 2500 structures containing many physiologically active members. Among the benzylisoquinoline alkaloids, morphine is one of the pharmaceutically important members that are still derived from the opium poppy *Papaver somniferum*, which produces over 80 alkaloids derived from L-tyrosine. Through the biosynthetic pathway that leads from L-tyrosine to morphine, salutaridinol is acetylated by salutaridinol 7-*O*-acetyltransferase (SalAT) and, subsequently, the acetate group is removed to form the pentacyclic morphinan ring system of thebaine. SalAT was initially identified and isolated as a cDNA clone that corresponds to the internal amino acid sequences of the native enzyme purified from a cell suspension culture of *Papaver somniferum* (Grothe et al., 2001). SalAT catalyzes the conversion of the phenanthrene alkaloid salutaridinol to salutaridinol acetate the immediate precursor of thebaine along morphine biosynthetic pathway. Because salutaridinol acetate non-enzymatically rapidly decomposes to thebaine, it was not clarified whether in vivo thebaine formation is an enzymatic or a non-enzymatic reaction. There were some indications which suggest that this elimination is an enzymatic - dependent process. Because of the instability of the acetate, this “thebaine synthase” was assumed to be physically correlated with salutaridinol 7-*O*-acetyltransferase. Based upon this hypothesis, a yeast two-hybrid system was used in an attempt to isolate a cDNA that encodes a putative “thebaine synthase”. The Cyto Trap yeast two-hybrid system is a new way to identify protein-protein interactions by searching the cytoplasm instead of the nucleus of the yeast cells. The project and its results could be summarized as the following.

1. Bait plasmid was constructed by cloning the cDNA of Salutaridinol 7-*O*-acetyltransferase into the pSos vector, though fusing the bait to human gene (hSos) product. The generated SalAT- hSos; fusion was transformed into yeast cdc25H strain.
2. A cDNA library from *Papaver somniferum* stems was prepared for protein- protein interaction screening, and cloned into pMyr vector which fuses the target gene to myristylation factor that anchors the protein to the yeast cell membrane.
3. Both fusion proteins (1 and 2) were co-transformed and co-expressed in the cdc25H yeast strain that harbors a temperature-sensitive mutation of the cdc25 gene and the yeast cells were incubated at the restrictive temperature of 37 °C on galactose

dependent medium for cDNA library screening and identification of putative positive interactors. Approximately 400 putative positive clones could be isolated from which 345 were sequenced and analyzed.

4. cDNA encoding the SalAT neighboring Salutaridine reductase (SalR) and the distant Norclaurine 6-*O*-methyl transferase (6OMT) were generated and unidirectional cloned into vector MCS as target proteins. SalAT show the ability to interact with SalR, but did not interact with 6OMT.
5. Gene expression of 400 interactors were analyzed along with alkaloid profiling by LC-MS in cell culture suspension, and developing poppy seedlings to correlate the expression of interactor cDNAs with the time of accumulation of morphinan alkaloids. LC-MS analysis of 4-months plants of *Papaver somniferum* shows morphine as main alkaloid followed by codeine and thebaine, respectively. Codeine was the first alkaloid to be detected in the greenhouse seedlings (12 days) meanwhile morphine was detected after 20 days, other alkaloids were in very low concentrations during the first month. Morphine contents continue to increase in much higher rates than codeine during the second month. One of the interactors showing high expression during alkaloid accumulation, the major latex protein 146, was selected for further characterization.
6. Salutaridinol 7-*O*-acetyltransferase (SalAT) which catalyzes the conversion of salutaridinol to salutaridinol-7-*O*-acetate, and the “thebaine synthase” candidate protein recombinant major latex protein (MLP 146) were heterologously over-expressed in *E.coli* and purified for a potential role in enzymatic thebaine formation. Enzyme assays were performed by incubations of salutaridinol and SalAT in the presence or absence of MLP146.
7. The product analysis was performed by LC-MS/MS and ESI selected reaction monitoring (SRM). The mass-spectrometric data exhibit signals for salutaridinol, salutaridinol acetate and thebaine in all incubations. Recombinant salutaridinol 7-*O*-acetyltransferase performance in converting salutaridinol into salutaridinol acetate was

very active in a wide pH range values (6.5-9) as observed by thebaine formation without any participation of MLP 146 protein.

8. Biochemical data from enzymatic activity assays suggests that salutaridinol acetate undergoes a subsequent spontaneous and non enzymatic elimination at pH 6.5 as well as in neutral and alkaline environment leading to the formation of thebaine suggesting that thebaine formation is not a pH dependent process. The presence of by-products at acidic and neutral conditions as described by Lenz and Zenk (1995a) were not detectable. Full scan data show no signals for neodihydrothebaine, nudaurine, reticuline, and [8, 9-dihydro 5H-2, 12-dimethoxy-1-hydroxy-7-methyl-dibenz [*d,f*]azonium]acetate. The MS spectra shows an unknown compound with protonated molecular ion at m/z 332, where the structure is not elucidated.
9. Recombinant major latex protein (MLP 146) appeared as a regulatory factor in thebaine accumulation depending on pH value; e.g. the rate of thebaine accumulation was dramatically declined regardless of the amount of MLP 146 at acidic conditions

Conclusion

Yeast two-hybrid assays for isolation of SalAT interaction proteins pulled out a relatively high number of cDNA as candidates for “thebaine synthase”. One of those candidates was the MLP 146 which could not be identified biochemically as the putative “thebaine synthase”. Rather, thebaine was detected rapidly and directly after incubations of salutaridinol and the recombinant salutaridinol 7-*O*-acetyltransferase only, no other proteins were needed. Based on the previous observations we suggest that *in vivo* thebaine formation in opium poppy is a non enzymatic rather than enzymatic step, most likely influenced by major latex protein.

VI References

- **Amann, M., Nagakura, N., and Zenk, M.H.** (1988). Purification and properties of (S)-tetrahydroprotoberberine oxidase from suspension-cultured cells of *Berberis wilsoniae*. *Eur. J. Biochem*, **175**, 17-25.
- **Atsatt, P.** (1996). Plant defense guilds. *Science* **193**, 24-29
- **Bak, S., Tax, F.E., Feldmann, K.A., Galbraith, D.W., and Feyereisen, R.** (2001). CYP83B1, a cytochrome P450 at the metabolic branch point in auxin and indole glucosinolate biosynthesis in *Arabidopsis*. *Plant Cell*, **13**, 101-111.
- **Baulcombe, D.** RNA silencing in plants. (2004). *Nature*, **431**, 356-363.
- **Blechert, S., Brodschelm, W., Hölder, S., Kammerer, L., Kutchan, T.M., mueller, M.J., Xia, Z.Q., and Zenk, M.H.** (1995). The octadecanoid pathway: Signal molecules for the regulation of secondary pathways. *Proc. Natl. Acad. Sci.* **92**, 4099-4105.
- **Borevitz, J.O., Xia, Y., Blount, J., Dixon, R.A., and Lamb, C.** (2000). Activation tagging identifies a conserved MYB regulator of phenylpropanoid biosynthesis. *Plant Cell*, **12**, 2383-2394.
- **Boun, P.** (2005). Transcriptional control of flavonoid biosynthesis: a complex network of conserved regulators involved in multiple aspects in differentiation in *Arabidopsis*. *Cur. Op. Pl. Biol*, **8**, 272-279.
- **Bowles, D., Isayenkova, J., Lim, E.K., and Poppenberger, B.** (2005). Glycosyltransferase: managers of small molecules. *Cur. Op. Pl. Biol*, **8**, 254-263.
- **Brown, J.W.S.** (1996). *Arabidopsis* intron mutations and pre-mRNA splicing. *Plant J.* **10**, 771-780.
- **Carter, O.A., Peters, R.J., and Croteau, R.** (2003). Monoterpene biosynthesis pathway construction in *Escherichia coli*. *Phytochemistry*, **6**, 425-433.
- **Causier, C., and Davie, B.** (2002). Analysing protein-protein interactions with the yeast two-hybrid system. *Plant Mol. Biol.* **50**, 855-870.
- **Choi, K., Morishige, T. and Sato, F.** (2001). Purification and characterization of coclaurine *N*-methyltransferase from cultured *Coptis japonica* cells. *Phytochemistry* **56**, 649-655.

- **Choi, K.B., Morishige, T., Shitan, N., and Yazaki, K.** (2002). Molecular Cloning and Characterization of Coclaurine *N*-Methyltransferase from Cultured of *Coptis japonica*. *J. Biol. Chem.* **277**, 830-835.
- **Czechowski, T., Bari, R.P., Stitt, M., Scheible, W.R., and Udvardi, M.K.** (2004). Real-time RT-PCR profiling of over 1400 Arabidopsis transcription factors: unprecedented sensitivity reveals novel root- and shoot-specific genes. *Plant J*, **38**, 366-379.
- **D`Aura, J.C.** (2006). Acyltransferases in plants: a good time to be BAHD. *Cur. Op. Pl. Biol*, **9**, 331-340.
- **D`Aura, J.C., and Gershenzon, J.** (2005). The secondary metabolism of *Arabidopsis thaliana*: growing like a weed. *Cur. Op. Pl. Biol*, **8**, 292-300.
- **Davies, K.M., and Schwinn K.E.** (2003). Transcriptional regulation of secondary metabolism. *Funct Plant Biol*, **30**, 913-925.
- **De Luca, V. and St Pierre, B.** (2000). The Cell and developmental biology of alkaloid biosynthesis. *Trends Plant Sci.* **5**, 168-173.
- **Deavours, B.E., and Dixon, R.A.** (2005). Metabolic Engineering of isoflavonoid biosynthesis in alfalfa. *Plant physiology*, **138**, 2245-2259.
- **Decker, G., Wanner, G., Zenk, M.H. and Lottspeich, F.** (2000). Characterization of proteins in latex of the opium poppy (*Papaver somniferum*) using two-dimensional gel electrophoresis and microsequencing. *Electrophoresis* **21**, 3500-3516.
- **De-Eknamkul, W., Ounaron, A., Tanahashi, T., Kutchan, T. M., Zenk, M. H.** (1997). Enzymatic condensation of dopamine and secologanin by cell-free extract of *Alangiumlamarckii*. *Phytochemistry*, **45**, 477-484.
- **De-Eknamkul, W. and Zenk, M.H.** (1992). Purification and properties of 1, 2-dehydroreticuline reductase from *Papaver somniferum* seedlings. *Phytochemistry* **31**, 813-821.
- **Dittrich, H. and Kutchan, T.M.** (1991). Molecular cloning, expression, and induction of berberine bridge enzyme, an enzyme essential to the formation of benzophenanthridine alkaloids in the response of plants to pathogenic attack. *Proc. Natl. Acad. Sci. USA* **88**, 9969-9973.
- **Dixon, R.A.** (2005). Engineering of plant natural product pathways. *Cur. Op. Pl. Biol*, **8**:329-336.

-
- **Dixon, R.A. and Pavia, N.L.** (1995). Stress-induced phenylpropanoid metabolism. *Plant Cell* **7**, 1085-1097.
 - **Dixon, R.J., Eperon, I.C., Hall, L., and Samani, N.J.** (2005). A genome-wide survey demonstrates widespread non-linear mRNA in expressed sequences from multiple species. *Nucleic Acid Research*, **33**, 5905-5913.
 - **Endo, T., Hamaguchi, N., Hashimoto, T., Yamada, Y.** (1988). Non-enzymatic synthesis of hygrine from acetoacetic acid and from acetonedicarboxylic acid. *FEBS*, **234**, 86-90.
 - **Eilert, U., Kurz, W.G.W., and Constabel, F.** (1985). Stimulation of Sanguinarine accumulation in *Papaver somniferum* cell cultures by fungal elicitors. *J. Plant Physiol.* **199**, 65-76.
 - **Facchini, P.J. and De Luca, V.** (1994). Differential and tissue-specific expression of a gene family for tyrosine/dopa decarboxylase in opium poppy. *J. Biol. Chem.* **269**, 26684-26690.
 - **Facchini, P.J. and De Luca, V.** (1995). Phloem-specific expression of tyrosine/dopa decarboxylase genes and biosynthesis of isoquinoline alkaloids in opium poppy. *Plant Cell* **7**, 1811-1821.
 - **Facchini, P.J. and Park, S.U.** (2003). Development and inducible accumulation of gene transcripts involved in alkaloid biosynthesis in opium poppy. *Phytochemistry* **64**, 177-186.
 - **Facchini, P.J., Bird, D.A., St.-Pierre, B.** (2004). Can arabidopsis make complex alkaloids? *Trends Plant Sci*, **9**, 116-122.
 - **Fairbairn, J.W., Hakim, F., and El Kheir, Y.** (1974). Alkaloid storage metabolism, and translocation in the vesicles of *Papaver somniferum* latex. *Phytochemistry* **13**, 1133-1139.
 - **Frank, M.R., Deyneka, J.M., Schuler, and M.A.** (1996). Cloning of Wound-induced Cytochrome P450 Monooxygenase Expressed in Pea. *Plant Physiol.* **110**, 1035-1046.
 - **Frenzel, T. and Zenk, M.H.** (1990). *S*-Adenosyl-L-methionine:3'-Hydroxy-*N*-methyl-(*S*)-coclaurine 4'-*O*-methyltransferase, a region- and stereoselective enzyme of the (*S*)-Reticuline pathway. *Phytochemistry* **29**, 3505-3511.
 - **Frenzel, T. and Zenk, M.H.** (1990a). Purification and characterization of three isoform of (*S*)-adenosyl-L-methionine: (*R*, *S*)-tetrahydrobenzylisochinoline-*N*-

- methyltransferase from *Berberis koetianeana* cell cultures. *Phytochemistry* **29**, 3491-3497.
- **Frenzel, T. and Zenk, M.H.** (1990b). (*S*)-Adenosyl-L-methionine: 3'-hydroxy-*N*-methyl-(*S*)-coclaurine-4'-*O*-methyltransferase, a regio- and stereoselective enzyme of the (*S*)-reticuline pathway. *Phytochemistry* **29**, 3505-3511.
 - **Frick, S. and Kutchan T.M.** (1999). Molecular cloning and functional expression of *O*-methyltransferases common to isoquinoline alkaloid and phenylpropanoid biosynthesis. *Plant J.* **17**, 329-339.
 - **Frick, S., Chitty, J.A., Kramell, R., Schmidt, J., Allen, R.S., Larkin, P.J., and Kutchan, T.M.** (2004). Transformation of opium poppy (*Papaver somniferum* L.) with antisense berberine bridge enzyme gene (*anti-bbe*) via somatic embryogenesis results in an altered ratio of alkaloids in latex but not in roots. *Transgenic Res.* **13**, 607-613.
 - **Frick, S., Ounaroon, A. and Kutchan T.M.** (2001). Combinatorial biochemistry in plants: the case of *O*-methyltransferases. *Phytochemistry* **56**, 1-4.
 - **Fridman, E., and Pichersky, F.** (2005). Metabolomic, genomic, proteomics, and the identification of enzymes and their substrates and products. *Cur. Op. Pl. Bio.* **8**, 242-248.
 - **Gamborg. O.L., Miller, R.A. and Ojina, K.** (1968). Nutrient requirements of suspension cultures of soybean root cells. *Exp. Cell Res.* **50**, 151-158.
 - **Gerard, R. and Zenk, M.H.** (1993b). Purification and characterization of salutaridine: NADPH 7-oxidoreductase from *Papaver somniferum*. *Phytochemistry* **34**, 125-132.
 - **Gerardy, R., and Zenk, M.H.** (1993a). Formation of salutaridine from (*R*)-reticuline by a membrane-bound cytochrome P-450 enzyme from *Papaver somniferum*. *Phytochemistry* **32**, 79-86.
 - **Golemis, E., A., and Brent, R.** (1992). Fused protein domains inhibit DNA binding by LexA. *Mol Cell Biol.* **7**, 3006-3014.
 - **Gollwitzer, J., Lenz, R., Hampp, N. and Zenk, M.H.** (1993). The transformation of neopinone to codeinone in morphine biosynthesis proceeds non-enzymatically. *Tetrahedron Lett.* **34**, 5703-5706.
 - **Goossens, A., Ha kkinenm S., Laakso, I., Seppa" nen-Laakso, T., Biondi, S., De Sutter, V., Lammertyn, F., Nuutila, A.M., So" derlund, H., and Zabeau,**

- M. (2003). A functional genomics approach toward the understanding of secondary metabolism in plant cells. *Proc. Natl. Acad. Sci. USA*, **100**, 8595-8600.
- **Griffing, L.P., Nessler, C.L.** (1989). Immunolocalization of the major latex proteins in developing laticifers of opium poppy (*papaver somniferum* L.). *J Plant Physiol*, **134**, 357-363
 - **Grotewold, E.** (2003). The challenges of moving chemicals within and out of cells: insights into the transport of plant natural products. *Planta 2004*, **219**, 906-909.
 - **Grothe, T., Lenz, R. and Kutchan T.M.** (2001). Molecular characterization of the salutaridinol 7-O-acetyltransferase involved in morphine biosynthesis in opium poppy *Papaver somniferum*. *J. Biol. Chem.* **276**, 30717-30723.
 - **Harborne, J.B., and Williams, C.A.,** (1992). Advances in flavonoid research *Phytochemistry*. **2000**, **55**:481-504.
 - **Hausschild, K., Pauli, H.H., and Kutchan, T.M.** (1998). Isolation and analysis of a gene *bbe1* encoding the berberine bridge enzyme from the California poppy *Eschscholzia californica*. *Plant Mol. Biol.* **36**, 473-478.
 - **He, X.Z., Reddy, J.T. and Dixon, R.A.** (1998). Stress response in alfalfa (*Medicago sativa* L.) XXII. cDNA cloning and characterization of an elicitor-inducible isoflavone 7-O-methyltransferase. *Plant Mol. Biol.* **36**, 43-54.
 - **Heath, J.R., Phelps, M.E., and Hood, L.** (2003). NanoSystems biology. *Mol Imaging Biol*, **5**, 312-325.
 - **Huang, F. and Kutchan T.M.** (2000). Distribution of morphinan and benzo[c]phenanthridine alkaloid gene transcript accumulation in *Papaver somniferum*. *Phytochemistry* **53**, 555-564.
 - **Ibrahim, R.K., Bruneau, A. and Bantignies, B.** (1998). Plant O-methyltransferases: molecular analysis, common signature and classification. *Plant Mol. Biol.* **36**, 1-10.
 - **Ikezawa, N., Tanaka, M., Nagayoshi, M., Shinkyō, R., Sakaki, T., Inouye, K., and Sato, F.** (2003). Molecular Cloning and Characterization of CYP719, a Methylenedioxy Bridge-forming Enzyme That Belongs to a Novel P450 Family, from cultures *Coptis japonica* Cells. *J. Biol. Chem.* **278**, 38557-39565.
 - **Itoh, A., Tanahashi, T., Nagakura, N.** (1995). Five tetrahydroisoquinoline-monoterpene glucosides and a tetrahydro-®-carbolinemonoterpene glucoside from *Alangium lamarckii*. *J. Nat. Prod*, **58**, 1228-1239.

- **Jørgensen, K., Rasmussen, A.V., Morant, M., Nielsen, A.H., Bjarnholt, N., Zagrobelny, M., Bak, S., and Møller, L.** (2005). Metabolon formation and metabolic channeling in the biosynthesis of plant natural products. *Cur. Op. Pl. Biol.* **8**, 280-291.
- **Jørgensen, K., Vinther Rasmussen, A., Morant, M.; Nielsen, A.H., Bjarnholt, N., Zagrobelny, M., Bak, S., Lindberg and Møller, B.** (2005). Metabolon formation and metabolic channeling in the biosynthesis of plant natural products. *Cur. Op. Pl. Biol.* **8**, 280-291.
- **Joshi, C.P. and Chiang, V.L.** (1998). Conserved sequence motifs in plant S-adenosyl-L-methionine-dependent methyltransferases. *Plant Mol. Biol.* **37**, 663-674.
- **Jung, G.Y., and Stephanopoulos, G.** (2004). A functional protein chip for pathway optimization and in vitro metabolic engineering. *Science*, **304**, 428-431.
- **Karrer, E.E., Lincoln, J.E., Hogenhout, S., Bennett, A.B., Bostock, R.M., Martineau, B., Lucas, W.J., Gilchrist, D.G., and Alexander, D.** (1995). In situ isolation of mRNA from individual plant cells: creation of cell-specific cDNA libraries. *Proc Natl Acad Sci USA*, **92**, 3814-3818.
- **Kehr, J.** Single cell technology (2003). *Cur. Op. Pl. Biol.* **6**, 617-621.
- **Klein, M., Perfus-Barbeoch, L., Frelet, A., Gaedeke, N., Reinhardt, D., Mueller-Roeber, B., Martinoia, E., and Forestier, C.** (2003). The plant multidrug resistance ABC transporter AtMRP5 is involved in guard cell hormonal signalling and water use. *Plant J*, **33**, 119-129.
- **Krieger, C.J., Zhang, P., Mueller, L.A., Wang, A., Paley, S., Arnaud, M., Pick, J., Rhee, S.Y., and Karp, P.D.** (2004). MetaCyc: a multiorganism database of metabolic pathways and enzymes. *Nucleic Acids Res*, **32**, D438-D442.
- **Kutchan, T.M.** (1993). 12-Oxo-phytodienoic acid Induces accumulation of berberine bridge enzyme transcript in a manner analogous to methyl jasmonate. *J. Plant. Physiol.* **142**, 502-505.
- **Kutchan, T.M.** (1995). Alkaloid biosynthesis – the basis for metabolic engineering of medicinal plants. *Plant Cell*, **7**, 1059-1079.
- **Kutchan, T.M.** (1998). Molecular genetics of plant alkaloid biosynthesis. *The Alkaloids – chemistry and Biology* (Cordell, G.A. Hrsg.), *Academic Press, San Diego*. **50**, 267-316.
- **Kutchan, T.M.** (2005). A role for intra- and intercellular translocation in natural product biosynthesis. *Cur. Op. Pl. Biol.* **8**, 292-300.

-
- **Kutchan, T.M., and Dixon, R.A.** (2005). Secondary metabolism: nature's chemical reservoir under deconvolution. *Cur. Op. Pl. Biol*, **8**, 227-229.
 - **Lange, B.M., Wildung, M.R., Stauber, E.J., Sanchez, C., Pouchnik, D., and Croteau, R.** (2000). Probing essential oil biosynthesis and secretion by functional evaluation of expressed sequence tags from mint glandular trichomes. *Proc Natl Acad Sci USA*, **97**, 2934-2939.
 - **Lenz, R. and Zenk, M.H.** (1995a). Stereoselective reduction of codeinone, the penultimate enzymic step during morphine biosynthesis in *Papaver somniferum*. *Tetrahedron Lett.* **36**, 2449-2452.
 - **Lenz, R. and Zenk, M.H.** (1995b). Purification and properties of codeinone reductase (NADPH) from *Papaver somniferum*. Cell cultures and differentiated plants. *Eur. J. Biochem.* **233**, 132-139.
 - **Liu, C. and Dixon, R.A.** (2001). Elicitor-induced association of isoflavone *O*-methyltransferase with endomembranes prevents the formation and 7-*O*-methylation of daidzein during isoflavonoid phytoalexin biosynthesis. *Plant Cell* **13**, 2643-2658.
 - **Mahmoud, S.S., Williams, M., and Croteau, R.** (2004). Cosuppression of limonene-3-hydroxylase in peppermint promotes accumulation of limonene in the essential oil. *Phytochemistry*, **65**, 547-554.
 - **Markus, B.** (2005). Single-cell genomics. *Cur. Op. Pl. Biol*, **8**:236-241.
 - **Martinoia, E., Klein, M., Geisler, M., Bovet, L., Forestier, C., Kolukisaoglu, U., Muller-Rober, B., and Schulz, B.** (2002). Multifunctionality of plant ABC transporters more than just detoxifiers. *Planta*, **214**, 345-355.
 - **Maxwell, C.A., Harrison, M.J. and Dixon, R.A.** (1993). Molecular characterization and expression of alfalfa isoliquiritigenin 2'-*O*-methyltransferase, an enzyme specifically involved in the biosynthesis of and inducer of *Rhizobium meliloti* nodulation genes. *Plant J.* **4**, 917-981.
 - **Memelink, J.** (2005). The use of Genetics to dissect Plant secondary pathways. *Cur. Op. Pl. Biol*, **8**:230-235.
 - **Morishige, T., Tsujita, T., Yamada, Y., and Sato, F.** (2000). Molecular Characterization of the *S*-Adenosyl-L-methionine: 3'-Hydroxy-*N*-methylcoclaurine 4'-*O*-Methyltransferase Involved in Isoquinoline Alkaloid Biosynthesis in *Coptis japonica*. *J. Biol. Chem.* **275**, 23398-23405.

- **Mueller J., L., Rhee, S.Y., and Stitt, M.** (2004). MAPMAN: a user-driven tool to display genomics data sets onto diagrams of metabolic pathways and other biological processes. *Plant J.* **37**, 914-939.
- **Mueller, M.J., Brodschelm, W., Spannagl, E., and Zenk, M.H.** (1993). Signalling in the elicitation process is mediated through the octadecanoid pathway leading to jasmonic acid. *Proc. Natl. Acad. Sci.* **90**, 7490-7494.
- **Mure, M., Tanizawa, K.** (1997). Chemical and biochemical characteristic of topa quinine. *Biosci. Biochem.* **61**, 410-417
- **Nessler, C. L., Burnett, R.** (1992). Organization of the major latex protein gene family in opium poppy. *Plant Mol. Biol.* **20**, 749-752.
- **Nessler, C. L., Kurz, W.G.W. and Peicher, L.E.** (1990). Isolation and analysis of major latex protein of opium poppy. *Plant Mol. Biol.* **15**, 951-953.
- **Nessler, C.L.,** (1988). Comprative analysis of major latex proteins of opium poppy. *J Plant Physiol* **132**, 588-592.
- **Nessler, C.L.,** (1994). Sequence analysis of two new members of the major latex protein gene family supports the triploid-hybrid origin of the opium poppy. *Gene*, **139**, 207-209
- **Nielsen, B., Røe, J. and Brochmann-Hanssen, E.** (1983). Oripavine – A new opium alkaloid. *Planta Med.* **48**, 205-206.
- **Ogita, S., Uefuji, H., Yamaguchi, Y., Koizumi, N., and Sano, H.** (2003). Producing decaffeinated coffee plants. *Nature*, **423**, 823.
- **Ohara, K., Kokado, Y., Yamamoto, H., Sato, F., and Yazaki, K.** (2004). Engineering of ubiquinone biosynthesis using the yeast *coq2* gene confers oxidative stress tolerance in transgenic tobacco. *Plant J.* **40**, 734-743.
- **Ounaroon, A., Decker, G., Schmidt, J., Lottspeich, F., and Kutchan, T.M.** (2003). (*R,S*)-Reticuline 7-*O*-methyltransferase and (*R,S*)-nococlaurine 6-*O*-methyltransferase of *Papaver somniferum* – cDNA cloning and characterization of methyl transfer enzymes of alkaloid biosynthesis in opium poppy. *Plant J.* **36**, 808-819.
- **Panicot, M., Minguet, E.G., Ferrando, A., Alcazar, R., Blázquez, M.A., Carbonell, J., Altabella, T., Koncz, C., and Tiburcio, A.F.** (2002). A polyamine metabolon involving aminopropyl transferase complexes in *Arabidopsis*. *Plant Cell*, **14**, 2539-2551.

- **Park, S.U., Yu, M. and Facchini, P.J.** (2002). Antisense RNA-Mediated Suppression of Benzophenanthridine Alkaloid Biosynthesis in Transgenic Cell Cultures of California poppy. *Plant Physiol.* **128**, 696-706.
- **Park, S.U., Yu, M., and Facchini, P.J.** (2003). Modulation of berberine bridge enzyme levels in transgenic root cultures of California poppy alters the accumulation of benzophenanthridine alkaloids. *Plant Mol. Biol.* **51**, 153-164.
- **Pauli, H.H. and Kutchan T.M.** (1998). Molecular cloning and functional heterologous expression of two alleles encoding (*S*)-*N*-methylcoclaurine 3'-hydroxylase (CYP80B1), a new methyl jasmonate-inducible cytochrome P-450-dependent monooxygenase of benzyloquinoline alkaloid biosynthesis. *Plant J.* **13**, 793-801
- **Pighin, J.A., Zheng, H., Balakshin, L.J., Goodman, I.P., Western, T.L., Jetter, R., Kunst, L., and Samuels, A.L.** (2004). Plant cuticular lipid export requires an ABC transporter. *Science*, **306**,702-704.
- **Raes, J., Rohde, A., Christensen, J.H., Van de Peer, Y., and Boerjan, W.** (2003). Genome-wide characterization of the lignification toolbox in Arabidopsis.
- *Plant Physiol*, **133**, 1051-1071.
- **Rischer H, Oresic M, Seppanen-Laakso T, Katajamaa M, Lammertyn F, Ardiles-Diaz W, Van Montagu MC, Inzé D, Oksman-Caldentey KM, Goossens A.** (2006). Gene-to-metabolite networks for terpenoid indole alkaloid biosynthesis in *Catharanthus roseus* cells *Proc Natl Acad Sci U S A*, **336**, 5614-5619,
- **Rosco, A., Pauli, H.H., Priesner, W., and Kutchan, T.M.** (1997). Cloning and Heterologous Expression of NADPH-Cytochrome P450 Reductases from the *Papaveraceae*. *Arch. Biochem. Biophys.* **348**, 369-377.
- **Rueffer, M., Zenk, M. H.** (1987). Distant precursors of benzoisoquinoline alkaloids and their enzymatic formation. *Z. Naturforsch*, **42c**, 319-332.
- **Rush, M.D., Kutchan, T.M., and Coscia, C.J.** (1985). Correlation of the appearance of morphinan alkaloids and latificer cells in germinating *Papaver bracteatum* seedlings. *Plant Cell Rep.* **4**, 237-240.
- **Saldanha, A.J.** (2004). Java Treeview-extensible visualization of microarray data. *Bioinformatics* **20**, 3246-3248.
- **Samanani, N. and Facchini, P.J.** (2001) Isolation and partial characterization of norcoclaurine synthase, the first committed step in benzyloquinoline alkaloid biosynthesis, from opium poppy. *Planta* **213**, 898-906.

-
- **Samanani, N., Park, S.U., and Facchini P.J.** (2005). Cell type-specific localization of transcripts encoding nine consecutive enzymes involved in protoberberine alkaloid biosynthesis. *Plant Cell* **17**, 915-926.
 - **Saul, S. J., Sugumaran, M.** (1991). Quinone methide as a reactive intermediate formed during the biosynthesis of papiliochrome II, a yellow wing pigment of papilionid butterflies. *FEBS Lett.* **279**, 145-148.
 - **Sato, F., Hashimoto, T., Hachiya, A., Tamura, K.I., Choi, K.B., Morishige, T., Fujimoto, H., and Yamada, Y.** (2001). Metabolic engineering of plant alkaloid biosynthesis. *Proc. Natl. Acad. Sci.* **98**, 367-372
 - **Schumacher, H.M., Gundlach, H., Fiedler, F., and Zenk, M.H.** (1987). Elicitation of benzophenanthridine alkaloid synthesis in *Eschscholtzia* cell cultures. *Plant Cell Rep.* **6**, 410-413.
 - **Sheps, J.A., Ralph, S., Zhao, Z., Baillie, D.L., and Ling, V.** (2004). The ABC transporter gene family of *Caenorhabditis elegans* has implications for the evolutionary dynamics of multidrug resistance in eukaryotes. *Genome Biol.* **5**, R15
 - **Simkin, A.J., Schwartz, S.H., Auldridge, M., Taylor, M.G., and Klee, H.J.** (2004). The tomato CCD1 (CARTENOID CLEAVAGE DIOXGENASE 1) genes contribute to the formation of the flavor volatiles β -ionone, pseudoionone and geranylacetone. *Plant J.* **40**, 882-892.
 - **Singer, S.J., and Nicolson, G.L.** (1972). The fluid mosaic model of the structure of cell membranes. *Science*, **175**, 720-731.
 - **Taylor, L.P., and Grotewold, E.** (2005). Flavonoids as developmental regulators. *Cur. Op. Pl. Biol.* **8**, 317-323.
 - **Tomos, A.D., and Sharrock, R.A.** (2001). Cell sampling and analysis (SiCSA): metabolites measured at single cell resolution. *J Exp Bot.* **52**, 623-630.
 - **Unterlinner, B., Lenz, R. and Kutchan T.M.** (1999). Molecular cloning and functional expression of codeinone reductase: the penultimate enzyme in morphine biosynthesis in the opium poppy *Papaver somniferum*. *Plant J.* **18**, 465-475.
 - **Wagner, G.J., Wang, E., and Shepherd, R.W.,** (2004). New approaches for studying and exploiting an old protuberance, the plant trichome. *Ann Bot (Lond)*, **93**, 3-11.

- **Weid, M., Ziegler, J., and Kutchan, T.M.** (2004). The roles of latex and the vascular bundle in morphine biosynthesis in the opium poppy, *Papaver somniferum*. *Proc. Natl. Acad. Sci.* **101**, 13957-13962.
- **Willits, M.G., Giovanni, M., Prata, R.T.N., Kramer, C.M., De Luca, V., Steffens, J.C., and Graser, G.** (2004). Bio-fermentation of modified flavonoids: an example of in vivo diversification of secondary metabolites. *Phytochemistry*, **65**, 31-41.
- **Winkel, B.S.J.** (2002). Biosynthesis of flavonoids and effects of stress. *Cur. Op. Pl. Biol*, **5**, 218-223.
- **Winkel, B.S.J.** (2004). Metabolic channeling in plants. *Annu Rev Plant Biol*, **55**, 85-107.
- **Yazaki, K.** (2002). Transporters of secondary metabolites. *Cur. Op. Pl. Biol*, **8**, 301-307.
- **Ye, Z.H.** (2002). Vascular tissue differentiation and pattern formation in plants. *Annu Rev Plant Biol*, **53**, 183-202.
- **Zenk, M.H.** (1991). Chasing the enzymes of secondary metabolism: Plant cell cultures as a pot of gold. *Phytochemistry*, **30**, 3861-3863.

Appendix VI.1 Sequenced SalAT Interactors/P1

№	SalAT Interactor	Gene	PCR Size (bp)	Accession number
1	P1A5	expressed protein [Arabidopsis thaliana]	550	NP_568601.1
2	P1A6	alpha-hemolysin [Aeromonas hydrophila]	625	AAB81227.1
3	P1A1	unnamed protein product	400	EAA17321.1
4	P1A3	unknown protein	450	NP_440212.1
5	P1A9	hypothetical protein XP_358683	600	XP_358683.1
6	P1A2	Eukaryotic translation initiation factor 5A-1	600	P26564 IF51
7	P1A8/Ma1	major latex protein-related / MLP-related	650	NP_177245.1
	P1A8/Ma2	major latex protein MLP146 - opium poppy		pir T09697
8	P1Co(B11,B3)	Metallothionein-like protein type 3 (MT-3)	400	Q40256 MT3
9	P1B6	hypothetical protein CaO19.7359	400	EAK97605.1
10	P1B1	hypothetical protein	350	NP_702191.1
11	P1B5	1-aminocyclopropane-1-carboxylate synthase (ACS4)	1650	AAC32428.1
12	P1B4	CG14605-PC [Drosophila melanogaster]	350	AAN13348.2
13	P1B2	No matching sequences reported	500	
14	P1B10	unknown [Arabidopsis thaliana]	500	AAM62969.1
15	P1B7	unnamed protein product [Tetraodon nigroviridis]	400	CAG07262.1
16	P1B12	Eukaryotic translation initiation factor	600	Q945F4 IF52
17	P1C4	photosystem I reaction center subunit III	400	AAD27880.2
18	P1C1	hypothetical protein	450	NP_909739.1
19	P1Con(C9,C10)	unknown	700	NP_957538.1
20	P1C2	F-box family protein	650	NP_201515.

				1
21	P1C7	CP12 domain-containing protein	700	NP_191800.1
22	P1C6	No matching sequences reported	200	
23	P1C5	Ribulose biphosphate carboxylase small chain, chloroplast precursor	350	Q42823 RB S
24	P1C8	putative microtubial binding protein	800	BAD05590.1
25	P1C11	hypothetical protein	600	NP_909739.1
26	P1D6	No matching sequences reported	400	
27	P1D1	No matching sequences reported	400	
28	P1D9	protein kinase family protein	700	NP_195303.2
29	P1D4	Major latex protein MLP146 opium poppy	850	pir T09697
30	P1D3	ABC transporter from Spirodelapolyrrhiza	850	AAD39650.1
31	P1D2	ENSANGP0000000258	400	XP_316614.1
32	P1D7	metallothionein-like protein	450	CAA07565.1
33	P1D8	Potential calcium-transporting ATPase 9, plasma membrane-type (Ca(2+)-ATPase isoform 9)	450	Q9LU41 A CA9
34	P1D5	coat protein [Turnip mosaic virus]	500	CAA70331.1
35	P1E8	hypothetical protein	400	EAA16395.
36	P1E10	glycoprotein gp2	850	AAK61480.1
37	P1E11	No matching sequences reported	400	
38	P1E12	expressed protein [Arabidopsis thaliana]	800	NP_563868 .1
39	P1E2	src-p52 phosphoprotein	200	AAA42575.1
40	P1E3	hypothetical protein	300	NP_701628.1
41	P1E5	No matching sequences reported	350	
42	P1E6	putative lipid transfer protein	600	AAT39256.1
43	P1E1	alpha tubulin subunit	500	AAK81858.1
44	P1F9	Binding Protein of TOR; Tsc11p	650	NP_011018.1
45	P1F1	unknown [Arabidopsis thaliana]	700	AAM63041.1

46	P1F4	preprotein translocase SecA subunit	700	NP_964701.1
47	P1F2	F-box family protein	500	NP_201515.
48	P1F10	Metallothionein-like protein type 3 (MT-3)	550	Q40256IMT3
49	P1F12	Unknown (protein for MGC:78286)	500	AAH71252.1
50	P1F8	putative ubiquitin conjugating enzyme	1000	NP_914863.1
51	P1F6	DNA-binding bromodomain-containing protein	900	INP_181036.2
52	P1G2	No matching sequences reported	350	
53	P1G6	hypothetical protein	400	BAD25288.1
54	P1G10	No matching sequences reported	300	
55	P1G4	NADH dehydrogenase subunit 2	350	YP_026105.1
56	P1G5	src-p68 phosphoprotein	--	IAAA42570.1
57	P1G8	No matching sequences reported	400	
58	P1G11	immunoglobulin-like family member	350	NP_504586.2
59	P1G9	No matching sequences reported	300	
60	P1G1	ribosomal protein L21	550	pirIT50602
61	P1Co(H7,H8)	No matching sequences reported	400	
62	P1H3	P0514G12.26	250	NP_910252.1
63	P1H4	P0514G12.26	250	NP_910252.1
64	P1H2	expressed protein [Arabidopsis thaliana]	550	NP_567596.1
65	P1H12	Photosystem I reaction center subunit IV	600	P12354IPSAE
66	P1H5	class IV chitinase	600	AAM95447.1
67	P1H10	malate dehydrogenase	700	AAD23506.1
69	P1H1	No matching sequences reported	400	
70	P1H9	No matching sequences reported	500	

Appendix VI.2 Sequenced SalAT Interactors/P2

№	SalAT Interactor	Gene	PCR Size (bp)	Accession number
1	P2Con(A8,A9, A2)	PREDICTED: non-tyrosine protein kinase	500	XP_425696.1
2	P2A11	OSJNBb0078D11.11	550	CAD41413.2
3	P2A12	unnamed protein product	700	BAB08813.1
4	P2A4	No matching sequences reported	300	
5	P2A3	No matching sequences reported	600	
6	P2A7	metallothionein-like protein	550	CAA07565.1
7	P2A6	small GTP-binding protein	600	AAA80678.1
8	P2A5	60S ribosomal protein L10 (QM protein homolog)	550	Q9SPB3 RL10_VITRI
9	P2A4	SNF8 like protein	550	CAB79559.1
10	P2B9	abscisic acid insensitive 5 (ABI5)	500	AAD21438.1
11	P2B10	Bax inhibitor	400	AAR28754.1
12	P2B12	putative histone H2A protein	500	AAL33777.1
13	P2B2	hypothetical protein F36H2.2 - <i>Caenorhabditis elegans</i>	900	pir T21887
14	P2B3	metallothionein-like protein	650	CAA07565.1
15	P2B4	hypothetical protein XP_358683	450	XP_358683.1
16	P2B5	No matching sequences reported	400	
17	P2B6	No matching sequences reported	450	
18	P2B7	protein kinase-like protein	300	CAB41178.1
19	P2B8	unknown protein	950	AAO50693.1
20	P2B1	No matching sequences reported	400	
21	P2Con(C11,C7)	PREDICTED: non-tyrosine protein kinase	900	XP_425696.1
22	P2C12	phosphate transporter 1	350	AAK01938.1
23	P2C9	putative protein	500	CAB80081.1
24	P2C2	No matching sequences reported	950	
25	P2C3	putative histone-like/ribosomal-like protein	350	YP_053689.1
26	P2C10	hypothetical protein	650	EAA17097.1
27	P2C4	protein of photosystem II	700	CAA59409.1
28	P2C5	MATE efflux family protein	800	NP_174585.1
29	P2C1	oxygen evolving complex 33 kDa photosystem II protein	800	AAP03871.1
30	P2C8	putative protein phosphatase type 2C	1400	AAM91671.1
31	P2Con (D11,D12)	CP12 protein precursor, chloroplast	400	pir T06562

32	P2D10	No matching sequences reported	200	
33	P2D4	At1g02780/T14P4_3	500	AAQ22647.1
34	P2D3	No matching sequences reported	620	
35	P2D2	putative Rieske iron-sulfur protein	550	AAD23030.1
36	P2D5	At3g53020 [Arabidopsis thaliana	850	AAP21353.1
37	P2D7	putative senescence-associated protein	1600	BAB33421.1
38	P2D1	1-aminocyclopropane-1-carboxylate oxidase	500	CAA66631.1
39	P2Con(E11,E12)	PREDICTED: non-tyrosine protein kinase	350	XP_425696.1
40	P2E2	liver aldehyde oxidase	700	AAD17000.1
41	P2E3	No matching sequences reported	400	
42	P2E4	No matching sequences reported	1500	
43	P2E6	Oligosaccharyl transferase 3; wu:fc14a12	450	NP_955955.1
44	P2E7	No matching sequences reported	200	
45	P2E8	metallothionein-like protein	500	CAA07565.1
46	P2E1	1-aminocyclopropane-1-carboxylate oxidase homolog	600	CAA66631.1
47	P2Con(F6,F7,F10)	PREDICTED: non-tyrosine protein kinase	600	XP_425696.1
48	P2F11	histone H1C	450	AAD48472.1
49	P2F4	protein of photosystem II	600	CAA59409.1
50	P2F3	coat protein [Turnip mosaic virus]	400	CAA70331.1
51	P2F1	unnamed protein product [Arabidopsis thaliana]	650	BAA96919.2
52	P2F8	No matching sequences reported	400	
53	P2F2hit1	trans-cinnamate 4-monooxygenase (EC 1.14.13.11) cytochrome P450 C4H - mung bean	500	pir JC1458
	P2F2hit2	cytochrome P450 - alfalfa		pir S36878
	P2F2hit3	cinnamate 4-hydroxylase (CYP73) [Catharanthus roseus]		CAA83552.1
	P2F2hit4	cytochrome P450 [Triticum aestivum]		AAG17469.1
	P2F2hit5	elicitor-inducible cytochrome P450[Nicotiana tabacum]		AAK62344.1
54	P2F3	coat protein [Turnip mosaic virus]	450	CAA70331.1
55	P2G3	SocE [Myxococcus xanthus]	--	AAF91388.1

56	P2G9	PREDICTED: non-tyrosine protein kinase.	450	XP_425696.1
57	P2G11	No matching sequences reported	400	
58	P2G2	AT3g06050/F24F17_3 [Arabidopsis thaliana]	500	AAK96471.1
59	P2G10	No matching sequences reported	200	
60	P2G4	Unknown protein [Arabidopsis thaliana]	600	AAD25619.1
61	P2G5	No matching sequences reported	400	
62	P2G7	putative photosystem II polypeptide [Arabidopsis thaliana]	200	AAM20194.1
63	P2G1	expressed protein [Arabidopsis thaliana]	350	NP_680430.1
64	P2Con(H11,H9, H10,H12)	NAD kinase, active as a hexamer; enhances the activity of ferric reductase (Fre1p)	100-150	NP_012583.1
65	P2H2	No matching sequences reported	200	
66	P2H5	Cytochrome B6-F complex iron-sulfur subunit 1, chloroplast precursor	200	P30361 UCR A_TOBAC
67	P2H6	histone H1-II - Volvox carteri	300	pir IJN0748
68	P2H7	12 kD protein [Potato virus M]	400	CAA40689.1
69	P2H8	Kinesin motor domain, putative	400	EAA18770.1
70	P2H1	lipid transfer protein precursor	850	AAR90329.1

Appendix VI.3 Sequenced SalAT Interactors/P3

№	SalAT Interactor	Gene	PCR Size (bp)	Accession number
1	P3Con (A11)	No matching sequences reported	650	
2	P3A3	Xnr-1	900	AAA97392.1
3	P3A4	OJ991214_12.3	350	CAE01514.1
4	P3A2	Unknown [Arabidopsis thaliana]	900	AAM61545.1
5	P3A7	Unknown protein	700	XP_469486.1
6	P3A8	putative gibberellin beta-hydroxylase [Arabidopsis thaliana]	700	AAD20145.1
7	P3A6	No matching sequences reported	350	
8	P3B11	No matching sequences reported	400	
9	P3B12	GNog1p. GTPase [Cryptosporidium parvum]	400	EAK87950.1
10	P3B2	NADH dehydrogenase 6	300	CAD61192.2
11	P3B3	SRC_AVIST Tyrosine-protein kinase transforming protein SRC (P60-SRC)	400	splP14085
12	P3B4	translationally controlled tumour-like protein	400	CAD31719.1
13	P3B6	plasma membrane H ⁺ ATPase	850	CAB69823.1
14	P3B7	putative ATP citrate lyase	500	AAL33788.1
15	P3B8	putative protein, with 3 coiled coil-4 domains (1F800)	700	NP_491546.2
16	P3B1	No matching sequences reported	500	
17	P3C11	No matching sequences reported	400	
18	P3C12	alpha tubulin subunit	450	AAK81858.1
19	P3C2	No matching sequences reported	100	
20	P3C3	type XII collagen NC1 domain long type splicing isoform	500	BAC79012.1
21	P3C4	hypothetical protein	300	XP_464482.1
22	P3C5	protein-tyrosine kinase (EC 2.7.1.112) src - Rous sarcoma virus	500	pirII52313
23	P3C6	At3g59010/F17J16_60 [Arabidopsis thaliana]	950	AAN46858.1
24	P3C7	ubiquitin-conjugating protein	400	AAR83898.1

25	P3C8	No matching sequences reported	650	
25	P3bCon(D10,D12,)	PREDICTED: hypothetical protein XP_498810	600	XP_498810.1
26	P3D9	protein src	650	prfl0610239A
27	P3D4	hypothetical protein	350	NP_909739.1
28	P3D7	No matching sequences reported	350	
29	P3D3	At4g33110 [Arabidopsis thaliana]	700	AAP42757.1
30	P3D6	unknown protein	700	pirllD96742
31	P3D8	OSJNBa0018M05.11	800	CAE03236.2
32	P3D2	chlorophyll A-B binding protein 4 precursor homolog	550	AAN15412.1
33	P3D1	No matching sequences reported	350	
	P3E1	No matching sequences reported	350	
34	P3E3	OSJNBa0063C18.17	450	CAE05976.2
35	P3 Con(E4,E9)	protein v-src	200	prfl0903255A
36	P3E2	Dipeptide ABC transporter, periplasmic dipeptide binding protein (dppA)	4000	NP_343949.1
37	P3E6	hypothetical protein	500	XP_504843.1
38	P3E7	major latex-like protein 1 [Plantago major]	400	CAH59440.1
39	P3E12	No matching sequences reported	450	
40	P3F1	hypothetical protein FG00351.1	400	EAA69611.1
41	P3bF2	No matching sequences reported	300	
42	P3F7	chlorophyll a/b-binding protein type I precursor (cab-6A) - tomato	300	pirllS00443
43	P3F9	unknown protein	450	XP_478221.1
44	P3F11	EST AU065533(C2174)	950	NP_910543.1
45	P3F8	truncated PDR5	--	AAO38684.1
46	P3F6	No matching sequences reported	400	BAA03104.1
47	P3F3	light-harvesting chlorophyll a/b-binding protein (LHCP) precursor	400	BAA03104.1
48	P3F4	P0518C01.25	--	NP_914359.1
49	P3 Con(G6,G9)	SocE [Myxococcus xanthus]	450	AAF91388.1
50	P3G7	hypothetical protein	400	NP_704040.1
51	P3G10	Metallothionein-like protein	650	CAA07565.1
52	P3G11	At1g79210/YUP8H12R_1	600	AAM67426.1
53	P3G2	T8K14.10 [imported]	1500	pirllA96826
54	P3G4	Major latex-like protein 15	550	AAC64917.1
55	P3G3	No matching sequences reported	--	

56	P3G12	No matching sequences reported	300	
57	P3G1	auxin-repressed protein like-protein [500	AAK25768.1
58	P3H7	hypothetical protein	--	CAH10374.1
59	P3H10	No matching sequences reported	200	
60	P3H12	LP01645p	300	AAR88554.1
61	P3H2	No matching sequences reported	400	
62	P3H6	RIKEN cDNA 1110059H15	650	XP_485005.1
63	P3H5	coat protein [Potato virus M]	700	AAP76211.1
64	P3H4	STARP antigen	500	AAF21035.1
65	P3H1	chlorophyll a/b binding protein	750	CAA28639.1
66	P3H8	unnamed protein product [Arabidopsis thaliana]	350	BAA94989.1
67	P3H3	thioredoxin	450	AAS88427.1
68	P3H9	hypothetical protein	500	EAA18061.1
69	P3H11	metallothionein-like protein	550	CAA07565.1

Appendix VI.4 Sequenced SalAT Interactors/P4

№	SalAT Interactor	Gene	PCR Size (bp)	Accession number
1	P4Con(A9,A10)	NAD kinase, active as a hexamer; enhances the activity of ferric reductase	300	NP_012583.1
2	P4A3	hypothetical protein	900	pirllC84900
3	P4A4	MRP-like ABC transporter[<i>Oryza sativa</i> (japonica cultivar-group)]	400	CAD59448.1
4	P4A5	Cytochrome B6-F complex iron-sulfur subunit 2, chloroplast precursor	550	splQ02585
5	P4A6	hypothetical protein	400	EAA74231.1
6	P4A8	KIAA0851 protein	500	CAB95945.1
7	P4A1	fiber lipid transfer protein	800	AAN77147.1
8	P4Con(B3,B10)	hypothetical protein	400	AAM94882.1
9	P2B7	photosystem II polypeptide	400	AAP72269.1
10	P4B11	enoyl-CoA hydratase	550	AAM18495.1
11	P4B4	dehydrin 13	650	AAT81473.1
12	P4B9	COG3497: Phage tail sheath protein FI	400	ZP_00110801.1
13	P4B1	hypothetical protein	350	XP_464482.1
14	P4B8	No matching sequences reported	400	
15	P4B11	histone H1D	500	AAN37904.1
16	P4C2	trans-cinnamate 4-monooxygenase (EC 1.14.13.11) cytochrome P450	500	pirllT06522
17	P4C3	polyprotein precursor	400	BAA01452.1
18	P4C4	IAP100 protein	400	NP_113434.1
19	P4C5	NAD kinase, active as a hexamer; enhances the activity of ferric reductase	550	NP_012583.1
20	P4C7	putative glycine-rich protein	400	NP_921766.1
21	P4C8	No matching sequences reported	500	
22	P4C1	transcriptional factor B3 family protein	650	NP_200636.1
23	P4Con(D11,D12)	PREDICTED: non-tyrosine protein kinase	550	XP_425696.1
24	P4D10	No matching sequences reported	950	
25	P4D4	hypothetical protein CaO19.7905	1400	EAL01248.1
26	P4D6	hypothetical protein	550	NP_704964.1
27	PD1	Sensory transduction histidine kinase	300	NP_347467.1
28	P4E12	similar to expressed sequence AI841794	400	XP_230055.2
29	P4E8	hypothetical protein CaO19.8741	250	EAK93927.1
30	P4E9	CP12 protein precursor, chloroplast	450	pirllT02941
31	P4E11	cytochrome P450-3 [<i>Musa acuminata</i>]	--	AAL38986.1

32	P4E2	putative Rieske iron-sulfur protein Tic55	600	XP_468226.1
33	P4E1	putative iron deficiency protein Ids3	600	XP_483774.1
34	P4E4	At1g02780/T14P4_3	500	AAQ22647.1
35	P4E3	No matching sequences reported	650	
36	P4E5	60S ribosomal protein L24	850	AAG13986.1
37	P4F3	No matching sequences reported	450	
38	P4F10	No matching sequences reported	600	
39	P4F2	cytochrome P450-3 [<i>Musa acuminata</i>]	600	AAL38986.1
40	P4F4	protein of photosystem II	650	CAA59409.1
41	P4F5	MATE efflux family protein	700	NP_174585.1
42	P4F6	putative LEA III protein isoform 1	700	CAC39160.1
43	P4F7	No matching sequences reported	300	
44	P4F8	OSJNBa0085I10.2	1450	CAE03557.1
45	P4F1	33kDa precursor protein of oxygen-evolving complex	750	CAA78043.1
46	P4G10	Bax inhibitor	400	AAR28754.1
47	P4G2	hypothetical protein F36H2.2	850	pirllT21887
48	P4G3	metallothionein-like protein	650	CAA07565.1
49	P4G4	P0514G12.26 [<i>Oryza sativa</i>]	300	NP_910252.1
50	P4G5	No matching sequences reported	400	
51	P4G8	unknown protein	950	AAM14161.1
52	P4G1	unknown protein	400	XP_475419.1
53	P4Con(H8)	NAD kinase, active as a hexamer; enhances the activity of ferric reductase (Fre1p); Utr1p	600	NP_012583.1
54	P4H12	unnamed protein product	650	BAB08813.1
55	P4H11	patched family protein	500	NP_195548.2
56	P4H9	unknown protein	400	AAL85038.1
57	P4H4	Sulfite reductase [NADPH] flavoprotein alpha-component	400	AAP11656.1
58	P4H5	QM-like protein	400	AAG27431.1
59	P4H6	small GTP-binding protein	450	AAA80678.1
60	P4H7	metallothionein-like protein	500	AAG44759.1
61	P4H1	SNF8 like protein [<i>Arabidopsis thaliana</i>]	550	CAB79559.1

Appendix VI.5 Sequenced SalAT Interactors/P5

№	SalAT Interactor	Gene	PCR Size (bp)	Accession number
1	P5Con(A2,A9)	pp60-c-src protein	300	CAA23696.1
2	P5A12	No matching sequences reported	350	
3	P5A1	ABC-type sugar transport systems, permease components	500	ZP_00337429.1
4	P5A10	AT5g02020/T7H20_70 [Arabidopsis thaliana]	500	AAM16209.1
5	P5A4	unknown protein [Arabidopsis thaliana]	450	BAC42366.1
6	P5A5	No matching sequences reported	300	
7	P5A3	unnamed protein product	400	CAF99566.1
8	P5A8	metallothionein-like protein	550	AAG44759.1
9	P5A6	LOS2 [Capsella bursapastoris]	700	AAS66001.1
10	P5B11	hypothetical protein	350	AAM94882.1
11	P5B8	unknown [Escherichia coli]	--	NP_957538.1
12	P5B9	No matching sequences reported	400	
13	P5B5	No matching sequences reported	600	
14	P5B2	chlorophyll a/b-binding protein CP26 in PS II	700	CAA65042.1
15	P5B10	hypothetical protein	850	BAD04851.1
16	P5B6	auxin-regulated protein-like protein	1200	XP_477897.1
17	P5B7	No matching sequences reported	550	
18	P5B1	hypothetical protein	250	XP_464482.1
19	P5C3	1700055O19Rik protein	350	AAH48635.1
20	P5C9	No matching sequences reported	300	
23	P5C1	major latex-like protein -Arabidopsis	500	CAC83579.1

		thaliana]		
24	P5C11	No matching sequences reported	500	AAR09603.1
25	P5C6hit1	(R,S)-reticuline 7-O-methyltransferase [Papaver somniferum]	350	AAR09603.1
	P5C6hit2	(R,S)-norcoclaurine 6-O-methyltransferase [Papaver somniferum]		AAQ01669.1
	P5C6hit3	O-methyltransferase [Mentha x piperita]		AAQ01668.1
	P5C6hit4	S-adenosyl-L-methionine:norcoclaurine 6-O- methyltransferase [Papaver somniferum]		AAP45315.1
26	P5C8	No matching sequences reported	350	
27	P5C7	coat protein [Turnip mosaic virus]	500	NP_734222.1
28	P5C1	S28 ribosomal protein [Triticum aestivum]	600	AAP80664.1
29	P5D11	SRC_AVISR Tyrosine-protein kinase transforming protein SRC (P60-SRC)	350	splP00525
30	P5D3	ENSANGP00000020336 [Anopheles gambiae]	400	XP_316160.1
31	P5D2	No matching sequences reported	450	
32	P5D5	Auxin response factor 6	500	splQ9ZTX8
33	P5D12	hypothetical protein	3000	NP_705155.1
34	P5D10	unknown protein	500	XP_469336.1
35	P5D4	dehydrin 13	600	AAT81473.1
36	P5D9	hypothetical protein	300	XP_325620.1
37	P5D7	translation initiation factor 5A precursor protein (eIF-5A)	650	CAB65463.1
38	P5D8	2-on-2 hemoglobin	600	CAD33536.1
39	P5E10	unknown [Arabidopsisthaliana]	500	AAM62557.1
40	P5E11	No matching sequences reported	200	

Appendix IV.2 Time course analysis of alkaloid seedlings content

Probe	Sum	morphine	codeine	papaverine	reticuline	sangunarine	laudanine	thebaine	laudanoline	FM mg
4d	0,0	0,0	0,0	0,0	0,0	0,0	0,0	0,0	0,0	10
8d	0,0	0,0	0,0	0,0	0,0	0,0	0,0	0,0	0,0	40
12d	2,2	0,0	2,2	0,0	0,0	0,0	0,0	0,0	0,0	120
16d	2,2	0,0	2,2	0,0	0,0	0,0	0,0	0,0	0,0	160
20d	3,3	1,3	2,0	0,0	0,0	0,0	0,0	0,0	0,0	210
24d	6,2	1,3	4,9	0,0	0,0	0,0	0,0	0,0	0,0	290
28d	4,2	2,1	2,0	0,0	0,0	0,0	0,0	0,0	0,0	390
32d	19,9	8,9	3,8	7,0	0,1	0,0	0,0	2,2	0,1	620
36d	8,1	3,8	3,3	0,4	0,2	0,0	0,0	0,1	0,2	340
40d	16,3	6,9	2,9	5,5	0,3	0,0	0,3	0,2	0,3	410
44d	11,5	8,8	1,9	0,1	0,2	0,0	0,2	0,1	0,2	530
48d	19,7	15,8	2,9	0,0	0,1	0,3	0,3	0,1	0,1	510
52d	15,0	9,8	1,4	0,0	0,7	0,8	1,2	0,5	0,6	460
56d	13,6	9,1	1,3	0,0	0,5	1,2	1,0	0,4	0,0	450
60d	18,0	12,5	4,5	0,0	0,2	0,2	0,4	0,1	0,0	540

Appendix VI.3 Enzymatic activity assays

SRM-AREA

Reaction	Thebaine-58	Salutaridinol-acetate	Salutaridinol
T0	0	0	1936719260
T5	0	0	2150015940
T10	0	0	1313372200
T20	0	0	1795386160
T40	0	0	981675220
T60	0	0	689990950
T0S	103.422.500	3.783.540	88195070
T5S	146.540.940	1.665.310	2.452.560
T10S	100.576.050	N D	N D
T20S	77.976.240	1.401.500	N D
T40S	50.707.940	N D	1495750
T60S	60.779.420	N D	1657130
T0SM	41.958.730	N D	24427230
T5SM	59.621.370	N D	N D
T10SM	42.823.700	N D	N D
T20SM	57.066.710	N D	N D
T40SM	37.020.800	N D	N D
T60SM	46.857.300	N D	N D
T0SM_5	48.322.946	2.531.513	65.101.230
T5SM_10	51.895.117	N D	N D
T10SM_20	46.671.175	N D	N D
T20SM_40	54.360.725	N D	N D
T40SM_80	52.140.175	N D	N D
T60SM_160	46.896.111	N D	N D

ND : not detectable

Concentration (ng/μl)

Reaction	Thebaine-58	Salutaridinol-acetate	Salutaridinol
T0	0,00	0,00	96,85
T5	0,00	0,00	107,5
T10	0,00	0,00	65,65
T20	0,00	0,00	89,75
T40	0,00	0,00	49,1
T60	0,00	0,00	34,50
T0S	5,15	0,19	4,40
T5S	7,35	0,08	1,25
T10S	5,00	ND	ND
T20S	3,90	0,07	ND
T40S	2,55	N D	0,07
T60S	3,03	N D	0,08
T0SM	2,10	N D	1,20
T5SM	2,95	N D	N D
T10SM	2,15	N D	N D
T20SM	2,85	N D	N D
T40SM	1,85	N D	N D
T60SM	2,30	N D	N D
T0SM_5	2,40	0,125	3,250
T5SM_10	2,55	N D	N D
T10SM_20	2,30	N D	N D
T20SM_40	2,70	N D	N D
T40SM_80	2,60	N D	N D
T60SM_160	2,30	N D	N D

ND : not detectable

ACKNOWLEDGEMENTS

Several people have been instrumental in the conceptualization and completion of this work and I hope they will find in these few lines my appreciation of their various efforts. I am most grateful to my supervisors, Prof. Dr. Toni M. Kutchan (The former managing director of the Institute of plant Biochemistry, Head of the Department, Natural Product Biotechnology, and Head of the Research Group Alkaloid Biosynthesis). Her cooperation, understanding, encouragement, and exceptional ideas during this research cannot be quantified; I am deeply indebted to her. My gratitude goes to the Institute of plant Biochemistry, for the financial support and for giving me the opportunity to study at IPB. I acknowledge all the staff in the Department of Natural Products Biotechnology for their candid support and sincere friendship. I also address my thanks to all administrative staff in the IPB who, in one way or another contributed to the realization of the present work specially Frau Christine Dietel and Frau Balkenhohl for creating an environment of mutual understanding and friendship in the institute. I also extend my thanks to my colleagues in the Department of Bioorganic chemistry Worthy of mention is Dr. Jürgen Schmidt, Frau Kuhnt and Dr. Robert Kramell from the NBT department for their help in enzymatic products analysis and Alkaloids detection. Many thanks also go for Dr. Thomas Vogt from the department of secondary metabolism for proof reading my thesis and many other things. For the current colleagues: Tobias, Katja, Susanne, Jörg, Alfonso, Andreas, Maria Luisa, Karin, Verona, Stefanie, Niels, Otto, Birgit, Domenika and Frau Wegener, I wish you all the best. It would be unbecoming not to acknowledge the love and understanding of all the Arabic friends in Halle: Khaled, Samir, Magdi, Abou Asef, Nasser, Fateh, Rashid, Jihad, for their unlimited support. Last but not least, love and sincere regards go to my family, especially to my mother may God bless her, my lovely wife Rouz and finally my daughter Lana for their endless sacrifices. Without them I would never have got so far in my education. I owe them my profound and sincere gratitude and every lasting love.

1/5/2006 Halle/Saale – Germany

Khaled

Curriculum Vitae

Name: Khaled Sabarna

Date of birth: Oct, 10, 1969

Place of Birth: Hebron, Palestine

Nationality: Palestinian

Education:

- **Bachelor of Science, Major in Biology (Oct, 1990 - Jan, 1995)**
Department of Life Sciences, Bethlehem University, Palestine
Diploma project: Physiological effects of smoking and the role of antioxidants in detoxification.
- **Diploma of Specialized Post-Graduate Studies (DSPU) (October, 1999 - June, 2000) in Natural Products and Biotechnology**
Department of Natural Products and Biotechnology,
Mediterranean Agronomic Institute of Chania (MAICh), Greece.
- **Master of Science (October, 2000 – March, 2002)**
Department of Natural Products and Biotechnology, Mediterranean Agronomic Institute of Chania (MAICh), Chania, Greece
Thesis title: Identification, purification, and enzymatic characterization of GST (omega)
- **Doctoral Student (May, 2002 - Present)**
Department of Natural Products Biotechnology at the Leibniz Institute of Plant Biochemistry (IPB), Halle (Saale), Germany
Thesis title: Approaches to isolating a cDNA encoding thebaine synthase of morphine biosynthesis from opium poppy *Papaver somniferum* L.

Publications:

- Kimiti, K.G., Atanassova, N., Vardanyan, A., Clatot, N., Al-Sabarna K., Kanellopoulos P. N., Makris, A. M., and Kampranis, S. C. Differential roles of tau class glutathione S-transferases in oxidative stress. *J. Bio. Chem.* 279, 24540-24551 (2004)
- Kimiti, K.G., P., Kanellopoulos P., Vardanyan, A., Clatot, N., Al-Sabarna, K., Makris, A. M., Kampranis, S. C. Antioxidant activity of tau-class glutathione S-transferases. *Free Radical Research* 37 (Supplement), 97 (2003).

Halle (Saale) 10.06.06

Declaration

Herewith, I declare that this thesis and its content were made solely on my work as a doctoral student of “Martin-Luther-Universität Halle-Wittenberg”. This work was done independently without any help from others. Other recourses and supports than that are stated in this thesis were not used. All citations are cited literally and the sources are acknowledged accordingly in this thesis as references. I certify that this thesis has never been submitted to other faculties or universities for examination

Halle (Saale)

.....

Date & Signature

Khaled Sabarna